Master's Thesis 2013

Candidate: Achini Weerasooriya

Title: Simulation of Flow in Sedimentation Tank Using Fluent

Telemark University College
Faculty of Technology
Kjølnes
3914 Porsgrunn
Norway

Telemark University College

Faculty of Technology
M.Sc. Programme

MASTER'S THESIS, COURSE CODE FMH606

Student:	**Achini Weerasooriya**		
Thesis title:	**Simulation of flow in sedimentation tank using Fluent**		
Signature:	. . . . .		
Number of pages:	**76**		
Keywords:	**Sewage Treatment, Sedimentation, CFD, Gambit, Fluent, Flow fields, Multiphase, Turbulent, Sedimentation Efficiency**		
Supervisor:	Knut Vågsæther	sign.:	. . . . .
2nd Supervisor:		sign.:	. . . . .
Censor:		sign.:	. . . . .
External partner:	VEAS	sign.:	. . . . .
Availability:	Open		

Archive approval (supervisor signature)**:** sign.: . . . . . **Date :** . . . . . .

Abstract:

Sewage treatment is the process which removes majority of the contaminants from a sewage stream and produces a liquid effluent suitable for safe disposal into the natural environment and sludge. Physical, chemical and biological processes are carried out in a typical WWTP and the sedimentation process is one of the major physical processes which commonly employed in a WWTP. The sedimentation process at VEAS was studied during this project. VEAS is a large scale sewage treatment plant which serves over 500 000 people in Oslo and Akershus.

An effective sedimentation process is important to get the required cleaning level of the effluents and it is very difficult to study or measure the flow fields and velocities inside the sedimentation tanks at VEAS because of the large capacity and the complex geometry. Therefore, a computation study was carried out for one of the sedimentation tanks which is currently operating at VEAS, as a remedy to this problem.

Gambit 2.4.6 software was used to generate the geometry and computational mesh of the sedimentation tank and ANSYS FLUENT 13.0 software was used to perform the simulations. Six different cases were studied during this thesis depending on the flow rate and the particle size of the solid phase.

Flow fields inside the sedimentation tank was evaluated during CFD simulations and it was observed that the flow currents inside the sedimentation tank are not short circuiting which prevents the mixing of partially settled liquid with unsettled influent. Similar velocity profiles were noticed for both liquid and solid phases. Solid volume fraction profiles for different cases at the outlets of the sedimentation tanks have fluctuating behavior and the highest sedimentation efficiency; 99.88% was observed with the case of 250 μm solid particle diameter with 0.5 m^3/h flow rate. Minimum settling efficiency; 1.97% was noticed with the case of 50 μm solid particle diameter with 0.5 m^3/h flow rate.

Furthermore, any specific trend for the velocity profiles at the outlets of the sedimentation tank couldn't be observed from the velocity contours and the velocity magnitudes at the inlet weirs are comparatively higher than the velocities near the outlets. Additionally, flow fields inside the tank are not symmetric even though the geometry of sedimentation tank is symmetric except the inlet.

Telemark University College accepts no responsibility for results and conclusions presented in this report.

Table of contents

PREFACE ..... **V**

NOMENCLATURE ..... **VI**

LIST OF TABLES ..... **VII**

LIST OF FIGURES ..... **VIII**

1 INTRODUCTION **1**

1.1 BACKGROUND 1
1.2 VEAS 2
1.3 OBJECTIVES 4
1.4 REPORT OUTLINE 4

2 LITERATURE REVIEW **5**

2.1 SEDIMENTATION PROCESS 5
2.2 FACTORS AFFECTING THE SEDIMENTATION PROCESS 6
2.2.1 Characteristics of the Fluids *6*
2.2.2 Characteristics of the Solids *6*
2.2.3 Physical Characteristics of the Design *7*
2.2.4 Miscellaneous Effects *8*
2.3 FLOW FIELD IN THE SEDIMENTATION TANKS 9

3 SEDIMENTATION TANK DESCRIPTION **11**

3.1 GEOMETRY 11
3.2 GEOMETRY GENERATION 13
3.3 MESH GENERATION 15

4 CFD MODEL DEVELOPMENT **17**

4.1 MULTIPHASE MODELS 17
4.1.1 Euler-Lagrange Approach *19*
4.1.2 Euler-Euler Approach *19*
4.2 TURBULENT MODELS 21
4.2.1 k – Epsilon (ε) Method *21*
4.2.2 k – Omega (ω) Model *23*
4.2.3 Reynolds Stress Models (RSM) *23*
4.3 SIMULATION DATA AND PARAMETERS 24
4.4 CASES 25

5 RESULTS AND DISCUSSION **27**

5.1 INLET ZONE FLOW BEHAVIOR 27
5.2 FLOW PATTERNS INSIDE THE SEDIMENTATION TANK 29
5.3 VELOCITY PROFILES INSIDE THE SEDIMENTATION TANK 31
5.4 CASE STUDIES 32
5.4.1 Case 1: 250μm Particle Diameter with 0.5 m^3/h Flow Rate *32*
5.4.2 Case 2: 100μm Particle Diameter with 0.5 m^3/h Flow Rate *35*
5.4.3 Case 3: 50μm Particle Diameter with 0.5 m^3/h Flow Rate *38*
5.4.4 Case 4: 340μm Particle Diameter with 1 m^3/h Flow Rate *41*

5.4.5 Case 5: 250μm Particle Diameter with 1 m^3/h Flow Rate 44
5.4.6 Case 6: 100μm Particle Diameter with 1 m^3/h Flow Rate 47

6 CONCLUSION 51

6.1 RECOMMENDATION FOR FUTURE WORKS 52

REFERENCES 53

APPENDIX A: THESIS TASK DESCRIPTION 54

APPENDIX B: VOLUME FRACTION PROFILES OF SOLID PHASE 56

APPENDIX C: VELOCITY PROFILES OF SOLID PHASE 61

APPENDIX D: DETAILED LAMELLA DESCRIPTION 66

Preface

This thesis is compiled to fulfill the requirement of the master's degree in Process Technology at Telemark University College, Norway and this report is an outcome of a collaborative effort of Telemark University College and VEAS.

I would like to express my deepest appreciation to all those who provided me the possibility to complete this report. A special gratitude I give to my supervisor, Associate Professor Knut Vågsæther, whose contribution in stimulating suggestions and encouragement, helped me to coordinate my thesis with VEAS and especially for providing helping hand to get familiarize with Gambit and FLUENT softwares. Moreover, I would like to thank the company VEAS for the collaboration extended during this project.

Furthermore I would also like to acknowledge with much appreciation the staff of IT department at Telemark University College for their great support by providing computers and necessary software.

Last but not least, many thanks go to my dear friends Sachira Kularathna and Chameera Jayarathna for their helping hand during this project.

Porsgrunn, June 5, 2013

Achini Weerasooriya

Nomenclature

WWTP	Waste Water Treatment Plant
CFD	Computational Fluid Dynamics
VOF	Volume of Fluid
RNG	Re-Normalization Group
SST	Shear Stress Transport
RSM	Reynolds Stress Models

List of Tables

Table 1-1: Key figures of the wastewater treatment plant at VEAS [4]. 3
Table 4-1: Summery of the cases 25

List of Figures

Figure 1-1: Schematic diagram of the wastewater threatment plant at VEAS [4]. 2
Figure 2-1: Different settling regimes and the variation of the settling velocity in the sedimentation tank [8]. 6
Figure 2-2: Simulated velocity fields. 9
Figure 2-3: Solid distribution in the center of the tank. a) without baffle; b) h = 1.5 m; c)h = 3m 10
Figure 3-1:Plan view of the selected sedimentation tank at VEAS. 11
Figure 3-2: Side view of the selected sedimentation tank at VEAS. (A = 2.55m; B = 4.2 m) 12
Figure 3-3: Flow fields through the Lamella part [13]. 13
Figure 3-4: Inlet zone geometry 14
Figure 3-5:Wireframe geometry of the sedimentation tank. 14
Figure 3-6: Side and plan veiws of the geometry 14
Figure 3-7: Computational geometry 15
Figure 3-8:Sedimentation tank after meshing the faces. 16
Figure 3-9: Computational mesh of the sedimentation tank. 16
Figure 4-1: Different flow patterns occur in flow regimes [18] 19
Figure 5-1:Velocity vector profile of the inlet zone. 28
Figure 5-2: Planes of the inlet zone. 28
Figure 5-3: Velocity vector profiles inside the inlet zone. 29
Figure 5-4: Solid phase behavior inside the tank at a) 100 s; b) 340 s; c) 550 s; d) 1598 s; e) 2698 s; f) 6098 s with 1 m3/h flow rate and particle size of 100 μm. 30
Figure 5-5: Velocity profile of the solid particles at 90 s; b) 310 s; c) 540 s; d) 6998 s with flow rate of 1m3/h and the diameter of 100μm. 31
Figure 5-6: Positions of the outlets that are going to be discussed. 32
Figure 5-7: Volume fraction profiles of the solid phase inside the tank for case 1. 33
Figure 5-8: Volume fraction profiles of the solid phase at outlets for case 1. 33
Figure 5-9: Volume fraction variation of solid phase with lenght of the tank for case 1. 34
Figure 5-10: Velocity profile variation of solid phase with lenght of the tank for case 1. 34
Figure 5-11: Velocity profile variation of liquis phase with lenght of the tank for case 1. 35
Figure 5-12: Volume fraction profiles of the solid phase inside the tank for case 2. 36
Figure 5-13: Volume fraction profiles of the solid phase at outlets for case 2. 36
Figure 5-14: Volume fraction variation of solid phase with lenght of the tank for case 2. 37
Figure 5-15: Velocity profile variation of solid phase with lenght of the tank for case 2. 37

Figure 5-16: Velocity profile variation of liquis phase with lenght of the tank for case 2. 38
Figure 5-17: Volume fraction profiles of the solid phase inside the tank for case 3. 39
Figure 5-18: Volume fraction profiles of the solid phase at outlets for case 3. 39
Figure 5-19: Volume fraction variation of solid phase with lenght of the tank for case 3. 40
Figure 5-20: Velocity profile variation of solid phase with lenght of the tank for case 3. 40
Figure 5-21: Velocity profile variation of liquis phase with lenght of the tank for case 3. 41
Figure 5-22: Volume fraction profiles of the solid phase inside the tank for case 4. 42
Figure 5-23: Volume fraction profiles of the solid phase at outlets for case 4. 42
Figure 5-24: Volume fraction variation of solid phase with lenght of the tank for case 4. 43
Figure 5-25: Velocity profile variation of solid phase with lenght of the tank for case 4. 43
Figure 5-26: Velocity profile variation of liquis phase with lenght of the tank for case 4. 44
Figure 5-27: Volume fraction profiles of the solid phase inside the tank for case 5. 45
Figure 5-28: Volume fraction profiles of the solid phase at outlets for case 5. 45
Figure 5-29: Volume fraction variation of solid phase with lenght of the tank for case 5. 46
Figure 5-30: Velocity profile variation of solid phase with lenght of the tank for case 5. 46
Figure 5-31: Velocity profile variation of liquis phase with lenght of the tank for case 5. 47
Figure 5-32: Volume fraction profiles of the solid phase inside the tank for case 6. 48
Figure 5-33: Volume fraction profiles of the solid phase at outlets for case 6. 48
Figure 5-34: Volume fraction variation of solid phase with lenght of the tank for case 6. 49
Figure 5-35: Velocity profile variation of solid phase with lenght of the tank for case 6. 49
Figure 5-36: Velocity profile variation of liquis phase with lenght of the tank for case 6. 50
Figure 5-37: Comparison of the settling efficiencies. 50

1 Introduction

An introduction to this thesis report will be presented in this chapter. Some background information related to this project will be discussed in the first part of this chapter and the second part will be presented the information about the wastewater treatment plant (WWTP) at VEAS. Then the next part describes the main objectives of this project and finally the outline of this report is presented.

1.1 Background

Wastewater problem is the world's biggest health risk, and continues to threaten both quality of life and public health in all around the world [1]. The main objective of the wastewater treatment is to allow human and industrial effluents to be disposed of without danger to human health or unacceptable damage to the natural environment [2]. Sewage treatment is one of the main areas that included in wastewater treatment and sewage treatment get higher important especially in the areas of highly populated.

Wide varieties of dissolved and suspended impurities are contained in the sewage. It amounts to a very small fraction of the sewage by weight, but it is large by volume and contains impurities such as organic materials and plant nutrients that tend to rot. Furthermore, the sewage contaminant water tends to increase the concentration of chemical elements required for life and it called eutrophication and therefore sewage need to be treated before it disposed to a water body [3]. Conventional wastewater treatment plants consist of a combination of physical, chemical and biological treatment processes and operate to remove solid, organic matter and sometimes nutrients from the wastewater [2].

Preliminary, primary, secondary and tertiary and/or advance wastewater treatment are used as general terms to describe the degree of the treatment in industry. The purpose of the preliminary treatment is the removal of coarse material from the raw wastewater. Afterwards wastewater flows through the primary treatment process which typically used the technique of sedimentation in order to remove settleable organic and inorganic solids and also to remove material that will float by skimming. Secondary treatment process is employed to further treat the effluent from primary treatment process to remove the residual organic and suspended solids. Typically secondary treatment process is equipped with biological treatment process which removes biodegradable dissolved and colloidal organic matters. The tertiary and/or advanced wastewater treatment processes are used to remove the specific wastewater constituents which cannot be removed by secondary treatment. However this advanced treatment process are sometimes combined with the other treatment processes and chemical addition to the wastewater before the sedimentation to enhance the settling speed can be given as an example [2].

In this report, sedimentation process of the sewage treatment plant is focused which belongs to VEAS.

1.2 VEAS

VEAS was created as an inter-municipal company in 1976 and it serves over 500 000 people in Oslo and Akershus. VEAS treats 100 – 110 million m^3 of waste water i.e. an average of 3500 liters per second and it use physical, chemical and biological process to treat the wastewater. Addition to the wastewater treatment VEAS is producing biogas from sewage and the total heat demand and the 50 % of the electricity demand in VEAS are covered from this biogas. Furthermore sludge is also treated and produces dry and highly demand VEAS soil. Purified water is discharged to approximately 50 m deep ocean. Figure 1-1 shows the schematic diagram of the waste water treatment plant [4].

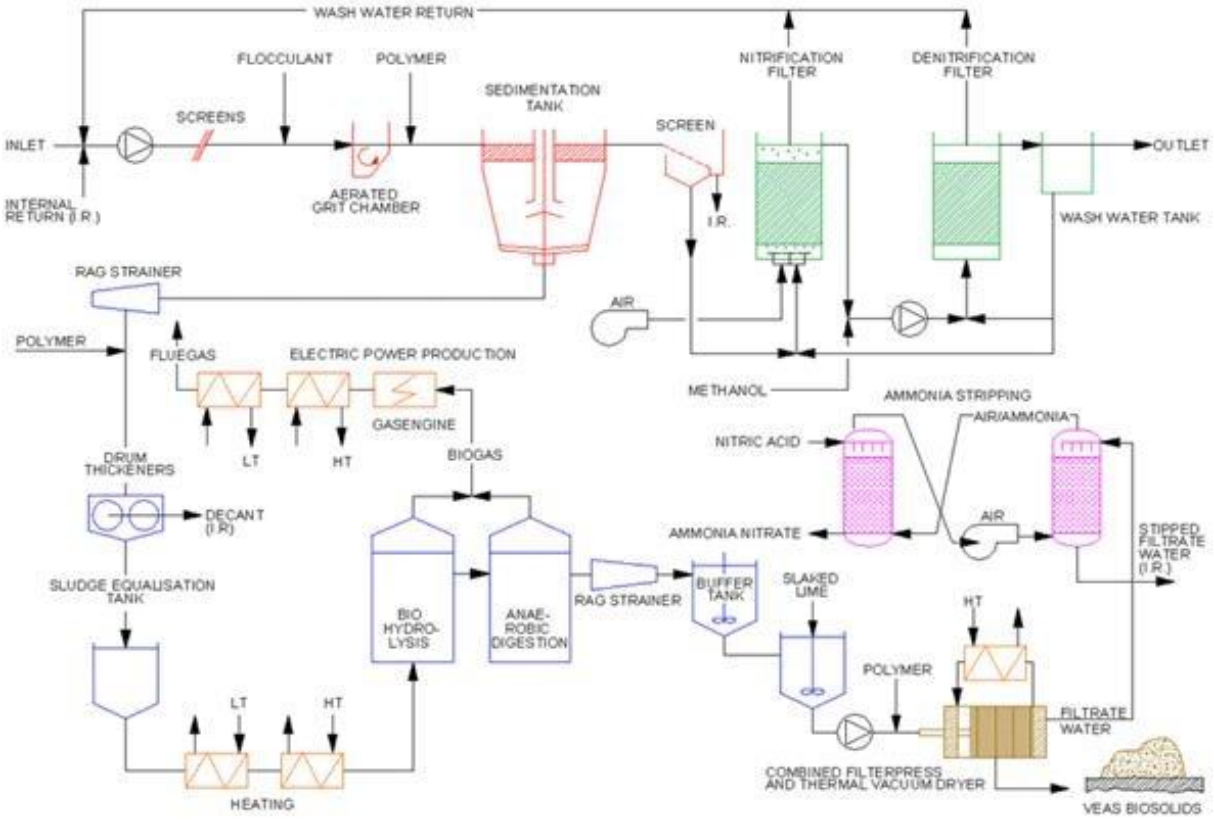

Figure 1-1: Schematic diagram of the wastewater threatment plant at VEAS [4].

Physical, chemical and biological processes are consisted in VEAS sewage treatment plant.

- Physical processes – Initially sewage flows through the shakers which contain coarse strainers that remove large particles. After the water is strained, it flows on to a sedimentation tank where small particles are sinking to the bottom.
- Chemical processes – chemicals are added to the waste water before the sedimentation tanks in order to achieve coagulations and agglomerates.

- Biological processes – Nitrate waste from the effluent is removed by using biological treatment and produce biogas.

Key figures of the sewage treatment plant are listed in the Table 1-1.

Table 1-1: Key figures of the wastewater treatment plant at VEAS [4].

The Treatment Plant		
Main sewer tunnel	Length	42.3 km
	Storage volume at 4 m^3/s	187 000 m^3
	Storage volume at 7.5 m^3/s	137 000 m^3
Transportation time	From Majorstua (Oslo) to Slemmestad	approx. 5 hours
Inlet pumps	8 in total, whereof 2 variable-speed	
	Capacity with 2m level on suction side	8 x 920 l/s = 7 360 l/s
	Capacity with 10m level on suction side	8 x1050 l/s = 8 400 l/s
Screens	4 with bar spacing of	3 mm
Aerated grit chamber	4 with a total volume of	3 320 m^3
Flocculation	Takes place in the aerated grit chamber	
Sedimentation tanks*	2 at 15.7m x 91.2m x 3.6m deep	10 300 m^3
Sedimentation tanks**	6 at 15.7m x 17.7m x 10.5m deep	17 500 m^3
Nitrification filters**	24 of 87 m^2, 4m depth of filter media	
Denitrification filters**	24 of 65 m^2, 3m depth of filter media	
Sludge thickening	2 rotary drum thickeners 1 storage thickener of 1 500 m^3	
Sludge dewatering	4 combined filter presses and thermal vacuum dryers, 140 chambers, 25 mm recess, plate size	1.5 m x 1.5 m
Deep sea discharge	4 diffusers, depth	40 - 55 m
Distribution depth		25-35 m

1.3 Objectives

The main objective of this thesis is to analyze the flow fields in one of the sedimentation tank which is currently operate in VEAS and this can be known as a beginning of the long term project. This report will provide the following main features;

- Make a literature review on sedimentation tanks in sewage treatment plants and solid – liquid flow in tanks.
- Make computational mesh of one of the sedimentation tanks at VEAS.
- Simulate the flow in the sedimentation tank with FLUENT.
- Investigate how the boundary conditions influence the flow field.
- Analyze data and discuss the behavior of the flow field.
- Provide recommendation for future work.

1.4 Report Outline

A brief introduction to the main theme of this thesis is provided at the beginning of this report. Literature review of the sedimentation process, factors affecting the sedimentation process and the flow fields inside the sedimentation tanks are presented in chapter 2. Sedimentation tank description which going to simulate is discussed in first section of the chapter 3 and the generation of geometry and computational mesh is presented in following sections of the chapter 3. In Chapter 4, development of CFD model is presented with the data, assumptions and model used during these simulations. Results and discussions are presented in the chapter 5 and the conclusions and recommendations for future work are presented in chapter 6.

References that used during this report writing are presented at the end of report and the appendixes are available after the references list. Gambit geometry, mesh and the FLUENT case files corresponding to the different cases are also attached with this report.

2 Literature Review

Literature review is an essential fragment of a project to gain knowledge and identify the research methodologies that related to the project which help to focus and refine the research problems by articulating the knowledge gap. Furthermore, the literature review will avoid the reproducing of technical errors and replicating existing knowledge [5]. Therefore the literature review was carried out for this project and the findings will be presented in this chapter. Process of the sedimentation will be described in the first section of this chapter and the following section will present the factors affecting the sedimentation process. Finally, the flow patterns inside the sewage sedimentation tank from literature are presented.

2.1 Sedimentation Process

Sedimentation is the process of separating suspended particles from the wastewater which is heavier than the fluid by using gravity effect [6]. This seemingly simple process proved as the bottle neck process in the many wastewater treatment plants and moreover better efficiencies are required in sedimentation process in order to obtain the specified efficiencies in whole treatment plant.

Four types of settling process can be occurred in the sedimentation tank depending on the particle size and the interactions between particles.

1. Discrete particle settling – Particles settle individually without interaction with neighboring particles and this scenario is happen when the solid concentration is low compared to the fluid concentration. Removal of sand particles are typical example for this settling process.
2. Flocculent settling – First stage of the settling is occurred due to the individual settling and afterwards particles will aggregate and this flocculation causes the particles to increase in mass and settle at a faster settling rate.
3. Hindered settling – This settling process is taken place due to the inter-particle forces and this forces are sufficient enough to hinder the settling of neighboring particles in this settling zone. Furthermore individual particles are remained in fixed position with respect to each other and due to that the mass of particles tends to settle as a unit.
4. Compression settling – The particle concentration is so high in this zone and due to that the particles at one level are mechanically influenced by the particles on the lower level. Therefore the sedimentation can only occur through compaction of the structure and the sedimentation velocity is very low at this zone [7].

Figure 2-1 illustrates these different settling regimes and the variation of the settling velocity in the sedimentation tank [8].

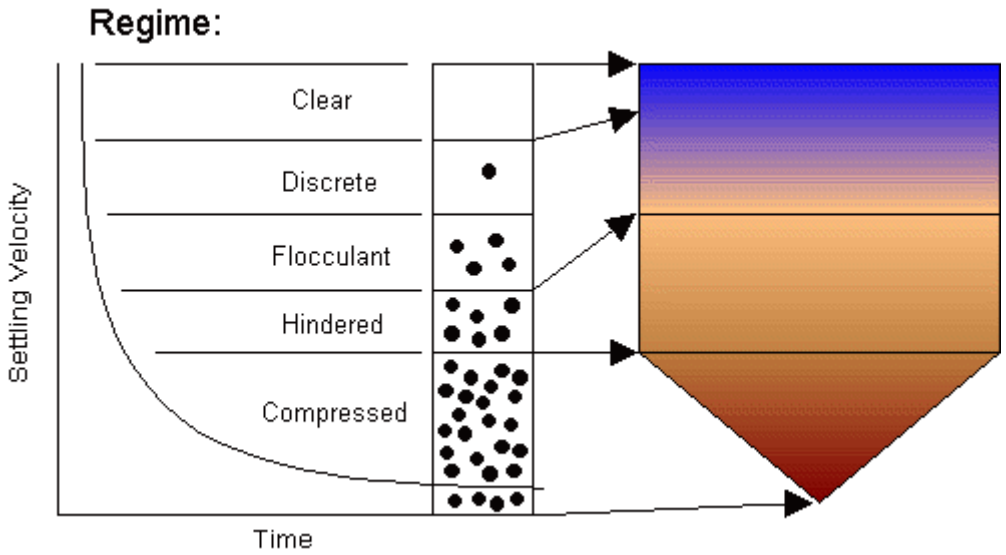

Figure 2-1: Different settling regimes and the variation of the settling velocity in the sedimentation tank [8].

2.2 Factors Affecting the Sedimentation Process

Sedimentation process of wastewater is affected by many factors and some of the more common types of factors to consider are;

- Characteristics of the fluid
- Characteristics of the solids
- Physical characteristics of the design
- Miscellaneous effects

2.2.1 Characteristics of the Fluids

Specific gravity and the viscosity of the fluid are the most significant parameters of the fluid that affect the sedimentation process. Both these parameters are affecting by the temperature. It is obvious that the particles in the fluids with lower specific gravity will be settled quickly due to the high density difference between the fluid and solid. Moreover specific gravity of the fluid will be decreased with the increasing temperature. Furthermore it is evident that the suspended particles, particularly more lighter and small particles settled down slowly through a high viscous fluid compare to the low viscous fluids due to the flow resistance for the particles are higher in high viscous fluids. Viscosity property of the fluid is also decreasing with increasing temperature as same as the specific gravity [9].

2.2.2 Characteristics of the Solids

Size, specific gravity, shape and concentration of the particles, flocculation, coagulation and coalescence are the main characteristics of the solid particles that affect to the efficient

sedimentation. It is obvious that larger particles with a given specific gravity have the high settling rate than the smaller particles due to the higher weight. Therefore to remove small particles and colloidal materials, chemicals are added to wastewater to initiate the coagulation and flocculation within particles.

Moreover it is apparent that with a given size of particles, higher the specific gravity of the particle the more rapidly it will settle down in the fluid. This causes the sand or silt can be removed easily from the wastewater because of the higher densities compared to the water. The shape of the particle is affecting to the settling rate by its effect on skin friction. Since the volume and hence the weight of the particle varies with the cube of the diameter and the surface area of the particle varies with the square of the diameter. Therefore the surface area per unit weight will have the inverse correlation with the diameter. In other words, small particle will have high skin friction while large particles have smaller skin friction [9]. Spherical solid particles have the smallest surface area per weight for a given size when comparing with other shapes and due to the round particles will settle down easily compared to particles that has ragged or irregular edges [10].

Concentration of the solid particles in the fluid affects the efficiency of the sedimentation. This is mainly due to the cohesion of the particles and their joining together into larger ones because of the higher solid particle concentration and these formulated flocs will lead the particles into the sedimentation with higher efficiencies. Additionally this action is a combined effect of the particle size and the flocculation. The effluent which carrying the heavier concentration of particles have the higher density when comparing the partially settled effluent in the sedimentation tank. It has been frequently observed that raw water carrying a high concentration of particles descends to the bottom of the tank and continues along until the part of the particles are settled and afterwards the water is dispersed with the partially settled water above.

Other main characteristics of solid are flocculation, coagulation and coalescence and flocculation is referred when the particles are joined into larger ones with naturally. Coagulation and coalescence is used when the large particles are formulated by means of chemicals. Formulation of the large flocs will increase the settling speed in the sedimentation tank as discussed in previous paragraphs. Moreover all particles have electrical charge and the particles have same electrical charge are tend to repel each other. The flocs formulation which is increasing the settling rate is disturbed by this repelling action [9].

2.2.3 Physical Characteristics of the Design

Retention time is the one of main physical characteristic that affects the efficiency of the sedimentation. It is obvious that the greater the retention time, greater the reduction of solid from the effluent. However the increasing retention time is not a good practice for all the application especially in sewage treatment as the increased retention time can lead the effluent

to degradation and the resulting gas buoyance of particles. Additionally it is proved that the actual retention time of the effluent in the sedimentation tanks is less than the designed retention time. Short circuit the flows, defective inlet and outlet construction, temperature effect or other causes are listed as the main reasons to occur this scenario.

The velocity of the flow in the sedimentation tank is one of the main factors that affecting the sedimentation efficiency and it is understandable that the higher velocities will reduce the solid deposition. The effect of the velocity of the flow depends on the size and specific gravity of the solid particles and also the dimensions of the sedimentation tank.

The factors of depth and ratio of length and depth of sedimentation tank are also affecting the sedimentation efficiency to some extent. Short circuiting and dead spaces in the sedimentation tank can directly affecting by this factor. Moreover it is been proven that the long shallow tanks reduce the effects of inlet and outlets and generally to promote conditions more favorably to efficient sedimentation. Additionally inlet and outlet positions are also the factors that affecting the effective sedimentation. When designing the inlet and outlets of the sedimentation tank, it is desired to produce conditions of uniform flow across substantially an entire vertical cross section and prevent partially settled effluent from being mixed with the unsettled incoming effluent. The most common outlet design that used in the sedimentation tank is overflow weirs.

Additional to the depth and the length of the sedimentation tank, there are some features that should be considered when designing the sedimentation tank. The tank with larger ratio of length to width is preferable to minimize the inlets and outlets effects and produce the uniform flow inside the sedimentation tank. Because of the economic construction and the bottom scraping mechanism typical sedimentation tanks are designed with uniform geometric shapes.

One of the remaining physical characteristic in the sedimentation tank is baffles and properly designed baffles can contribute to the increasing efficiency of the sedimentation tank. Baffles can provide several advantages to the settling tank such as;

- Reduce the effect of eddies at the inlet end of tank
- Produce the more uniform flow inside the tank and prevent “dead spaces”
- Prevent unsettled influent from mixing with partially settle liquid [9]

2.2.4 Miscellaneous Effects

Currents caused by the wind, eddies and difference of temperature are the great important factor that affecting the efficiency of the sedimentation. The settled and unsettled wastewater at the surface of the tank mixed due to the wind effect and carrying the inlet influent to the outlets in a short time which lead to the low efficiencies in the sedimentation tank. Eddies caused by the obstacles in the tank such as columns, scraping mechanism are serving low efficiency sedimentation when the velocity created by such actions is higher than the

hydraulic value of the particles. Furthermore these eddies act more important role in the case of high velocity and flows counters to the direction of influent travelling which lead the huge reduction in sedimentation efficiency. When the air and the wastewater temperature are quite different short circuiting, stratification, mixing may occur. As commonly observed when the air temperature is higher than the wastewater temperature, the effluent is tend to flow along the bottom of the tank because of the difference in specific gravity.

Another factor affecting the sedimentation is bottom reaction. Velocity of the liquid at the bottom is considerably low when comparing the liquid short distance above the bottom because of the wall friction at the bottom of the tank. So this effect leads to the lifting action on the particle which approaching the bottom of the tank [9].

2.3 Flow Field in the Sedimentation Tanks

Flow field inside the sedimentation tank is a wide topic and it depends on the factors described in the above section. Literature review on the flow patterns inside the sedimentation tanks which treat sewage for two cases are going to briefly describe in this section.

Matthieu *et al.* (2008) investigate the flow patterns inside the rectangular sewage treatment sedimentation tank by varying the depth of the water. When the water depth is high, overflow from the tank is occur and the flow fields consist of two circulations as shown on (a) in Figure 2-2. Furthermore, when the water depth is low, there is no overflow is take place and a large circulation dominates the flow field which present in the (b) in Figure 2-2 [11].

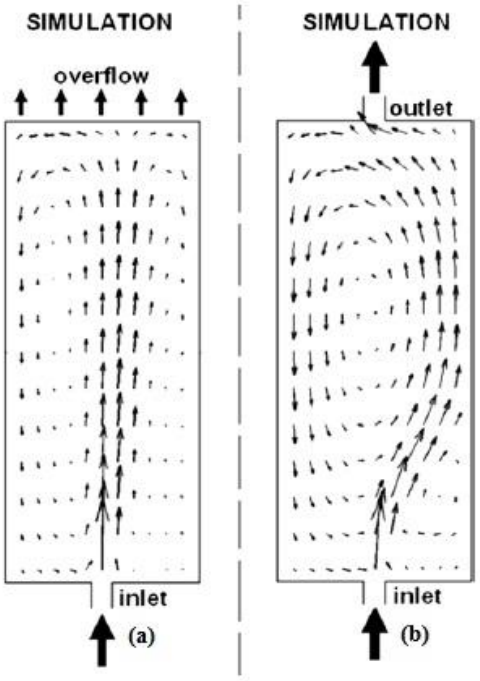

Figure 2-2: Simulated velocity fields.

Long Fan *et al.* (2007) demonstrated the flow patterns inside the sedimentation tank for urban wastewater. Rectangular tank was used to observe the flow fields and the inlet was placed the

center of tank and the outlets from tank were fitted to the ends of the tank. Influence of the baffle height was also studied. Figure 2-3 demonstrate the solid distribution in the center of the tank. Circulation loop was appeared below the entrance and however the flow is relatively simple near the outlets [12].

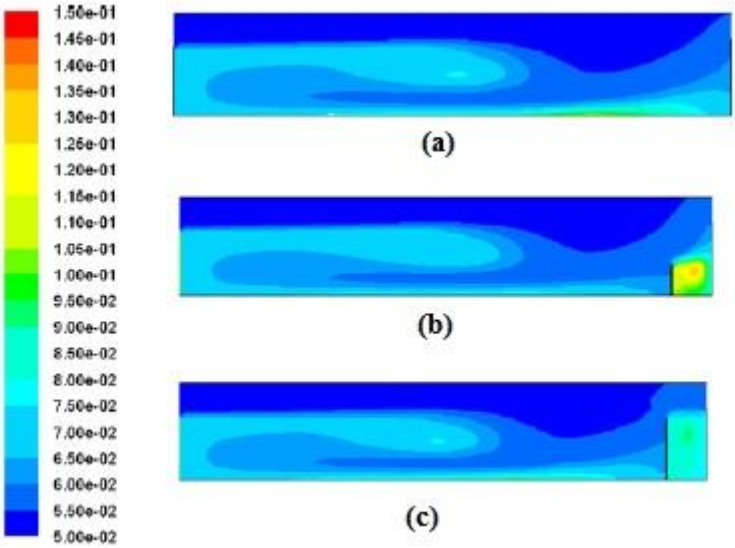

Figure 2-3: Solid distribution in the center of the tank. a) without baffle; b) h = 1.5 m; c)h = 3m

3 Sedimentation Tank Description

The flow field inside the sedimentation tank is a crucial factor on efficiency of the sedimentation process. One of the sedimentation tanks in VEAS is studied during this thesis as described in Chapter 1 and the flow field in these tanks can be very complicated and it is very difficult to measure velocities in such a large tank. Therefore it is important to have an overview of geometry of the sedimentation tank which is going to be simulated. The first part of this chapter is regarding the geometry of the sedimentation tank and the following subchapters will discuss the generation of geometry and the computational mesh by using Gambit.

3.1 Geometry

As discussed in the chapter 1, eight sedimentation tanks are used in the sewage treatment plant in VEAS and one sedimentation tank was selected from these tanks for this study. Figure 3-1 and Figure 3-2 show the schematic diagrams of the selected sedimentation tank.

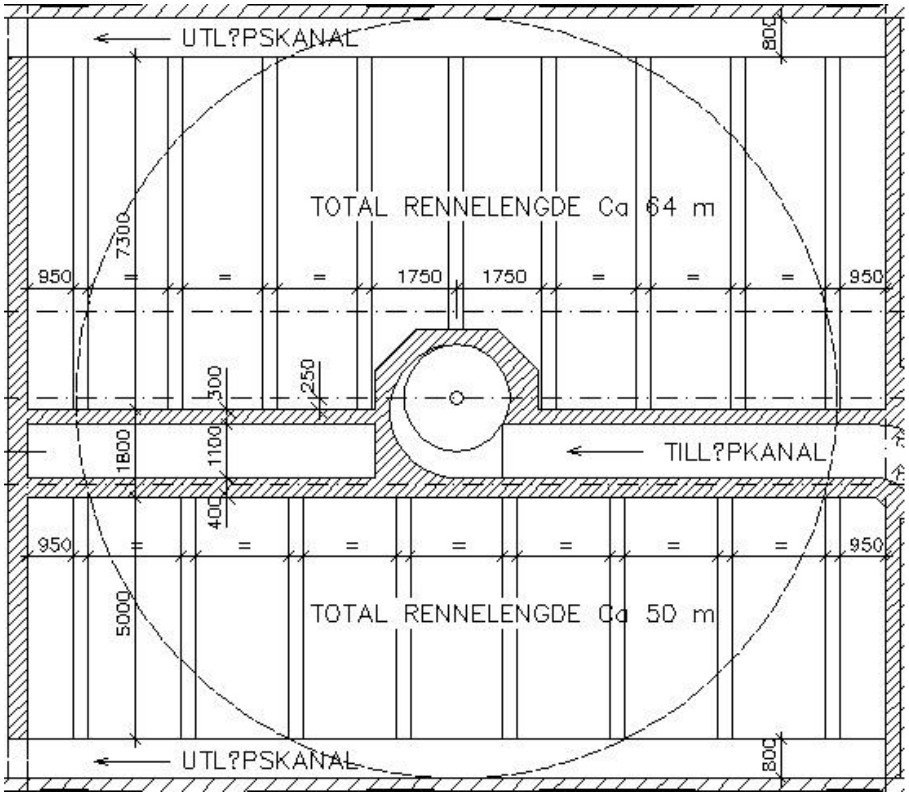

Figure 3-1:Plan view of the selected sedimentation tank at VEAS.

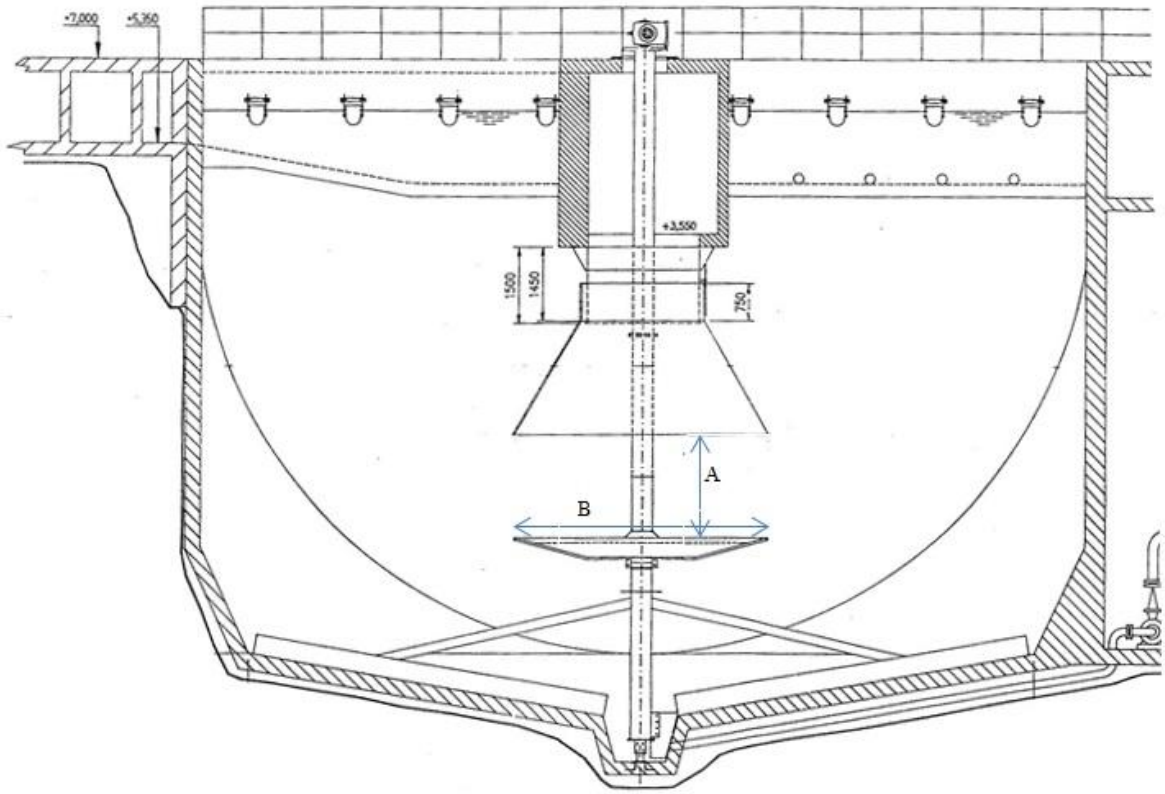

Figure 3-2: Side view of the selected sedimentation tank at VEAS. (A = 2.55m; B = 4.2 m)

Geometry of the sedimentation tank is a complex geometry and it occupied with two main components which help to increase the sedimentation efficiency.

- Middle part – This can be described as the inlet zone of the sedimentation tank and it introduces sewage into the bottom section of the sedimentation tank. Middle part of the sedimentation tank shows in Figure 3-2.
- Lamella part – Direction of the flow is changed by using this part and the detailed drawing of the Lamella part is attached in Appendix D. Lamella part consists set of parallel longitudinal profiles that are fitted in the tank under a certain rising angle and the Figure 3-3 shows the flow pattern trough the Lamella part. Each plate functions as a miniature sedimentation basin which helps to increase the settling area [13]. This type of sedimentation tanks is several times more efficient compared to simple sedimentation with a flow-through system and Lamella separators can reduce space requirements by up to 90% compared with a settling pond [14].

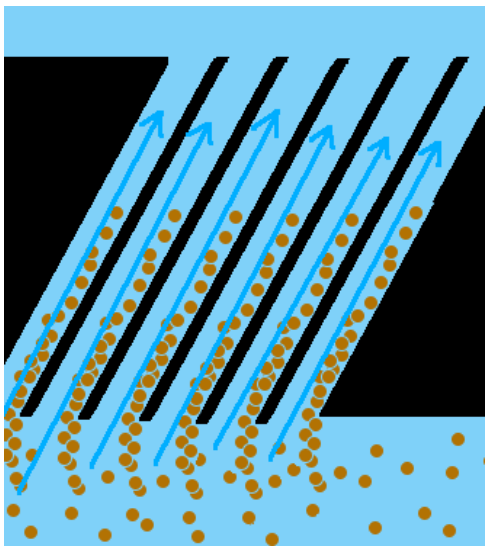

Figure 3-3: Flow fields through the Lamella part [13].

3.2 Geometry Generation

Gambit 2.4.6 was used to create computational geometry of the sedimentation tank. Due to the complexity of the geometry, the inlet zone was drawn separately and this part is shown in Figure 3-4. After completion of the tank geometry of the sedimentation tank, both tank and the inlet parts were merged to get the complete geometry. Afterward, the Lamella part was created in the geometry of the sedimentation tank. Figure 3-5, Figure 3-6 and Figure 3-7 illustrate the computational geometry that created using Gambit. Additionally, inlet, outlets and walls were specified as boundary types. Inlet was mentioned as the velocity inlet and the outlets of the sedimentation tank were specified as pressure outlets.

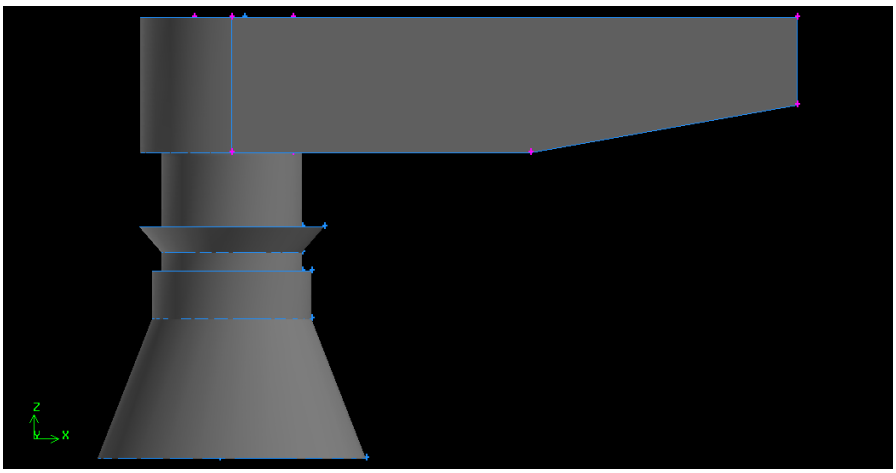

Figure 3-4: Inlet zone geometry

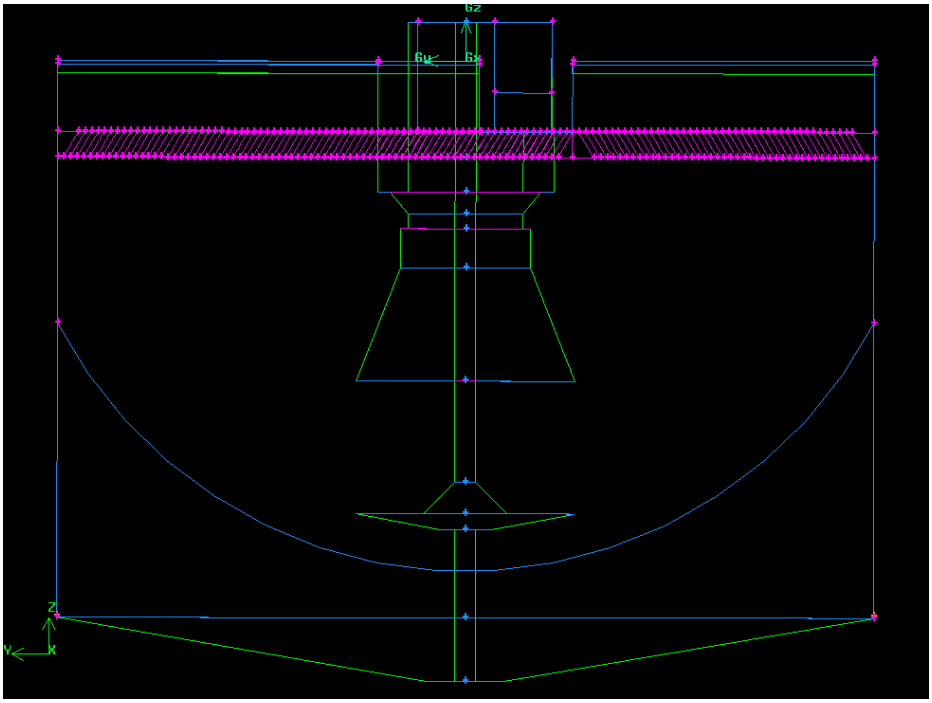

Figure 3-5:Wireframe geometry of the sedimentation tank.

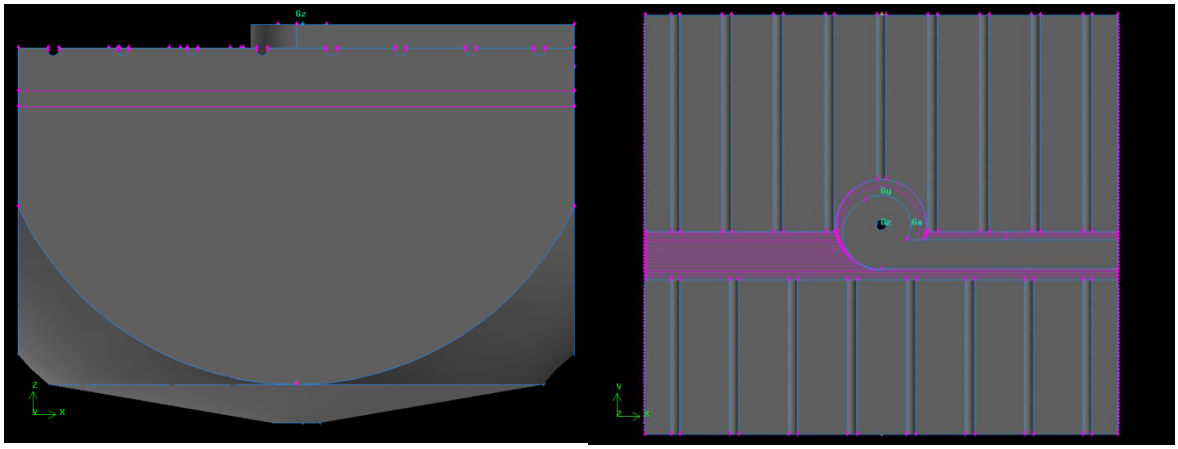

Figure 3-6: Side and plan veiws of the geometry

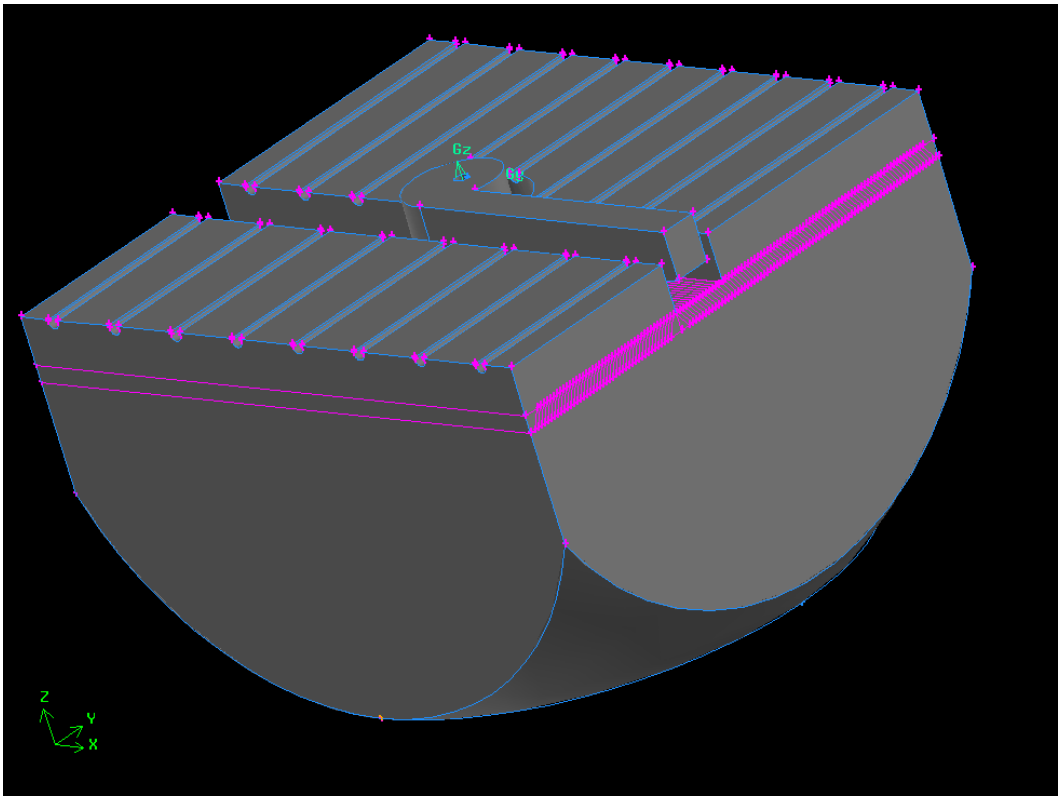

Figure 3-7: Computational geometry

3.3 Mesh Generation

Generating a good mesh is the most critical fragment of the Computational Fluid Dynamics (CFD) simulations and the creating good enough mesh is a hard job for the complex geometries. Generating proper mesh is a must in CFD simulations since the good mesh helps the CFD solver converge to the correct answer while minimizing the computer resources expended.

During the generation of computational mesh, some faces were meshed prior to the volume meshing in order to achieve a quality mesh. Those faces included the central axis of the tank and the each and every plate faces of the lamella part. Moreover, the following parameters are used to generate the face meshes that discussed above. Geometry of the sedimentation tank after meshing the faces is illustrated in the Figure 3-8.

- Elements – Tri
- Types – Pave
- Spacing – 0.2 m

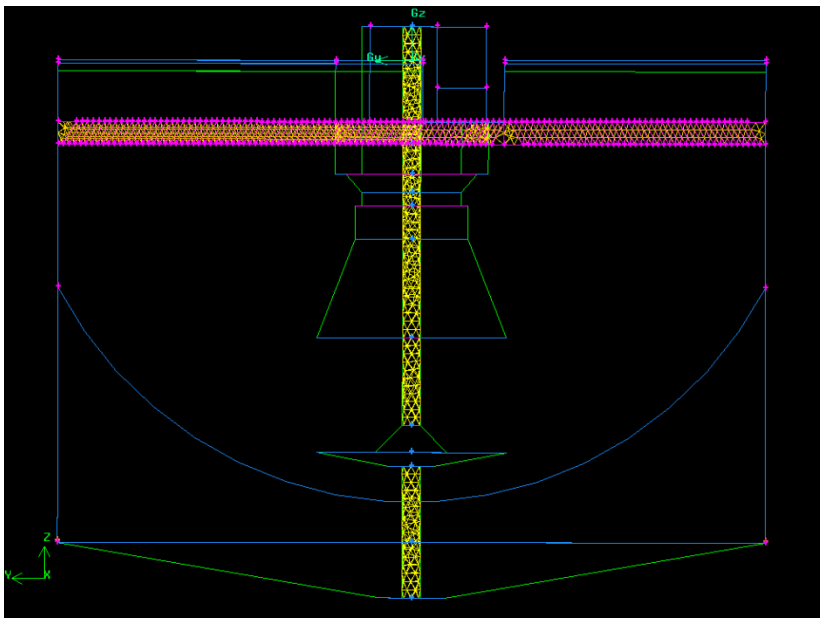

Figure 3-8:Sedimentation tank after meshing the faces.

Afterward, volume meshing was done and the volumes at Lamella part were meshed as the first step. Then the other volumes of the sedimentation tank were meshed one by one. The parameters used to mesh the volumes are as follows. Figure 3-9 shows the fully meshed geometry of the sedimentation tank.

- Elements – Tet/Hybrid
- Types – Tgrid
- Spacing – 0.3 m

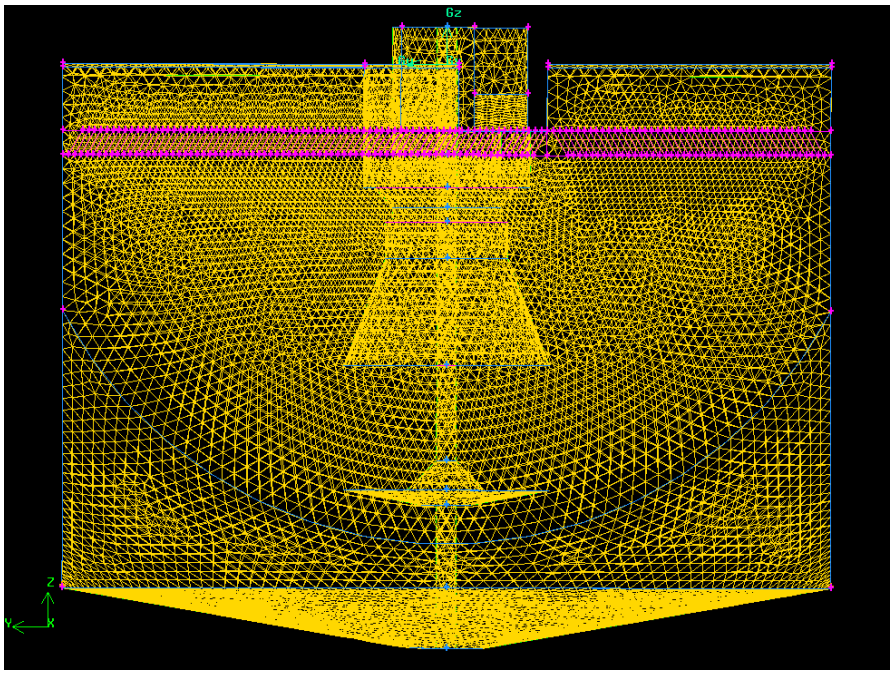

Figure 3-9: Computational mesh of the sedimentation tank.

4 CFD Model Development

In recent years, Computational Fluid Dynamics (CFD) has become an essential predictive tool for gathering information to be used for design and optimization for fluid systems [15]. Moreover, there are several unique advantages of CFD over the experimental approaches to fluid system design.

- Considerable reduction of lead time and the cost
- Ability to study the systems which difficult or impossible to perform experiments
- Ability to evaluate the systems under the hazardous conditions such as accident scenarios
- Can obtain the unlimited amount of results which practically impossible to gain [16]

ANSYS FLUENT 13.0 software was used in this study in order to perform the CFD simulations and this software contains the broad physical modeling capabilities needed to model flow, turbulence, heat transfer, and reactions. Today, thousands of companies around the world use the FLUENT software as an integral part of their design and optimization phases of product development. Advanced solver technology in FLUENT provides fast, accurate CFD results, flexible moving and deforming meshes and superior parallel scalability. Benefits can gain from FLUENT include the extensive range of physical modeling capabilities and fast, accurate CFD results and FLUENT has become the one of the most comprehensive software packages for CFD modeling available in the world today [17].

During the CFD simulations, both multiphase and turbulent models were used since the sedimentation tank has a complex geometry and the flow patterns. Following sections will describe about the multiphase and turbulent models which consist in FLUENT. After that, data, parameters and assumptions made during simulations and the cases that are going to simulate are presented.

4.1 Multiphase Models

The term multiphase flow was coined by the late Prof. Soo of the University of Illinois in 1965 and includes fluid dynamics motion of various phases. In the multiphase flow particle or secondary phase composition can be solid, liquid or gas while using of liquid or gas as primary phase [15]. Many flow patterns that occur in the nature and technology belong to the multiphase flow and multiphase flow can be divided in to four categories based on the flow regimes. Figure 4-1 illustrates the different flow patterns occur in these flow regimes.

1. Gas – liquid or liquid – liquid flow
    - Bubbly flow: discrete gaseous or fluid bubbles in a continuous fluid
    - Droplet flow: discrete fluid droplets in a continuous gas

- Slug flow: large bubbles in a continuous fluid
- Stratified/free-surface flow: immiscible fluids separated by a clearly-defined interface

2. Gas – solid flows
    - Particle-laden flow: discrete solid particles in a continuous gas
    - Pneumatic transport: dune flow, slug flow, packed beds, and homogeneous flow are the typical flow patterns belong to this regime and these flow pattern depends on factors such as solid loading, Reynolds numbers, and particle properties
    - Fluidized beds – Gas is introduced to the vertical cylindrical column which contain particles and particles are suspended in the gas

3. Liquid – solid flows
    - Slurry flow: transport of particles in liquids. The stroke number of the slurry flows is normally less than 1 and the flow become liquid – solid fluidization when the stroke number is larger than 1.
    - Hydrotransport: densely-distributed solid particles in a continuous liquid
    - Sedimentation

4. Three phase flow – combination of above flow regimes [18]

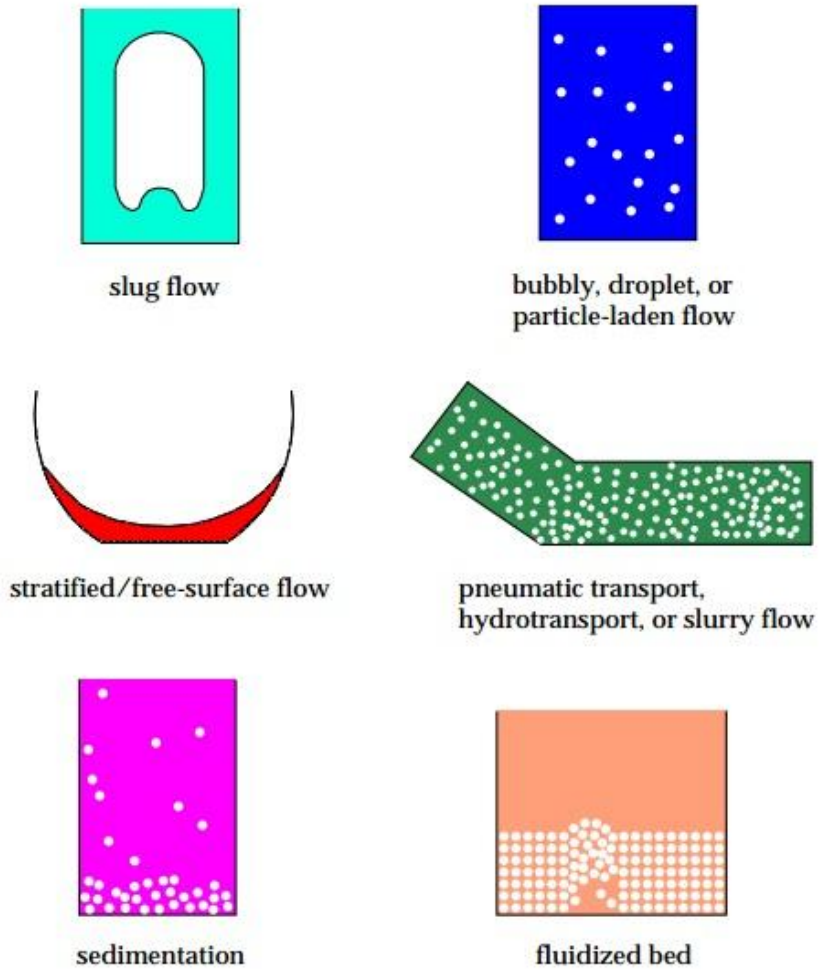

Figure 4-1: Different flow patterns occur in flow regimes [18]

There are two approaches for the numerical calculation of multiphase flow in CFD simulations.

- Euler-Lagrange approach
- Euler-Euler approach

4.1.1 Euler-Lagrange Approach

In this model, properties of continuous fluid phase is solved by using time-average Navier-Stokes equations while the dispersed phase is solved by tracking a large number of particles, bubbles, or droplets through the calculated flow field [19]. Most important assumption that made in this model is that the volume fraction of the dispersed phase is low, even though high mass loading is acceptable [18].

4.1.2 Euler-Euler Approach

In the Euler-Euler approach the different phases in the simulation are treated as the continuous phases [20]. The concept of phasic volume fraction is introduced in this approach

as the volume of a one phase cannot be occupied by the other phases. These volume fractions of the phases are assumed to be continuous functions of space and time and the sum of the volume fraction is equal to one. Set of equations are derived from the conservation equations for each phase.

Three different Euler – Euler multiphase models are available in the FLUENT [18].

- The VOF model
- The mixture model
- The Eulerian model

4.1.2.1 The VOF Model

Surface-tracking technique is applied in the VOF model and this model is designed for two or more immiscible fluids where the position of the interface between the fluids is of interest. A single set of momentum equations is shared by the fluids in this model and the volume fraction of each of the fluids in each computational cell is tracked throughout the domain [18].

4.1.2.2 The Mixture Model

The mixture model can be used for two or more phases and these phases may contain fluid or particles. The mixture momentum equation is solved in the mixture model and prescribes relative velocities to describe the dispersed phases. Mixture model can be applied for the particle-laden flows with low loading, bubbly flows and cyclone separators. Furthermore, mixture model can also be used without relative velocities for the dispersed phases to model homogeneous multiphase flow [18].

4.1.2.3 The Eulerian Model

The most complex multiphase model in the FLUENT is Eulerian model and it solves a set of momentum and the continuity equation for each and every phases. Coupling is achieved through the pressure and interphase exchange coefficients and the manner of coupling handling is depend on the type of phases involved in the simulation. The properties of the granular flow which contain the fluid and solid phases are calculated by using kinetic theory. Momentum exchange between the phases is also dependent upon the type of mixture being modeled. Large number of secondary phases can be simulated by using the Eulerian model and the number of secondary phases is only limited by the memory requirement and the convergence behavior [18].

The Eulerian model is recommended to observe the flow patterns in the sedimentation and this model is used as the multiphase flow model during this study. Moreover Eulerian model has some limitations also.

- The Reynolds Stress turbulence model is not available on a per phase basis.
- Particle tracking interacts only with the primary phase.

- Streamwise periodic flow with specified mass flow rate cannot be modeled when the Eulerian model is used
- Inviscid flow is not allowed.
- Melting and solidification are not allowed [18].

4.2 Turbulent Models

Main characteristic of the turbulent flows is the fluctuated velocity field. These fluctuated velocities will affect the transport properties such as momentum, energy and species concentration and cause the fluctuation in these properties as well. Simulate and calculate these fluctuations directly are expensive since these fluctuations can be in small scales with high frequency. As a remedy for this problem time averaged, ensemble – average or manipulated equations to remove small scales are used in simulations in order to decrease the computational expenses [18].

There are three main type of turbulent models are available in FLUENT while calculating the simulations with multiphase models.

1. k – epsilon (ε) method
    - Standard
    - RNG
    - Realizable
2. k – omega (ω) model
    - Standard
    - SST
3. Reynolds stresses
    - Linear pressure – strain
    - Quadratic pressure – strain

Standard k – ε model was used in this study to do simulation in the sedimentation tank and the following subchapters are used to discuss the properties and characteristics of these turbulent models.

4.2.1 k – Epsilon (ε) Method

All three model of the k – ε method have the similar forms with transport equations for k and ε and the main difference of these models are as follows [18].

- The method of calculating turbulent viscosity
- The turbulent Prandtl numbers governing the turbulent diffusion of k and ε
- The generation and destruction terms in the k equation

4.2.1.1 Standard k – ε Model

The standard k – ε model is proposed by Launder and Spalding and this model is using a lot to compute the practical engineering flow calculation since the time it was proposed. Moreover, this is one of the simplest and complete turbulent models which determine the turbulent velocity and the length scales by solving the two separate transport equations. The standard k – ε model can be used for a wide range of turbulent flows and the advantages of this model are robustness, economy and reasonable accuracy. The standard k – ε model is a semi-empirical model based on model transport equations for the turbulence kinetic energy (k) and its dissipation rate (ε) [18].

4.2.1.2 RNG k – ε Model

A mathematical technique called the "renormalization group" (RNG) is used to derive the RNG k – ε model from the instantaneous Navier-Stokes equations. This model is similar to the standard k – ε model, but includes following modifications to avoid the weaknesses of standard k – ε model.

- The RNG model has an additional term in its ε equation that significantly improves the accuracy for rapidly strained flows.
- The effect of swirl on turbulence is included in the RNG model, enhancing accuracy for swirling flows.
- The RNG theory provides an analytical formula for turbulent Prandtl numbers, while the standard k – ε model uses user-specified, constant values.
- While the standard k – ε model is a high-Reynolds-number model, the RNG theory provides an analytically derived differential formula for effective viscosity that accounts for low Reynolds number effects [18].

4.2.1.3 Realizable k – ε Model

The realizable k – ε model is satisfied certain mathematical constraints on the Reynolds stresses, consistent with the physics of turbulent flows and due to that the term “realizable” is given to this model. Neither the standard k – ε model nor the RNG k – ε model is realizable. Furthermore, the realizable k – ε model differ from the standard k – ε model in two important ways;

- The realizable k – ε model contains a new formulation for the turbulent viscosity.
- A new transport equation for the dissipation rate (ε) has been derived from an exact equation for the transport of the mean-square vorticity fluctuation [18].

4.2.2 k – Omega (ω) Model

The k – ω model is one of the most commonly used turbulence models. It is a two equation model, which includes two extra transport equations to represent the turbulent properties of the flow [18].

4.2.2.1 Standard k –ω Model

The Wilcox k – ω model is the based model for the standard k – ω model in the FLUENT, which incorporate modifications for low-Reynolds-number effects, compressibility and shear flow spreading. The standard k – ω model is based on the transport equations for the turbulence kinetic energy (k) and the specific dissipation rate (ω) and this is an empirical model [18].

4.2.2.2 SST k –ω Model

SST refers to the "Shear Stress Transport" and it is similar to the Standard k – ω model with transport equations for k and ω. Main modifications in the SST k – ω model when comparing with the standard k – ω model are listed below.

- The standard k – ω model and the transformed k – ε model are both multiplied by a blending function and both models are added together. The blending function is designed to be one in the near-wall region, which activates the standard k – ω model, and zero away from the surface, which activates the transformed k – ε model.
- The SST model incorporates a damped cross-diffusion derivative term in the equation.
- The definition of the turbulent viscosity is modified to account for the transport of the turbulent shear stress.
- The modeling constants are different.

The SST k – ω model is more accurate and reliable for a wider range of flows than the standard k – ω due to these modified features [18].

4.2.3 Reynolds Stress Models (RSM)

The Reynolds stress model is the most complicated model that offered by FLUENT and this RSM solves the Reynolds-averaged Navier-Stokes equations by solving transport equations for the Reynolds stresses, together with an equation for the dissipation rate. Due to that, seven additional transport equations are solved in FLUENT in 3D simulations. Moreover, the RSM predicts the accurate flow patterns for complex flows as it accounts the effect of streamline curvature, swirl, rotation, and rapid changes in strain rate in a more rigorous manner. The RSM computation is higher expensive than the simpler model due to the complexity and this model is not always yield the results. However, use of the RSM is a must when the flow features of interest are the result of anisotropy in the Reynolds stresses [18].

4.3 Simulation Data and Parameters

Data and parameters used in FLUENT simulations are listed below.

Phases:

- Liquid phase of the wastewater is assumed as water.
- Density of the solid phase – 1100 kg/m^3
- Solid particle size range – 250 to 340 μm

Models:

- Multiphase – Eulerian model
- Viscous model – Standard k – ε model

Velocity inlet boundary conditions:

- Volume fraction of the solid particles at the sedimentation tank inlet – 0.01%
- Flow rate – 0.5 to 1 m^3/s
- Inlet velocity – 0.35 to 0.67 ms^{-1}
- Turbulent intensity of the inlet of sedimentation tank – 10 %
- Hydraulic diameter – 1.2177 m
- Initial gauge pressure – 0 Pa

Pressure outlet boundary conditions:

- Turbulent intensity of the outlets of sedimentation tank – 5 %
- Length scale of the outlets of sedimentation tank – 0.35 m
- Back flow volume fractions for solid phase – 0

Operating conditions:

- Operational pressure – 101325 Pa
- Gravitational Acceleration – -9.81 ms^{-2}

Solution methods:

- Pressure – Velocity Coupling: Phase coupled simple
- Gradient – Least squares cell based
- Momentum – first order upwind
- Volume fraction – First order upwind
- Turbulent kinetic energy – First order upwind
- Turbulent dissipation rate – First order upwind

- Transient formulation – First order implicit

Calculations:

Hydraulic diameter calculation of the inlet of the sedimentation tank

$$HD = \frac{4A}{P} \qquad 4-1$$

Where;

HD – Hydraulic Diameter

A – Area of the inlet

P – Perimeter of the inlet

$$HD = \frac{4 * (1.1 * 1.36364)}{2 * (1.1 + 1.36364)} = 1.2177\ m$$

4.4 Cases

As discussed in chapter 4.3, effluent loading of the sedimentation tank can be varied from 0.5 – 1 m^3/s. Effluent loading is high at the end of winter because of the melting snow and in the raining periods. Due to these two different loadings, two cases are studied in this thesis depending on the inlet velocities. Moreover, screening process is occupied before the sedimentation tank and due to that the particle sizes are normally laying in the range of 340 – 250 μm as discussed in the above section. Six cases were studied during this thesis depending on the flow rate and the solid particle diameters and Table 4-1 shows the summery of these cases.

Table 4-1: Summery of the cases

Case	Flow Rate [m^3/h]	Particle Diameter [μm]
1	0.5	250
2	0.5	100
3	0.5	50
4	1	340
5	1	250
6	1	100

Sludge removal from the sedimentation tank is omitted while doing the simulation as it occurs intermittently over long intervals and it assumed that the influence of this sludge removal is very low compared to the flow behavior in the tank.

Computers with Intel® Core™ i5-2500 CPU @ 3.30 GHz 3.30 GHz processors, 8.00 GB memory and Windows 7 Enterprise Edition 64 bit operating system were used to run the simulations. Average simulation times for different cases were in the range of 2 – 3 days to get about 13 hour of flow time.

5 Results and Discussion

Overview of the results that obtained from the FLUENT simulations will be discussed in this chapter. Inlet zone flow behavior will be discussed in the first part of this chapter while the second part describes flow patterns inside the sedimentation tank. Velocity profiles inside the sedimentation tank will be presented in next section. Finally, the detailed discussions of case studies are presented.

5.1 Inlet Zone Flow Behavior

Flow behavior of the inlet zone was studied separately in order to get a better knowledge of the sedimentation process inside the tank. Velocity vector profile of the inlet zone is presented on Figure 5-1 and by analyzing this figure, it can be understood that the velocity magnitude of the inlet zone is decreasing from inlet to outlet. Furthermore, the velocity vector profiles in the inlet zone at different planes are going to be discussed in this chapter and Figure 5-2 will provide a better understanding of the places of planes that are going to be evaluated. Inlet flow behavior of the inlet zone can be understood by aid of plane A in Figure 5-3 and it clearly shows that the whole flow currents are rotating around the central axis of the inlet zone without short circuiting. Cross sections of two perpendicular planes of inlet zone are presented in planes B and C in Figure 5-3 and it demonstrate the complex flow behavior at the inlet zone. Velocity vectors tend to rotate around the axis at the top of the inlet zone and after that the flow tends to flow along the axis. Plane D can be used to describe the velocity vectors at the outlet of the inlet zone and by analyzing the velocity vectors at plane D; it can be understood that the velocity magnitude is decreasing from middle to the outer edge of plane D.

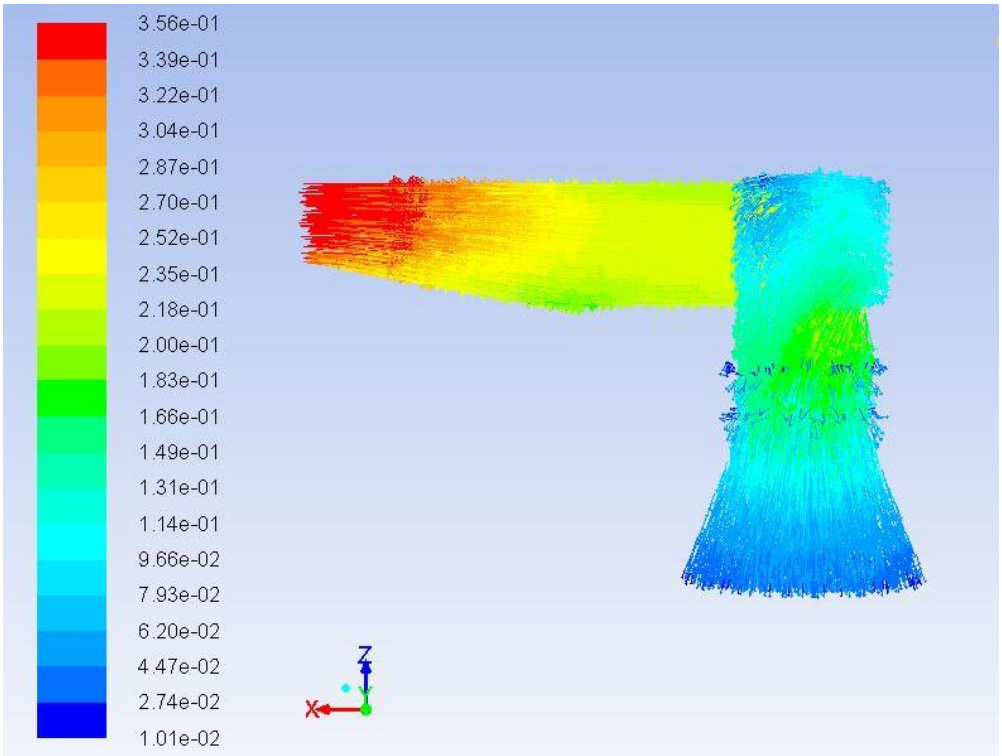

Figure 5-1:Velocity vector profile of the inlet zone.

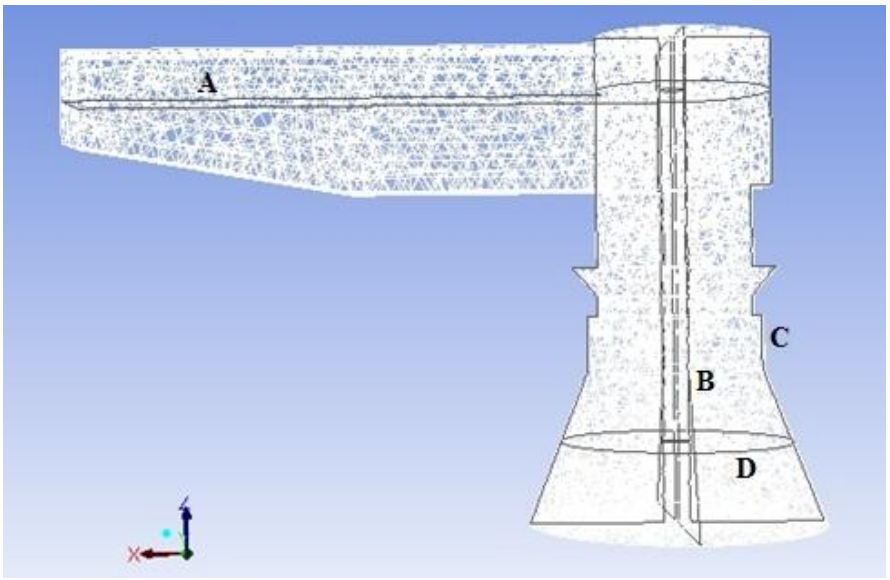

Figure 5-2: Planes of the inlet zone.

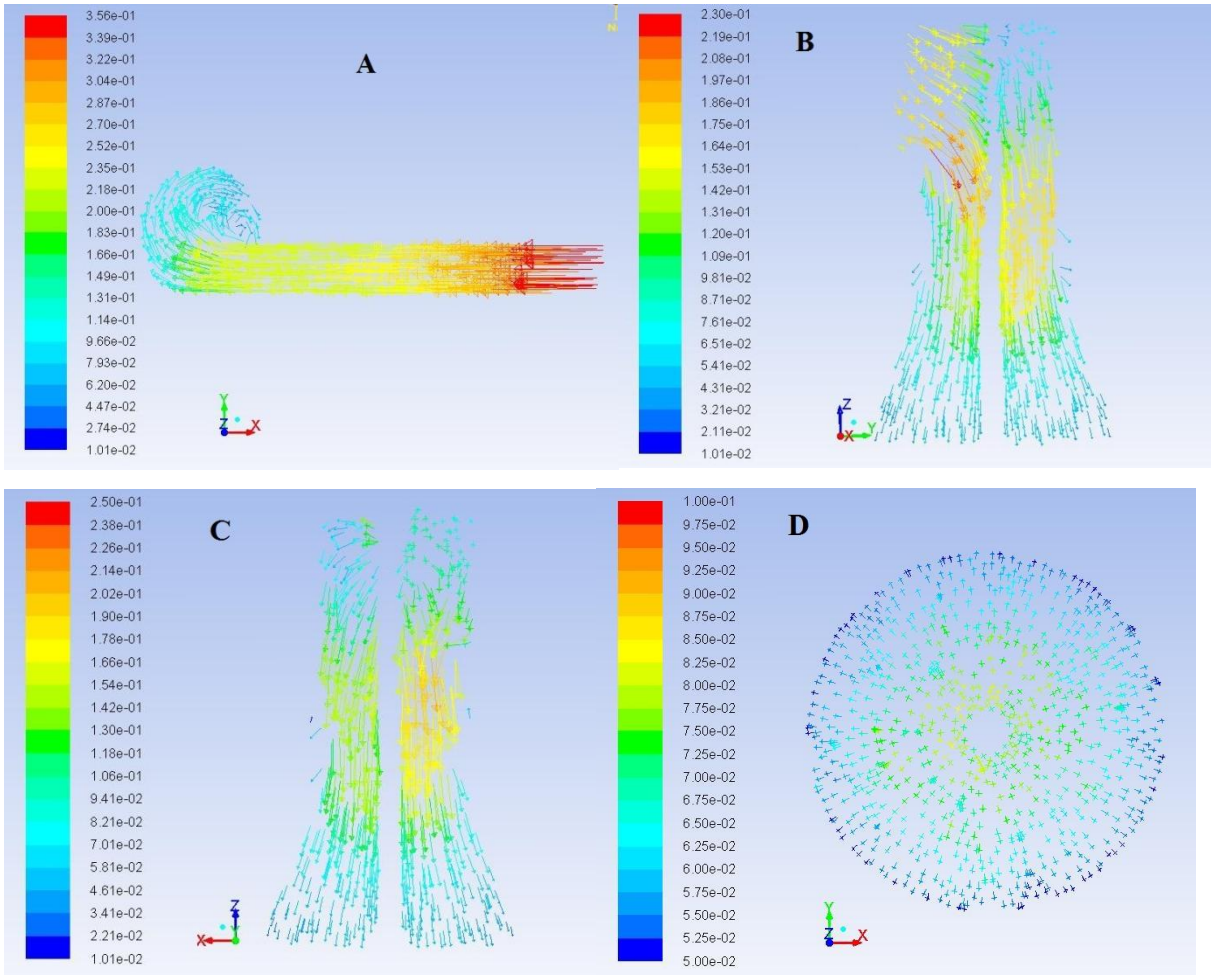

Figure 5-3: Velocity vector profiles inside the inlet zone.

5.2 Flow Patterns inside the Sedimentation Tank

Flow patterns inside the sedimentation tank were observed during the simulations. Figure 5-4 illustrates the solid phase behavior inside the tank at different flow times with 1 m^3/h flow rate and particle size of 100 μm. Solid phase profiles for other cases will be presented in Appendix B.

It was observed that the larger amount of effluent coming from inlet zone is directly contacting with the cone and plate that was placed below the inlet zone. Due to this behavior, some of the solid particles settled down on the plate and then these settled solid particles tend to move down to the bottom of the tank. Additionally, it was also noted that the flows inside the sedimentation tank was not short circuiting. Flow fields inside the sedimentation tank for other different cases were also similar to this case. That implies that the sedimentation tank at VEAS has a great design in order to prevent the mixing of partially settled influent with the settled effluent.

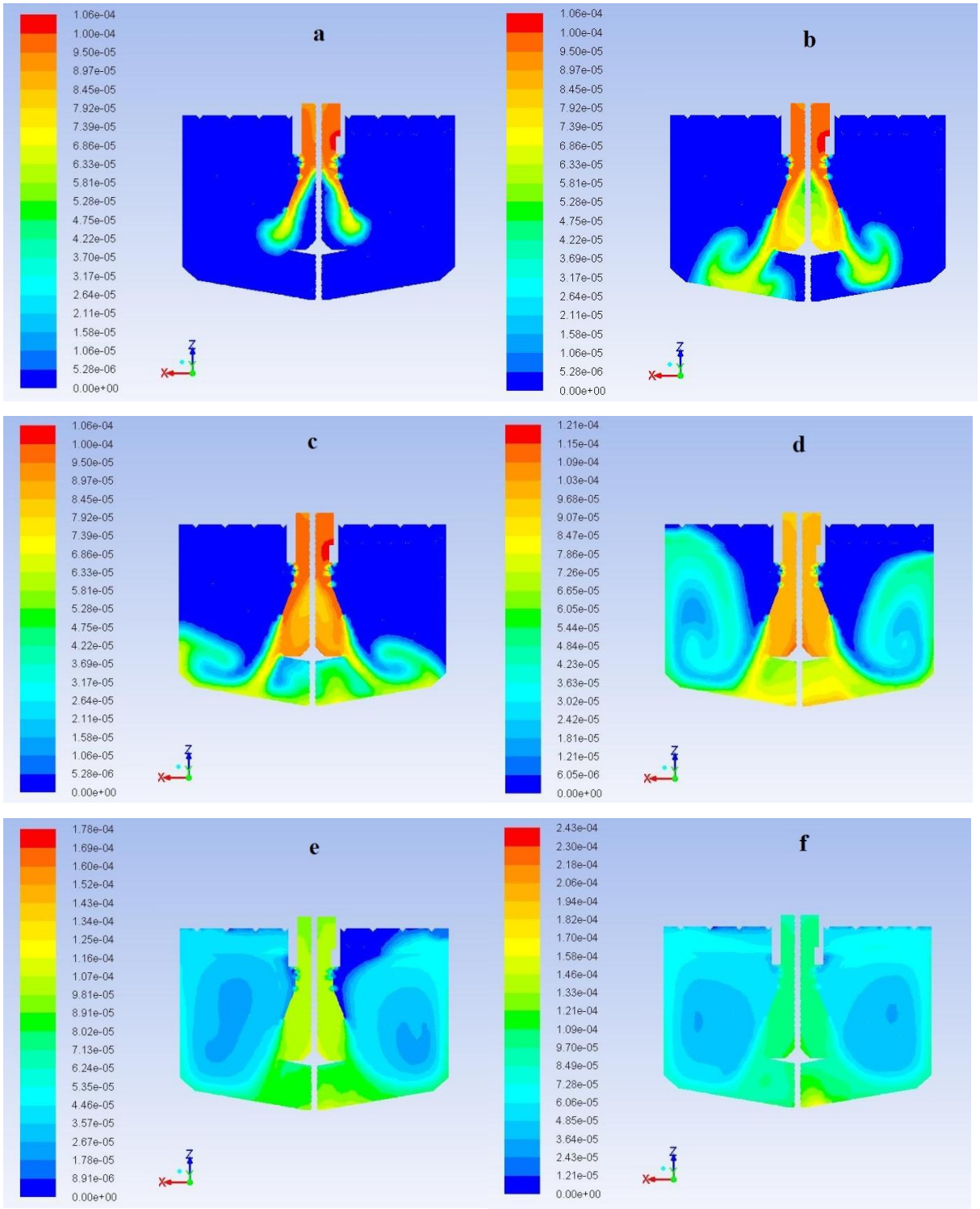

Figure 5-4: Solid phase behavior inside the tank at a) 100 s; b) 340 s; c) 550 s; d) 1598 s; e) 2698 s; f) 6098 s with 1 m3/h flow rate and particle size of 100 µm.

5.3 Velocity Profiles inside the Sedimentation Tank

Additionally, velocity profile of the solid phase was also observed during the simulations and Figure 5-5 demonstrates the velocity profile of the solid particles at different flow times with flow rate of 1m^3/h and the diameter of 100µm. Velocity profiles of the other cases have been attached in Appendix C It is observed that the velocity profiles of both liquid and solid phases are similar while doing the simulations and due to that only the velocity profiles of the solid phase is discussed in this report. By analyzing the Figure 5-5, it can be concluded that the flow field inside the sedimentation tank are following the design specifications of the tank since the flow fields are not short circuiting as discussed in chapter 5.2. Velocities of the solid particles are decreasing while flowing from inlet zone to the tank and it is evident that the velocity is further decreasing from bottom of tank to outlets. Smoother operating conditions have been provided by this flow field behavior with low fluctuations.

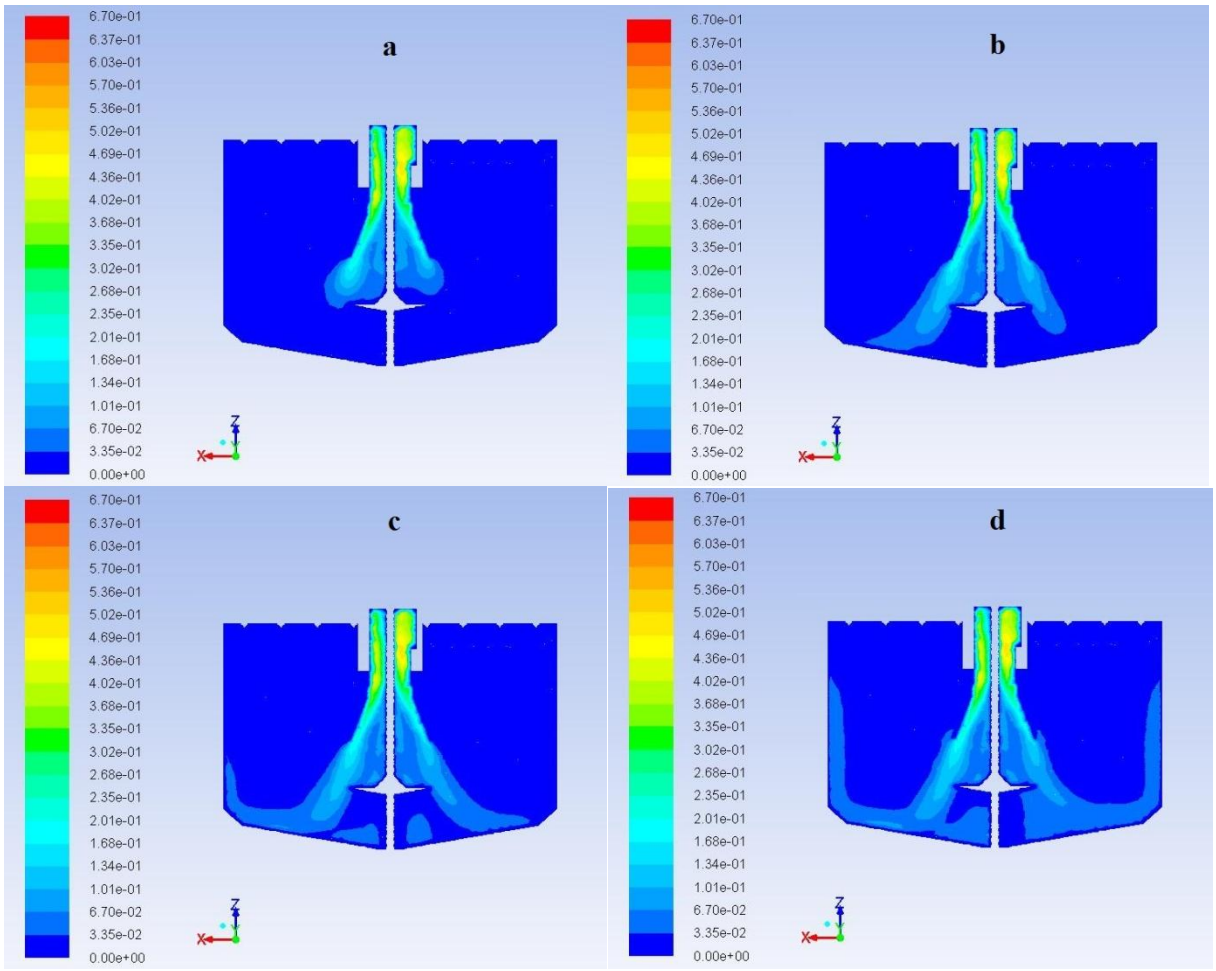

Figure 5-5: Velocity profile of the solid particles at 90 s; b) 310 s; c) 540 s; d) 6998 s with flow rate of 1m3/h and the diameter of 100µm.

5.4 Case Studies

Solid phase profiles have also been studied at the end of the simulation when the flow fields are stable in order get a better understanding of the sedimentation process inside the tank. Flow patterns at the outlets are analyzed since it is an important factor to measure the efficiency of the sedimentation. Velocity profiles of both liquid and solid phases and the volume fraction profile of the solid phase at outlets were studied during this thesis and Figure 5-6 illustrates the positions of the outlets that are going to be discussed in this chapter.

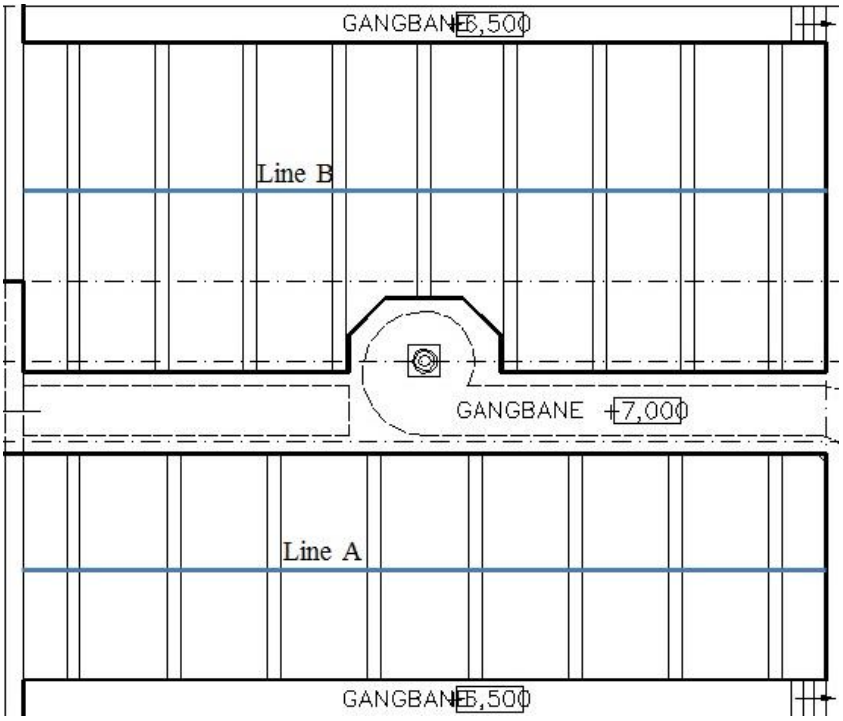

Figure 5-6: Positions of the outlets that are going to be discussed.

5.4.1 Case 1: 250μm Particle Diameter with 0.5 m^3/h Flow Rate

Figure 5-7 illustrates the solid phase behavior of the particle diameter of 250 μm with 0.5 m^3/h flow rate for two perpendicular planes of x = 0 and y = 0 inside the tank . Moreover, the volume fraction profile for solid phase is shown in Figure 5-8 and the detailed analysis of the variation of this profile is shown in Figure 5-9. Variations of outlet velocity profiles of solid phase and liquid phase with the length of the sedimentation tank are depicted in Figure 5-10 and Figure 5-11 respectively. By analyzing the Figures from 5-7 to 5.9, it is observable that most of the solid particles of 250 μm diameter with low flow rate , that is 0.5 m^3/h is settling down through the sedimentation process and the sedimentation efficiency for this case is 99.88 %. By studying the figures of outlets, it is observable that most of the solid particles appear at the area of line B and also at the area between 4 m to 6.15 m have the highest

particle concentration. Furthermore, volume fraction of the solid particles near the area of line A is almost zero and due to this the velocity of the solid phase along line A is also zero. Additionally, velocity profiles of liquid phase are varying through both A and B lines and the higher velocities can be clearly observed at the outlets weirs, and also the velocity profile of the solid phase through line B also has similar deviation.

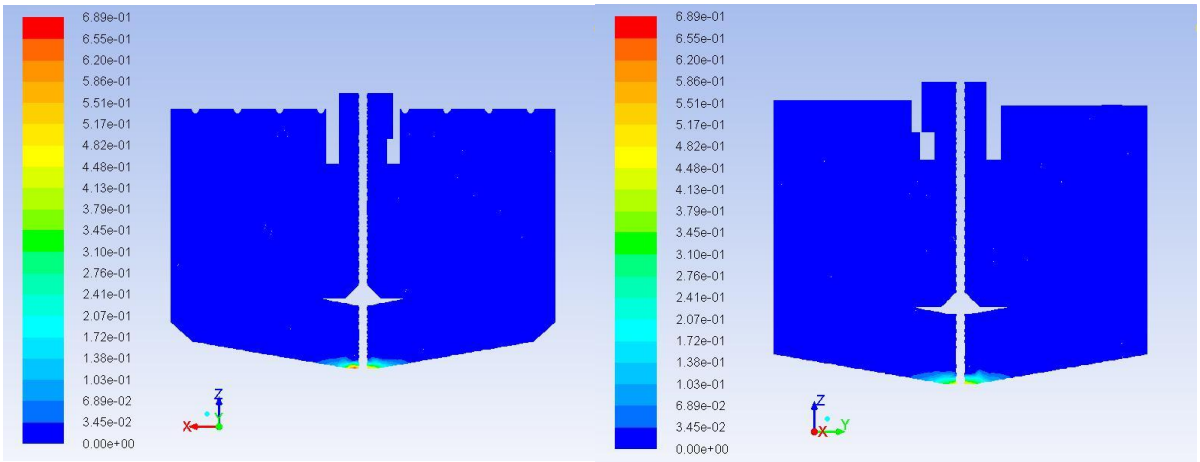

Figure 5-7: Volume fraction profiles of the solid phase inside the tank for case 1.

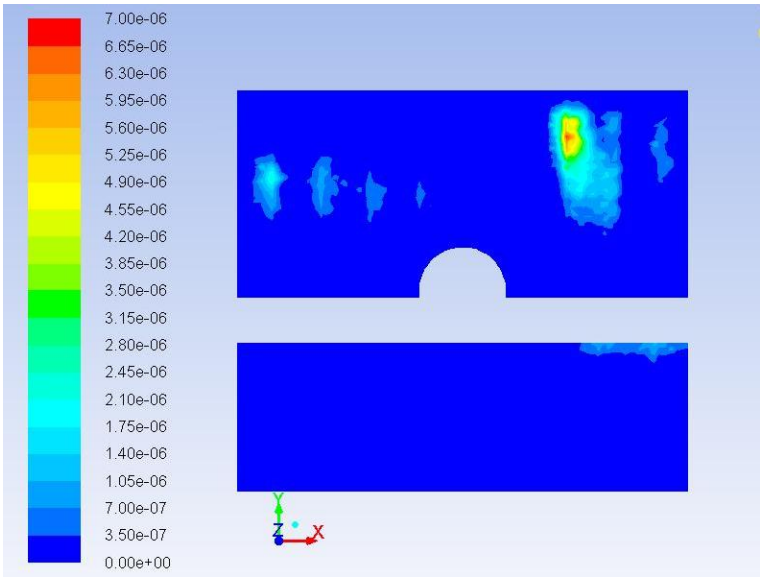

Figure 5-8: Volume fraction profiles of the solid phase at outlets for case 1.

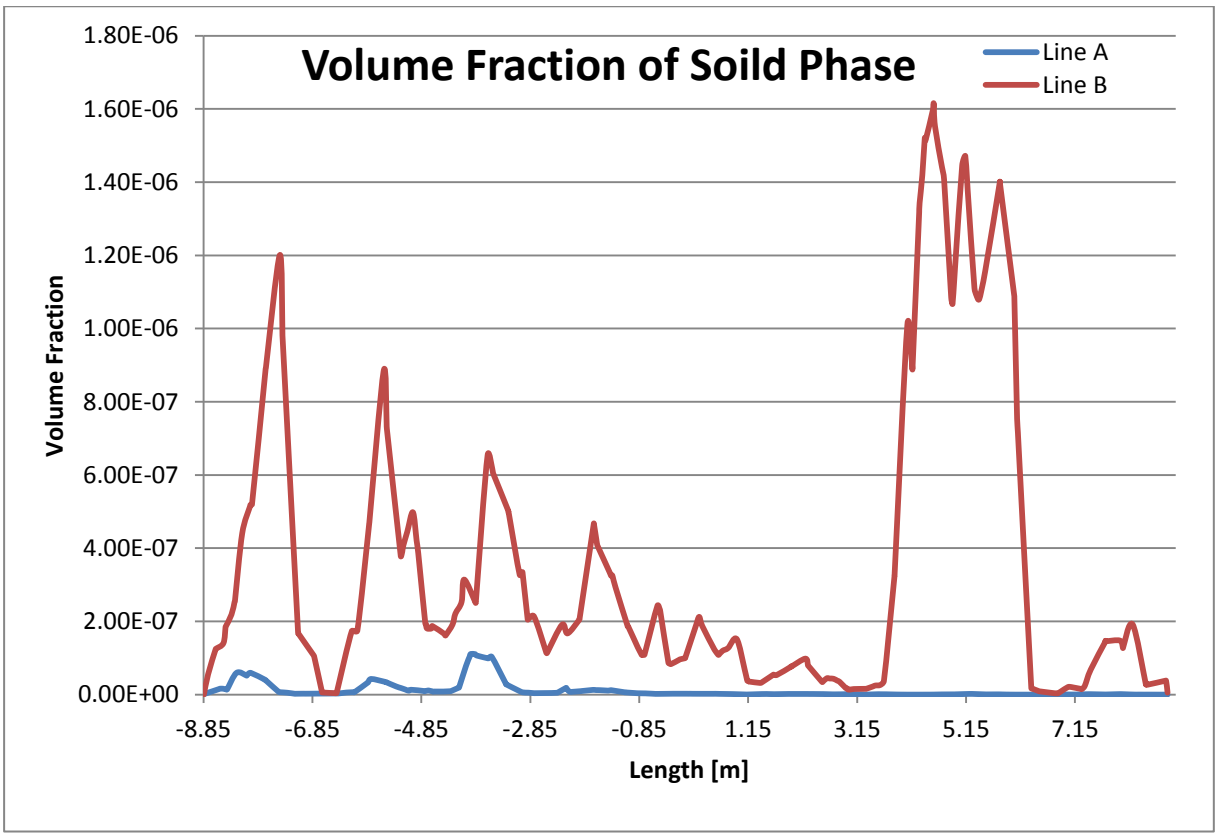

Figure 5-9: Volume fraction variation of solid phase with lenght of the tank for case 1.

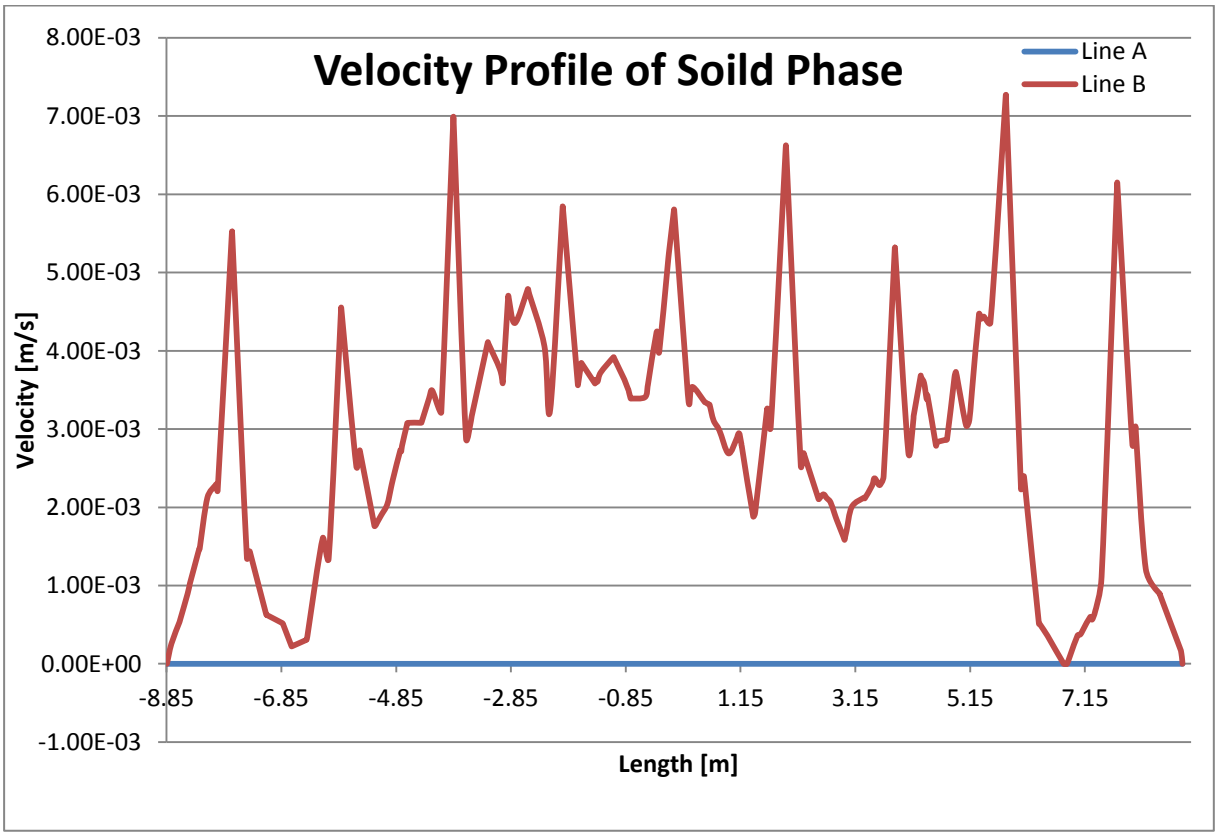

Figure 5-10: Velocity profile variation of solid phase with lenght of the tank for case 1.

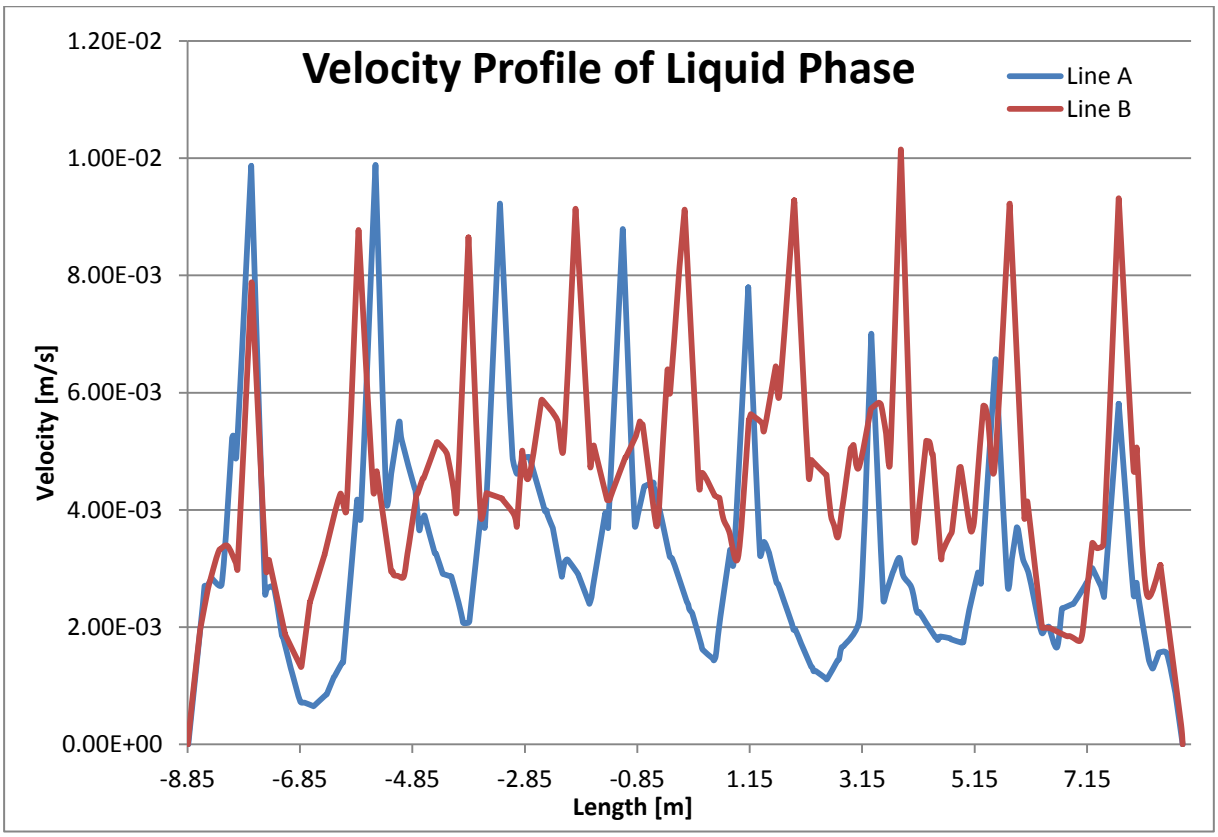

Figure 5-11: Velocity profile variation of liquis phase with lenght of the tank for case 1.

5.4.2 Case 2: 100µm Particle Diameter with 0.5 m^3/h Flow Rate

Solid phase behavior inside the sedimentation tank for the case with 100 µm particle diameter and the 0.5 m^3/h flow rate has been demonstrated in the Figure 5-12 by using two perpendicular cross sections. Furthermore, Figure 5-13 illustrates the volume fractions of solid phase at outlets and detailed demonstration of the volume fraction of solid particles are given in Figure 5-14. Figure 5-15 and Figure 5-16 show the variation of velocity profiles of the solid phase and the liquid phase with length of the sedimentation tank respectively. It can be noticed that the considerable amount of solid particles are escaping from outlets without settling down and the sedimentation efficiency for this case is 3.02 % which is very low compare to the case 1. It can be said that the volume fractions of solid particle along both A and B lines are fluctuating a lot by observing the detailed graph of the volume fractions and have the minimum values around 2.15 m to 4.15 m of line B. Detailed velocity graphs also have the high fluctuation effects for both solid and liquid phases and cannot observe a prominent trend. But from these graphs it can be seen that the velocities at the outlet weirs are higher compare to the velocities near the weirs for both liquid and solid phases.

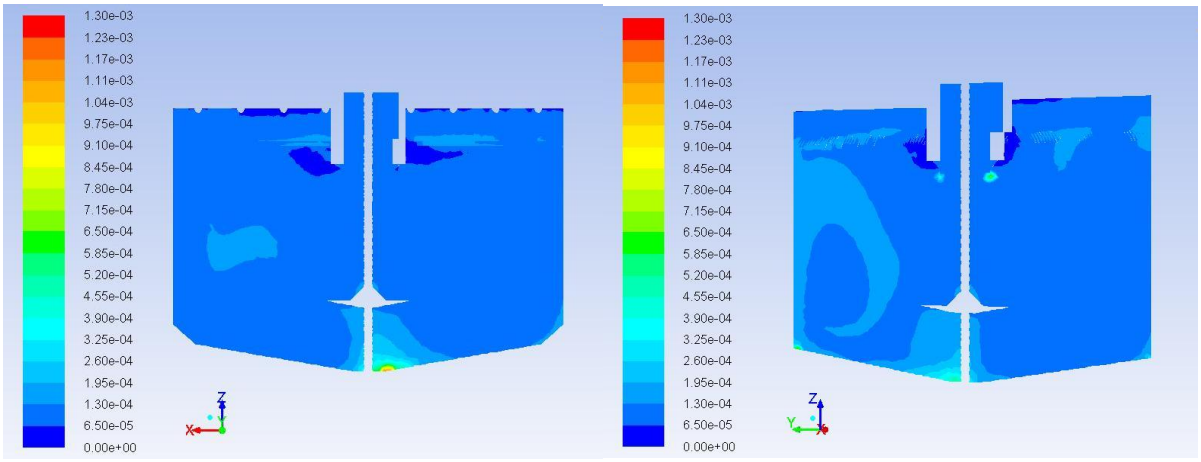

Figure 5-12: Volume fraction profiles of the solid phase inside the tank for case 2.

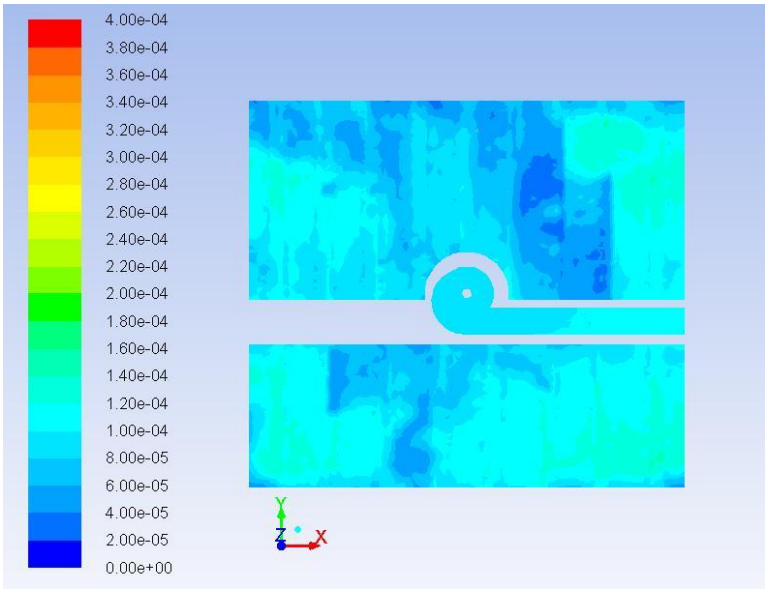

Figure 5-13: Volume fraction profiles of the solid phase at outlets for case 2.

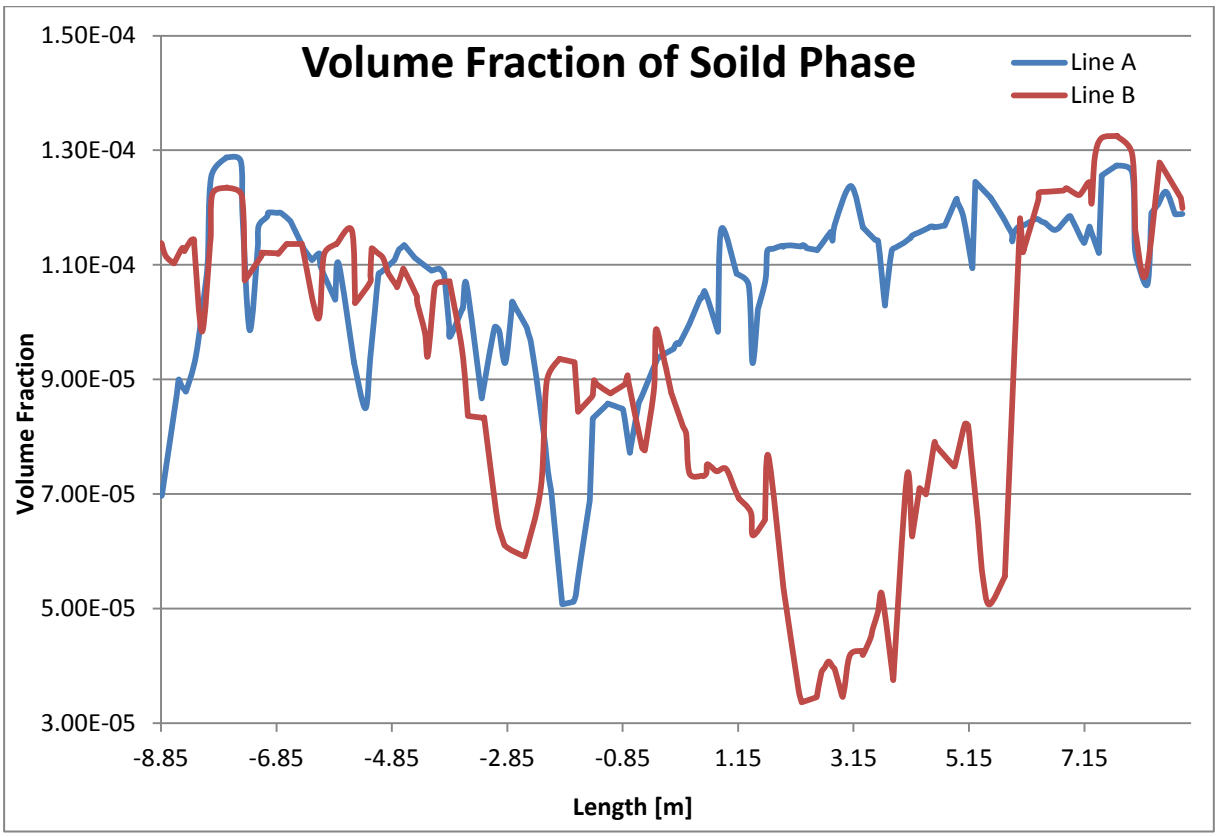

Figure 5-14: Volume fraction variation of solid phase with lenght of the tank for case 2.

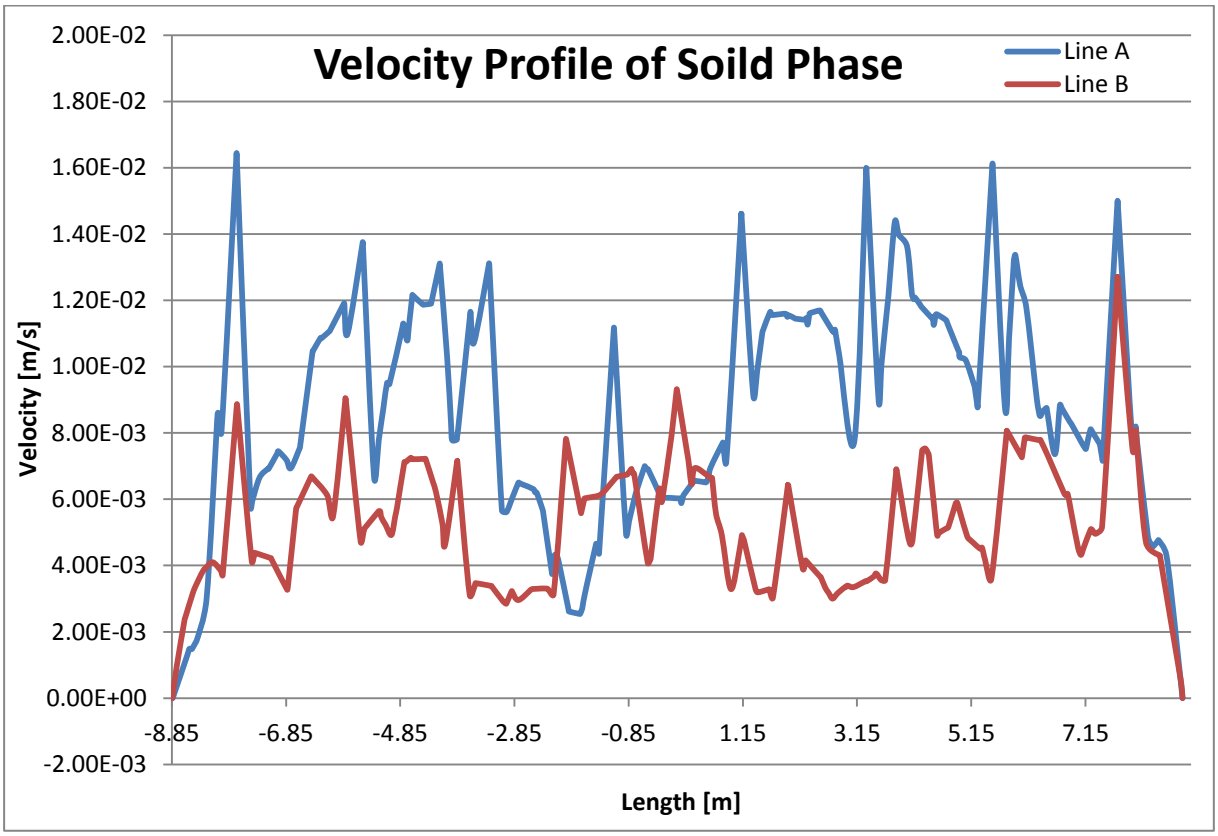

Figure 5-15: Velocity profile variation of solid phase with lenght of the tank for case 2.

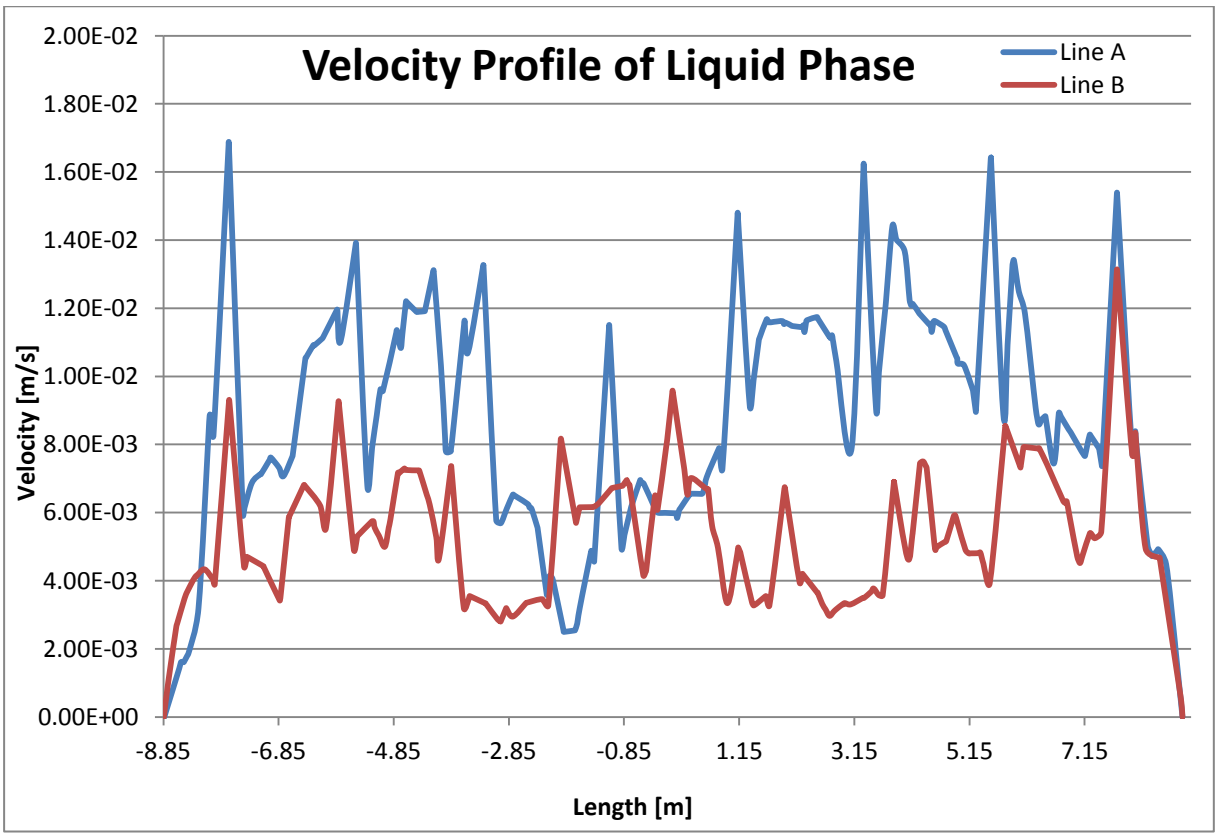

Figure 5-16: Velocity profile variation of liquis phase with lenght of the tank for case 2.

5.4.3 Case 3: 50µm Particle Diameter with 0.5 m^3/h Flow Rate

Moreover, the flow patterns of perpendicular cross sections of the tank while having the 50 µm particle diameter and the 0.5 m^3/h flow rate is shown in the Figure 5-17 and Figure 5-18 demonstrates the volume fraction of solid phase at the outlets. Figure 5-19 illustrates the detailed variation of the volume fraction of solid phase at the outlets while Figure 5-20 and Figure 5-21 present the velocity variation at outlets for both solid and liquid phases. It can be observed that the solid particles with 50 µm diameter have not settled down properly but the flow fields inside the tank follow the designed path, i.e. from inlet zone to bottom of tank and then to outlets. This case has the lowest sedimentation efficiency which is 1.97 %. Volume fractions of solid phase at the outlets have lot of fluctuations and also any specific trend cannot be noticed. Moreover velocity profiles at the outlets are also showing the oscillated behavior for both liquid and solid phases and as discussed in previous section, the velocity magnitude at the outlet weirs are higher compare to the velocities near the outlets.

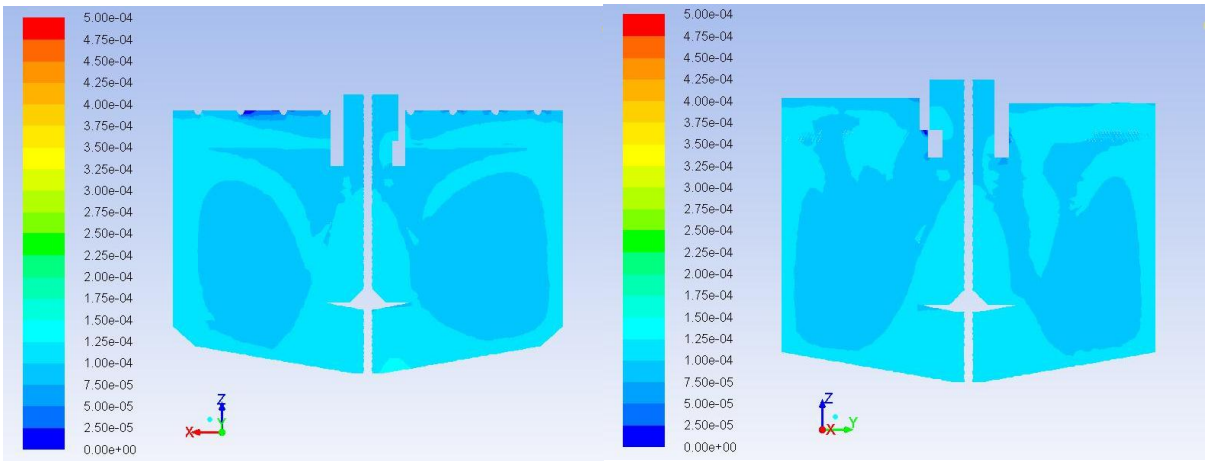

Figure 5-17: Volume fraction profiles of the solid phase inside the tank for case 3.

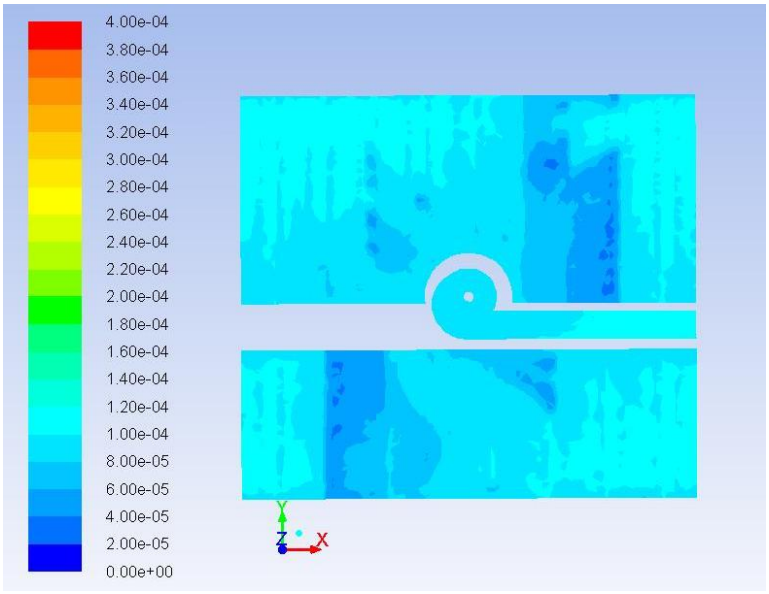

Figure 5-18: Volume fraction profiles of the solid phase at outlets for case 3.

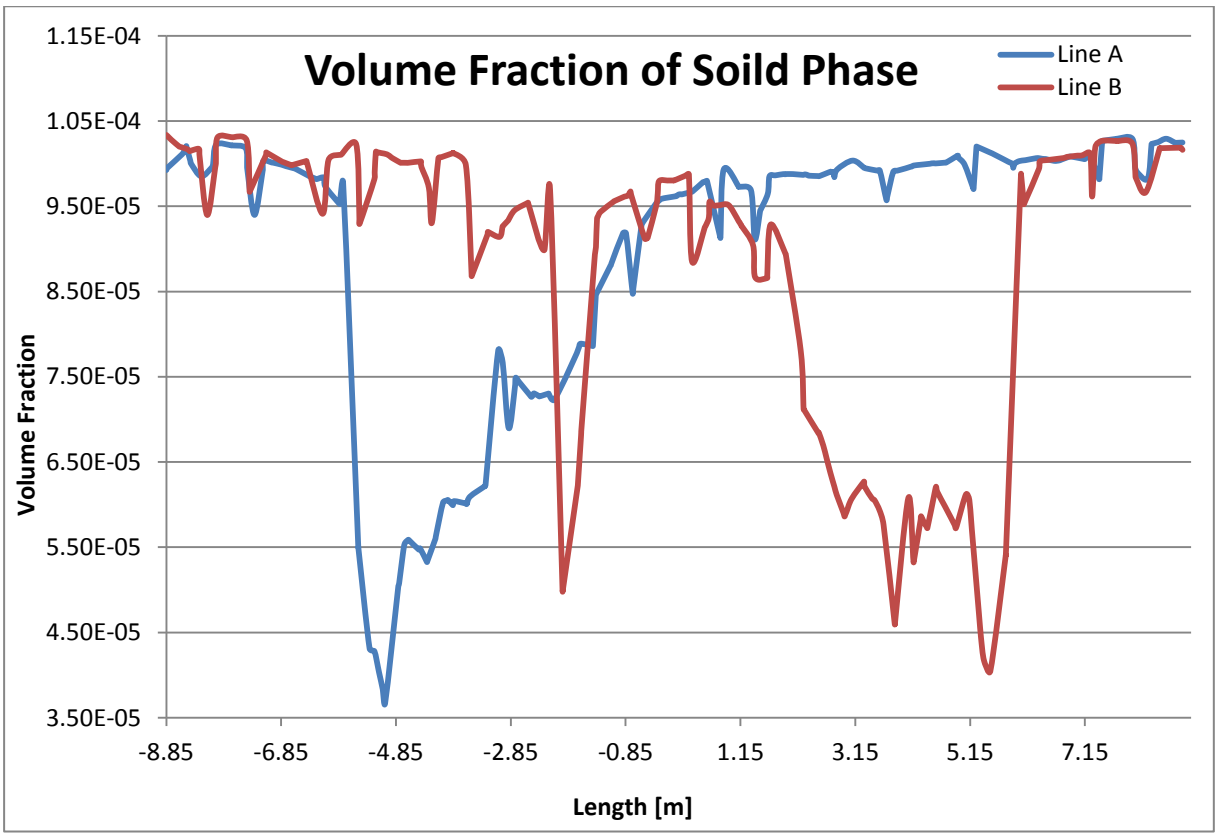

Figure 5-19: Volume fraction variation of solid phase with lenght of the tank for case 3.

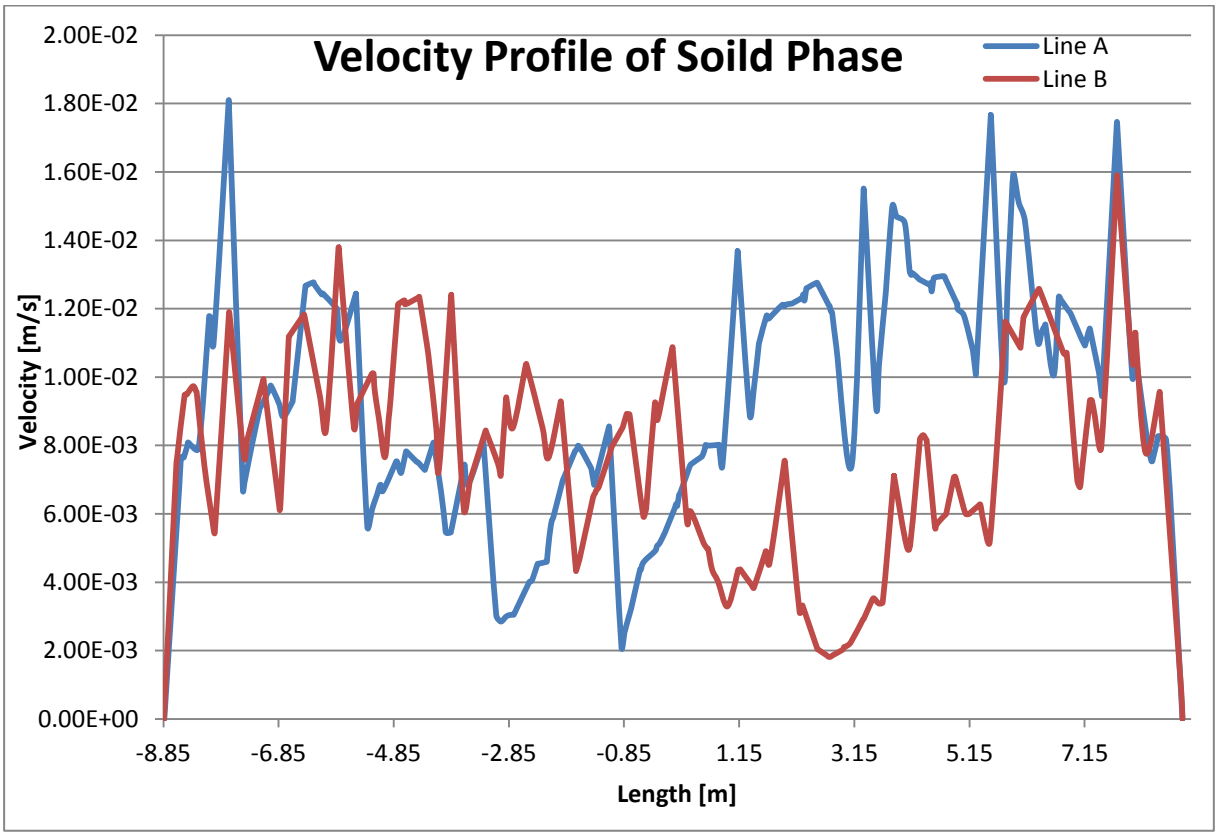

Figure 5-20: Velocity profile variation of solid phase with lenght of the tank for case 3.

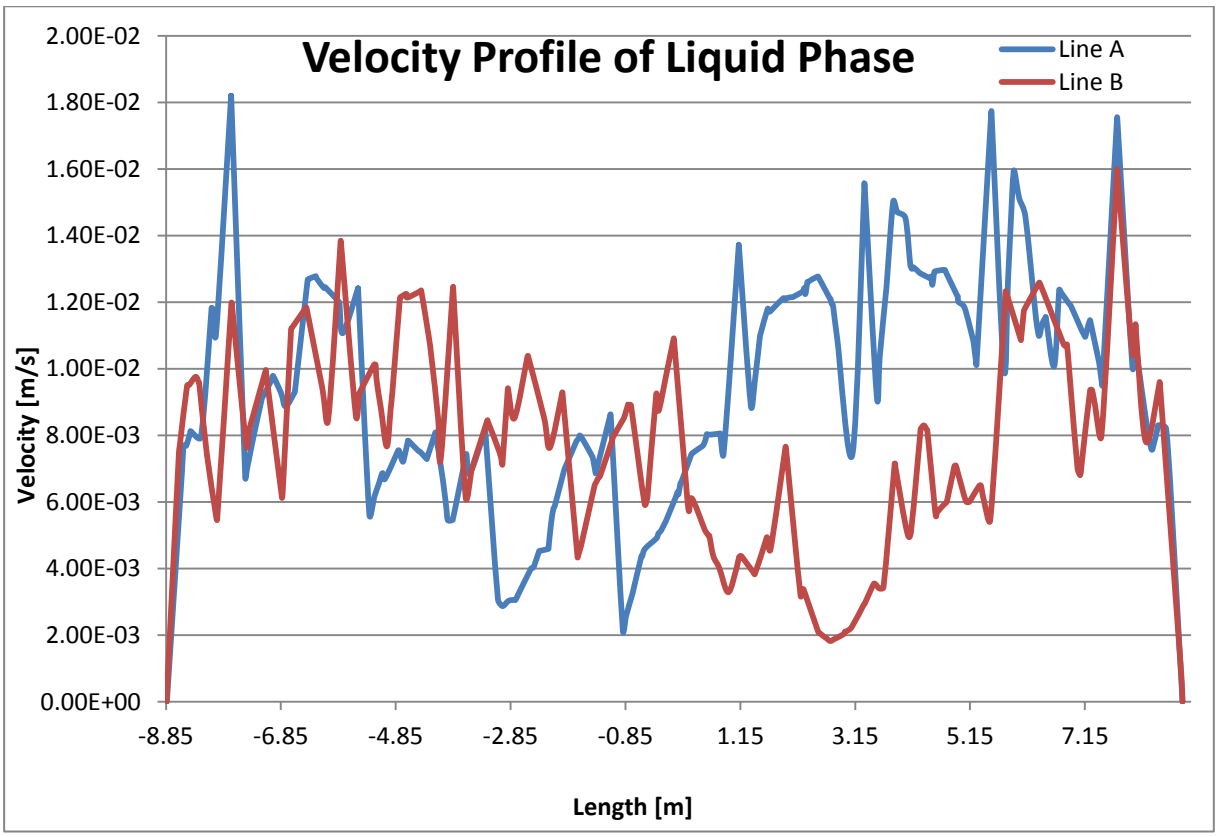

Figure 5-21: Velocity profile variation of liquis phase with lenght of the tank for case 3.

5.4.4 Case 4: 340µm Particle Diameter with 1 m^3/h Flow Rate

The volume fraction profiles of solid phase in the sedimentation tank for 1 m^3/h flow rate with 340 µm particle diameter are illustrated in Figure 5-22 for perpendicular planes at x = 0 and y = 0. Solid phase volume fraction profiles at the outlets are shown in Figure 5-23 and Figure 5-24. Velocity profiles of the outlets for both solid and liquid phases are shown in Figure 5-25 and Figure 5-26 respectively. Even though the particle size is larger than the case 1, all the particles have not settled down because of the high flow rate. This phenomenon can be observed from Figure 5-23 and still some percentage of particles are escaped from the outlets of the tank can be observed from Figure 5-23 and Figure 5-24 and also 85.45 % settling efficiency is reported for this case. It can be noticed that the solid volume fractions of the outlets along the line A is minimized around -4.84 m to -1.85 m and minimum solid volume fractions for line B can be observed from -4.85 m to 4.15 m and magnitude of the volume fractions are almost zero. Magnitude of the outlets velocities at line A is higher than the velocity at line B and this scenario can be observed for both phase while analyzing the Figure 5-25. and Figure 5-26. Moreover, prominent trend cannot be seen from the velocity profiles of both phases as same as previous cases and the velocity at outlet weirs have higher magnitude when comparing the velocity around the outlets.

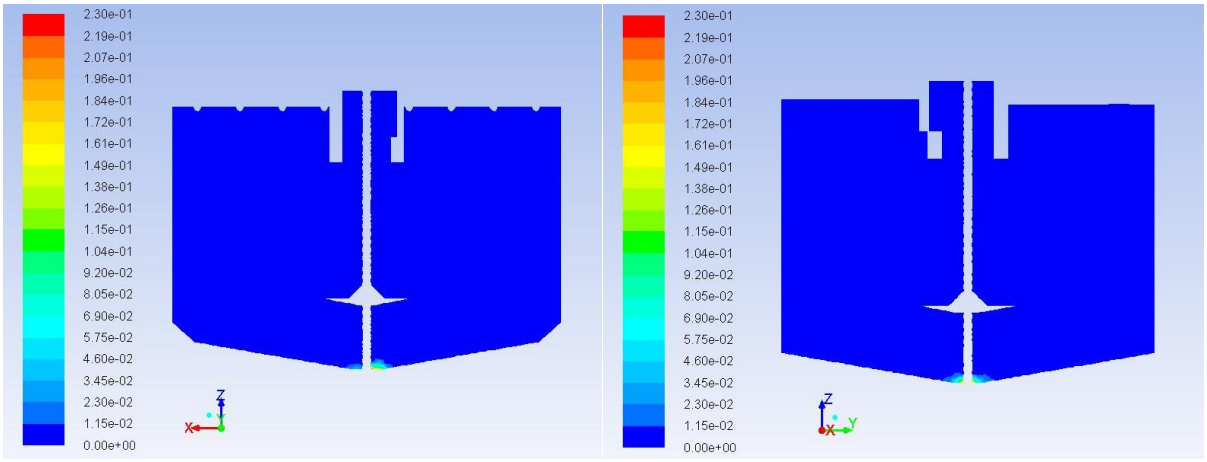

Figure 5-22: Volume fraction profiles of the solid phase inside the tank for case 4.

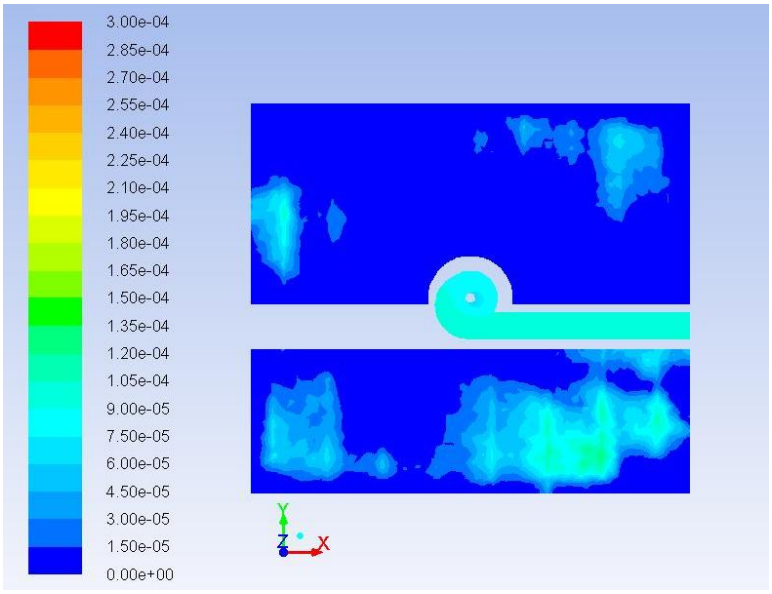

Figure 5-23: Volume fraction profiles of the solid phase at outlets for case 4.

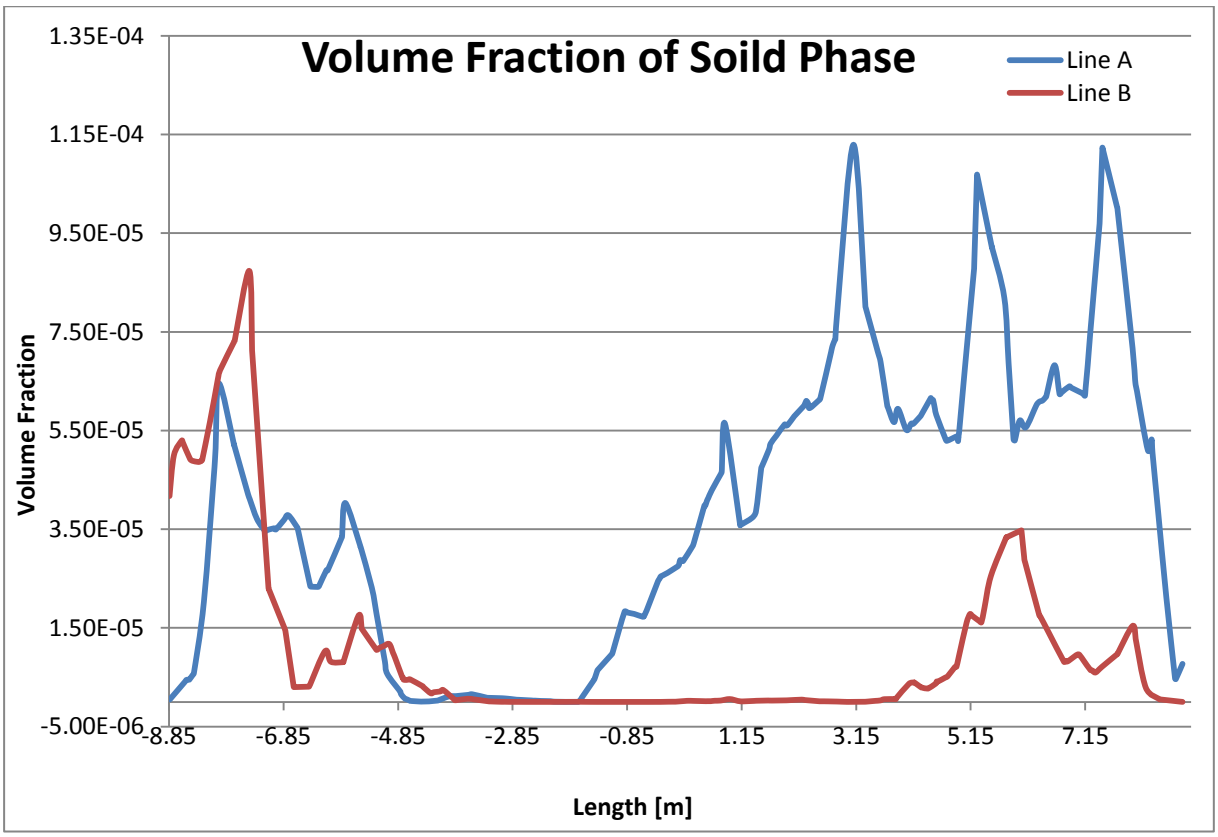

Figure 5-24: Volume fraction variation of solid phase with lenght of the tank for case 4.

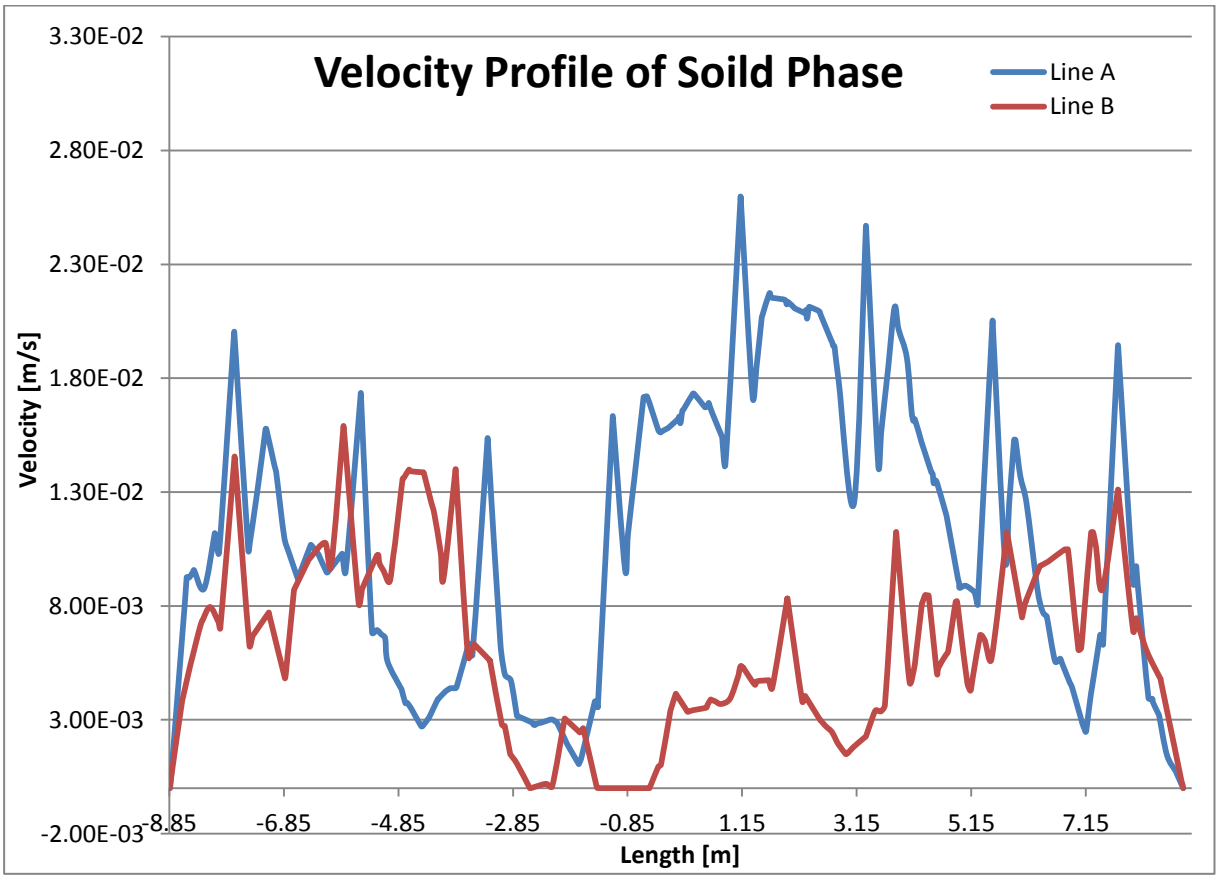

Figure 5-25: Velocity profile variation of solid phase with lenght of the tank for case 4.

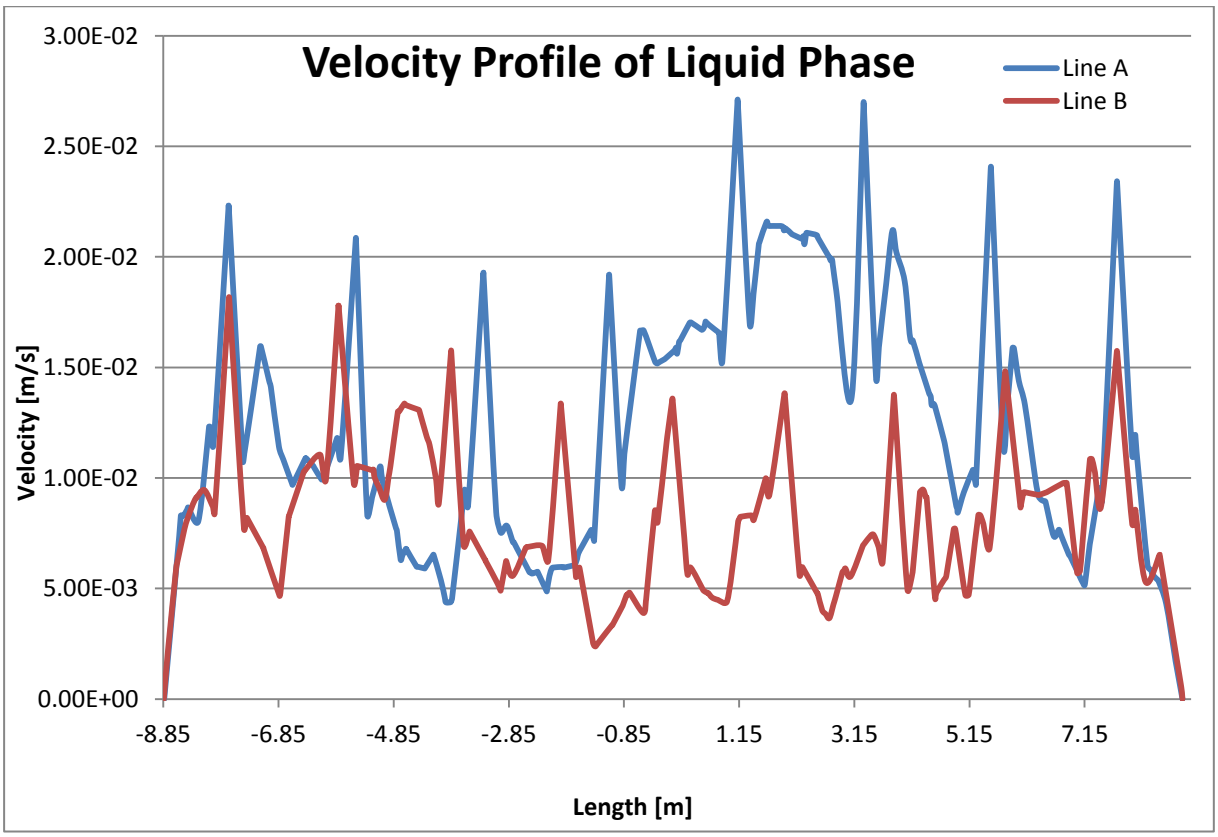

Figure 5-26: Velocity profile variation of liquis phase with lenght of the tank for case 4.

5.4.5 Case 5: 250µm Particle Diameter with 1 m^3/h Flow Rate

Figure 5-27 illustrates the solid phase behavior of the particle diameter of 250 µm with 1 m^3/h flow rate for two perpendicular planes of x = 0 and y = 0 inside the tank. Moreover the Figure 5-28 and Figure 5-29 demonstrated the solid volume fraction profiles at outlets. It can be noticed that the some parentage of the solid particles are settled down at the bottom of the tank and large amount of particles are escaping from the tank without settling down while having 4.14 % settling efficiency. By analyzing the Figure 5-29 it can be said that lowest solid volume fraction of line A occurs approximately around -3 m and it shows the increasing trend along the length of the tank. But minimum solid volume fraction for line B appears around the 7 m and deceasing trend can be observed for line B along the length of the tank. Velocity profiles of the outlets for solid phase and the liquid phase are shown in Figure 5-30 and Figure 5-31 respectively. Similar to the previous cases, the specific trend cannot be observed from these figures and the velocity magnitude at line A is higher at outlets compare to the velocity magnitude near the outlets for both phases. However, this kind of trend cannot be observed for line B for both phases.

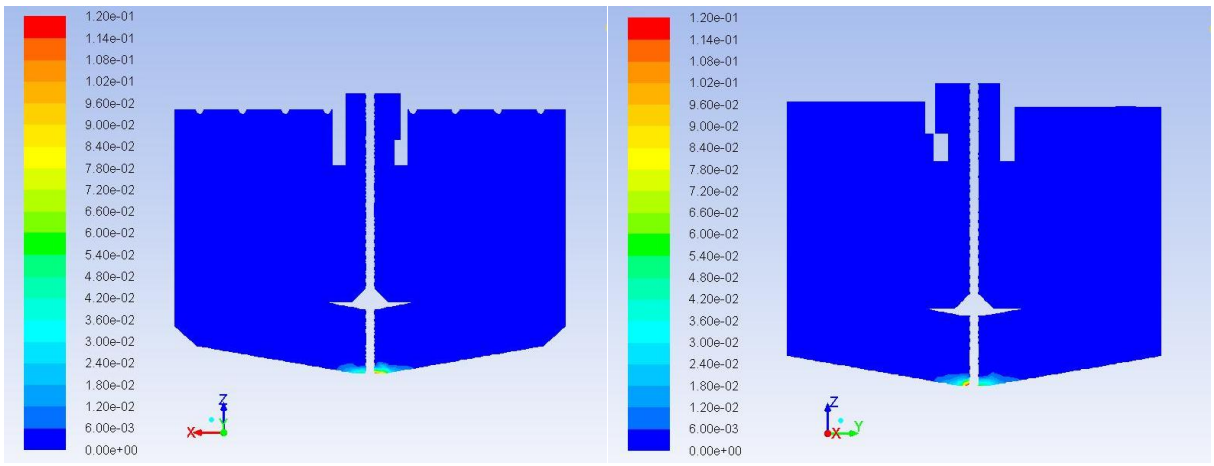

Figure 5-27: Volume fraction profiles of the solid phase inside the tank for case 5.

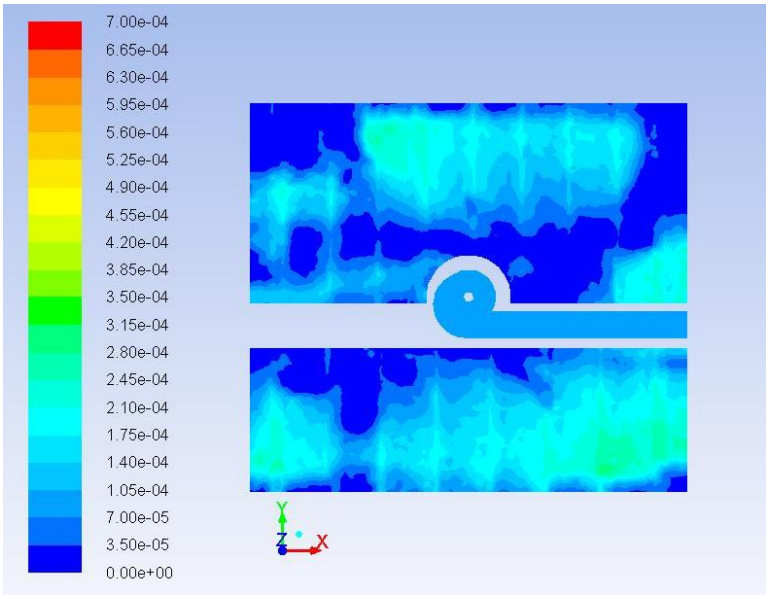

Figure 5-28: Volume fraction profiles of the solid phase at outlets for case 5.

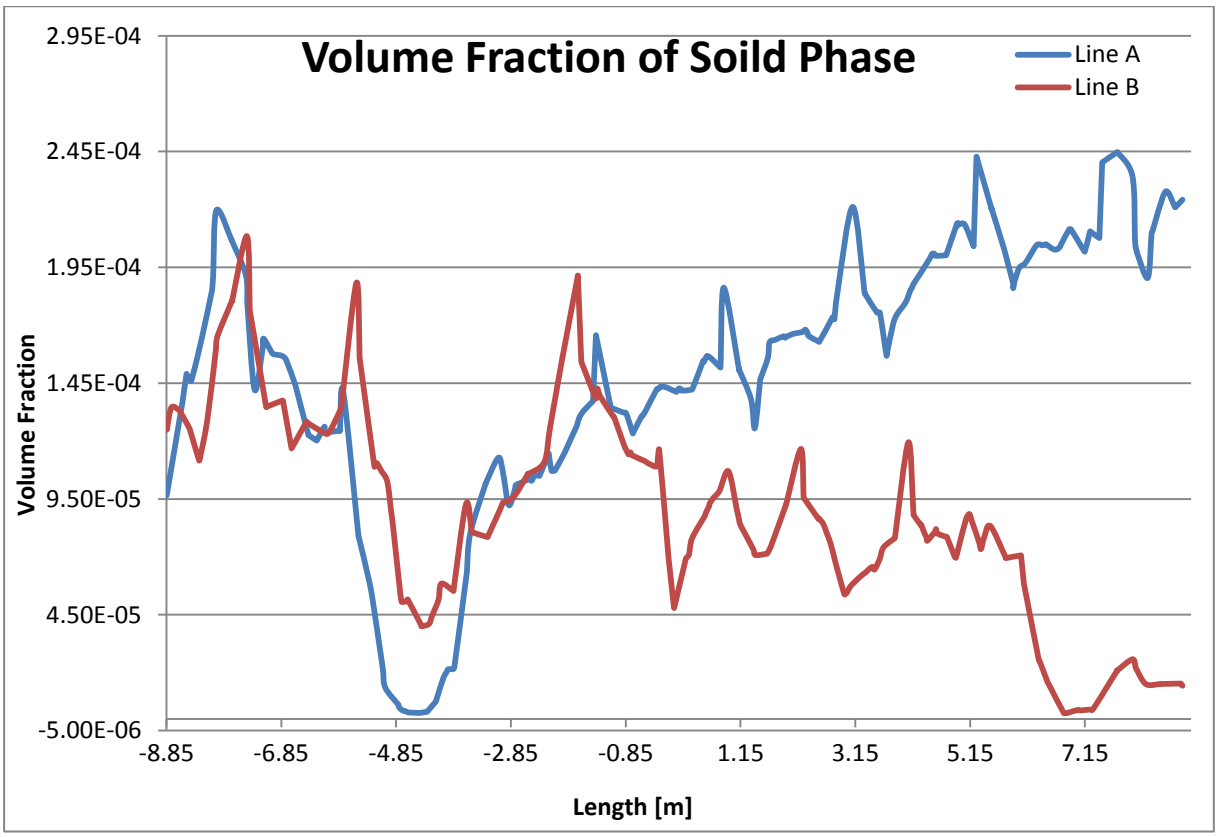

Figure 5-29: Volume fraction variation of solid phase with lenght of the tank for case 5.

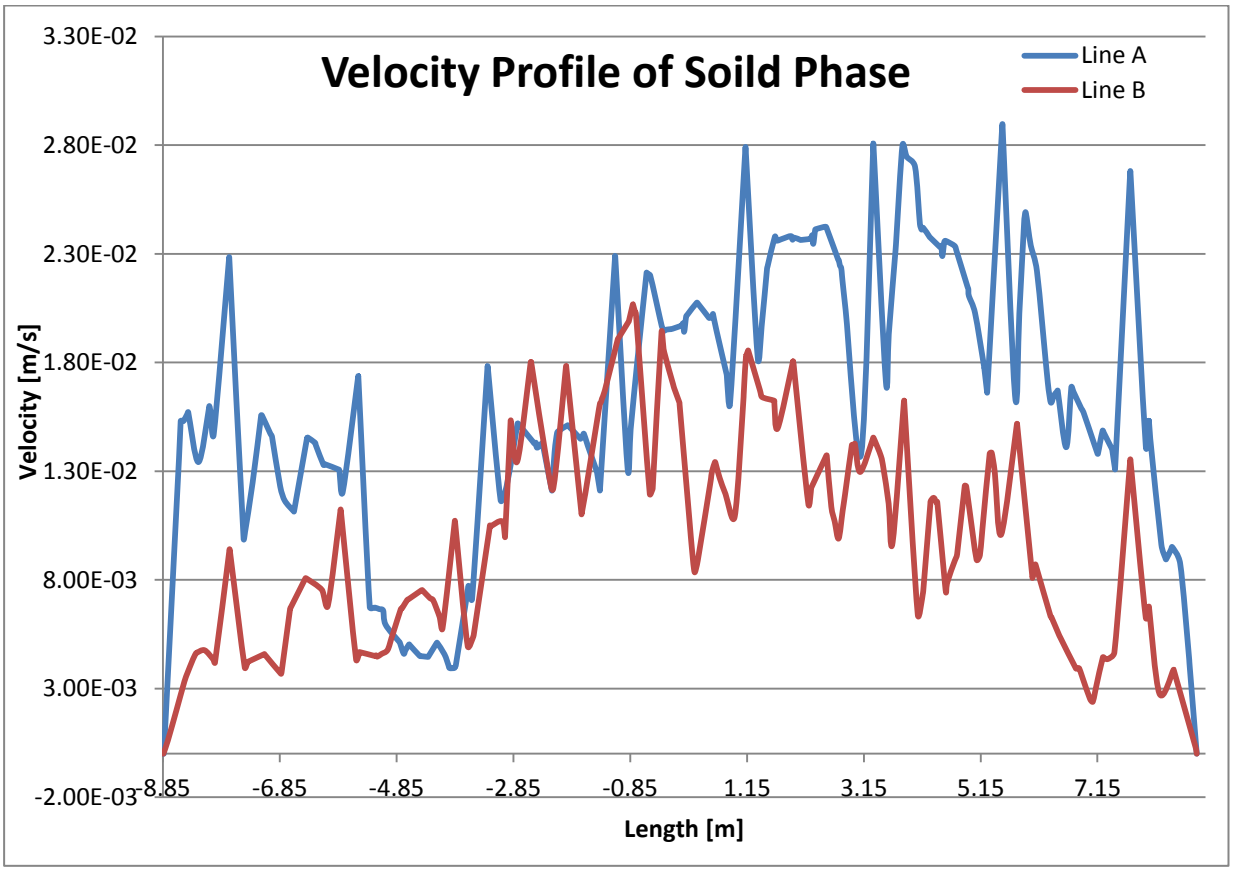

Figure 5-30: Velocity profile variation of solid phase with lenght of the tank for case 5.

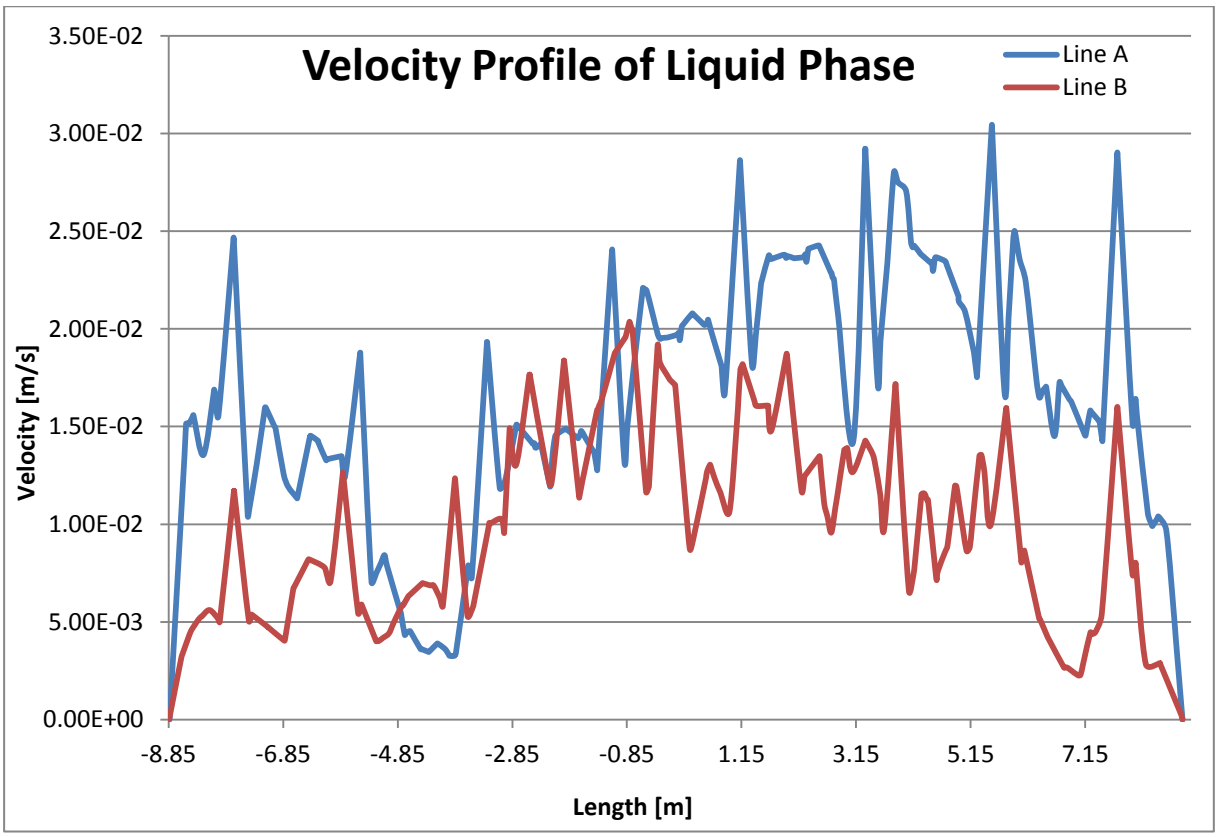

Figure 5-31: Velocity profile variation of liquis phase with lenght of the tank for case 5.

5.4.6 Case 6: 100µm Particle Diameter with 1 m^3/h Flow Rate

In Figure 5-32, two solid phase behavior of the perpendicular planes inside that tank with particle with 100 µm diameter and the flow rate of 1 m^3/h are presented. Additional to those figures, Figure 5-33 and Figure 5-34 demonstrate the solid volume fractions of the outlets. Settling efficiency for this case is 2.42 % and by evaluating the Figure 5-34, it can be understood that the lowest solid volume tractions for line A is occur around the length between the -4.85 m to -2.85m and the minimum solid volume fractions for line B is appear approximately around 3.15 m to 5.15 m. Velocity profiles at the outlets are shown in Figure 5-35 and Figure 5-36 for solid and liquid phases respectively. Because of the fluctuation, prominent trend for outlet velocities cannot be observed for neither solid phase nor liquid phase.

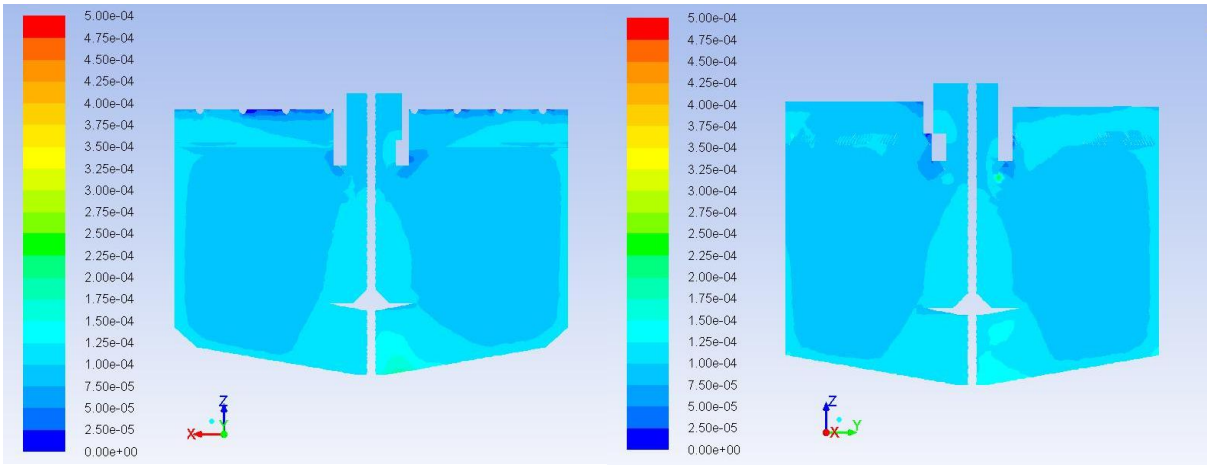

Figure 5-32: Volume fraction profiles of the solid phase inside the tank for case 6.

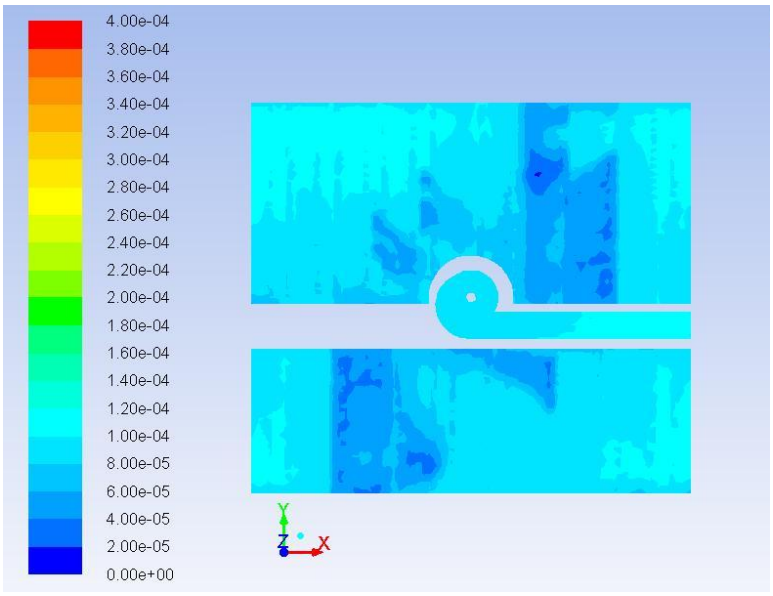

Figure 5-33: Volume fraction profiles of the solid phase at outlets for case 6.

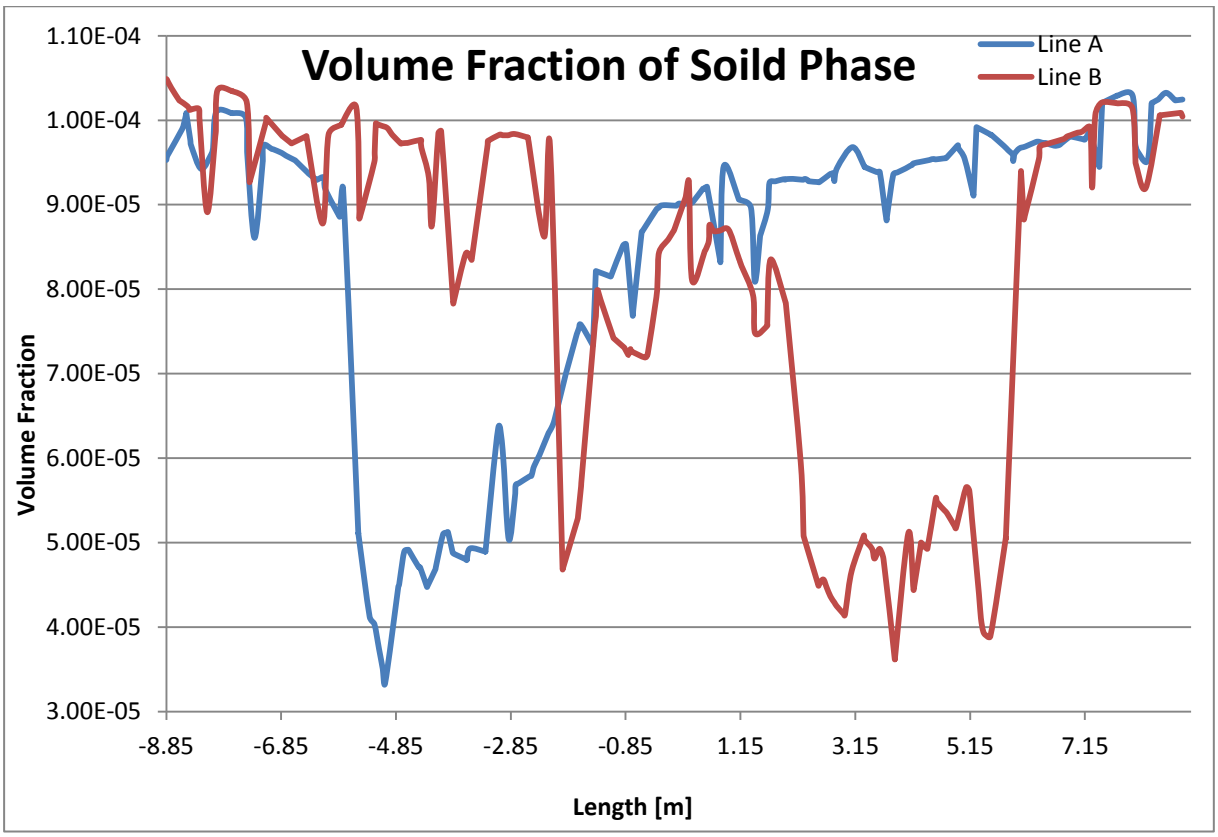

Figure 5-34: Volume fraction variation of solid phase with lenght of the tank for case 6.

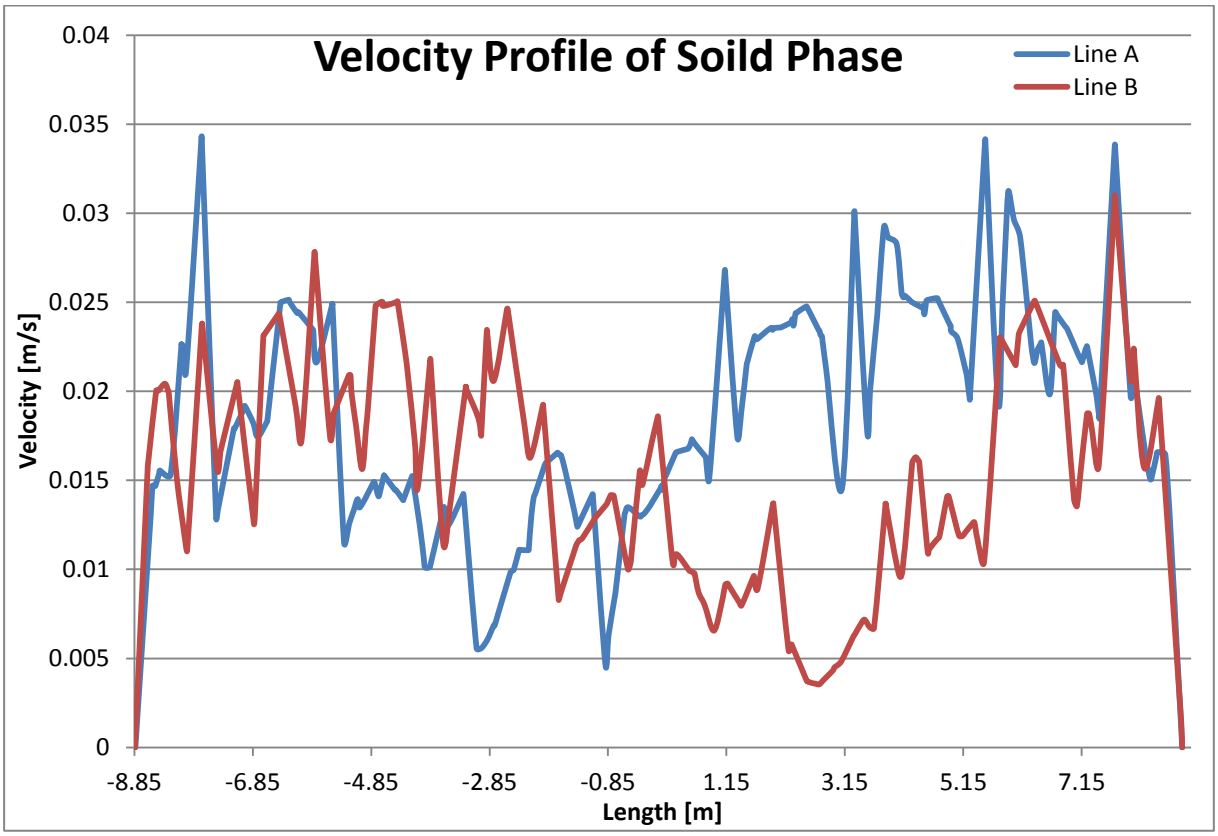

Figure 5-35: Velocity profile variation of solid phase with lenght of the tank for case 6.

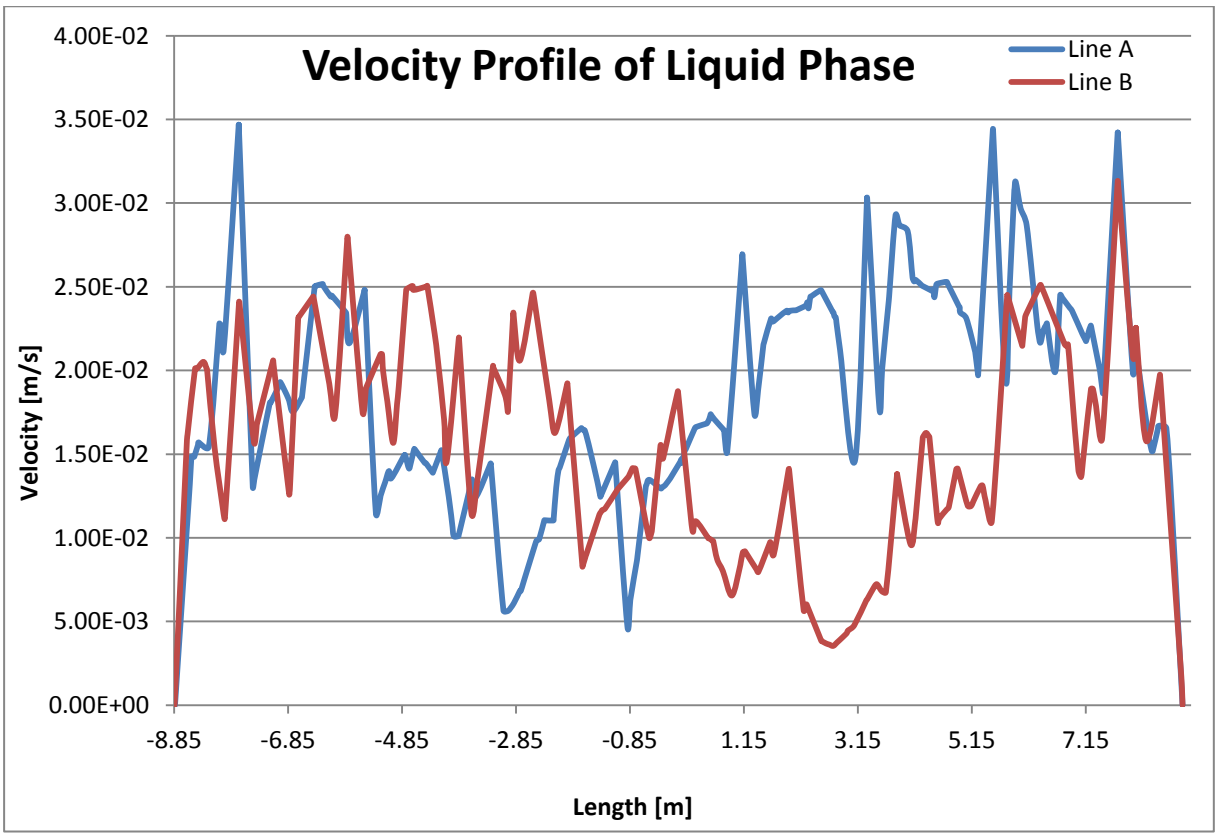

Figure 5-36: Velocity profile variation of liquis phase with lenght of the tank for case 6.

Comparisons of the efficiencies in the sedimentation tank for different cases are presented in Figure 5-37. It can be observed that the highest settling velocity can be obtain from the particles with 250 µm diameter with 0.5 m^3/h flow rate and the minimum settling efficiency is reported with the case 6; 100 µm particle diameter with 1 m^3/h flow rate.

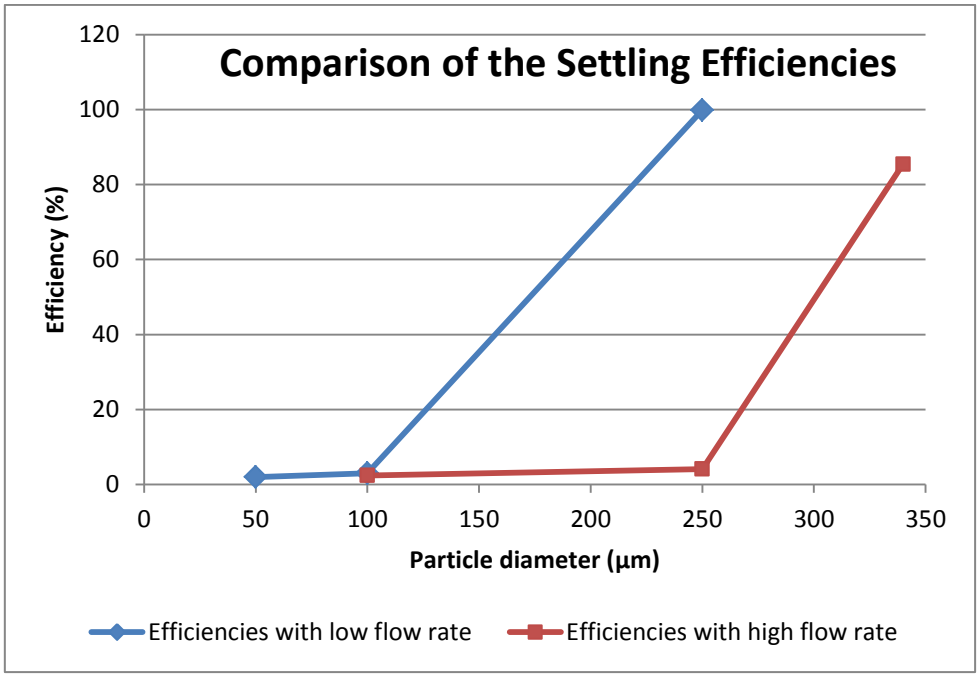

Figure 5-37: Comparison of the settling efficiencies.

6 Conclusion

Sewage treatment is the process of removing the contaminants from sewage to produce liquid and solid (sludge) suitable for discharge to the environment or for reuse. During this study, the flow fields inside one of the sedimentation tanks at VEAS were evaluated. Gambit 2.4.6 software was used to generate the geometry and the computational mesh and the ANSYS FLUENT 13.0 software was used as the CFD tool during this thesis.

Eulerian model was used as the multiphase model and the Standard k – ε model was used as the turbulent model while doing the simulations. Six cases were analyzed during this study depending on the size of the solid particle and the flow rate of the tank. Results were taken after the flow is stabilized and around 13 hours of flow time is required to stabilize one case of simulations.

While evaluating the flow patterns inside the sedimentation tank for all cases, it was noticed that the design of the sedimentation tank is suitable since the short circuiting of the flow currents do not take place inside the tank which prevents the unsettled influent from mixing with partially settle liquid. Moreover, the velocity profiles for both solid and liquid phases have similar behavior which decreases gradually from inlet to outlets of the sedimentation tank.

It is obvious that the sedimentation efficiency of the particles with larger diameters have higher efficiency than the small diameter particles. Therefore, it is needed to add suitable chemicals to enhance the coagulation rate to increase the efficiency of the sedimentation process.

Furthermore, the efficiency of the sedimentation gets lower with the higher flow rates since the higher retention time will improve the sedimentation efficiency. It is observed that the solid particles with 340 μm diameter and 1 m^3/h flow rate have lower sedimentation efficiency than the 250 μm diameter particles with flow rate of 0.5 m^3/h. Additionally, the sedimentation efficiencies for cases with 100 μm and 50 μm solid particles diameter with 0.5 m^3/h and the diameters of 250 μm and 100 μm solid particles with 1 m^3/h are observed very low. Hence to get a better settling efficiency, it is important to control the flow rate of the tank.

Solid volume fractions at outlets have fluctuating behaviors for different cases and prominent trend cannot be observed for many cases. Likewise, the velocity fields at outlets are also varying and it is obvious that the velocities at outlet weirs are little bit higher than the velocity near the outlets and this phenomenon can be observed from the results of simulations.

Finally, it can be concluded that the flow fields inside this sedimentation tank is not symmetric by analyzing the simulated results even though the tank is symmetric except at the inlet of the tank.

6.1 Recommendation for Future Works

Even though the different simulation cases that depend on the flow rate and the size of the particles were carried out during this study, only one particle size was focused in one case. But in the real life, sewage will have a particle size distribution and it is recommended to add the real particle distribution to the simulations which result in more than two phases in the sedimentation tank. More than one phase of solid particles with different diameters were tried out in simulations during this study. However due to the limitation of the computer performance it takes a significantly long time, hence it is recommended to have high performance computers for more than two phase simulations.

It can be notices that validation of results is common practice while doing the literature review. Therefore, it is recommended to do the validation of the CFD results with experiments. The radioactive particles or colored particles can be injected to the inlet of the sedimentation tank to validate the results from simulations and then the flow fields of these particular particles can be analyzed.

Due to the tight deadlines of this project, only the minimum and maximum flow rates were taken as cases, but to enhance the predictive capacity and the accuracy of these simulations it is suggested to do simulations with the flow rates between the lowest and highest.

CFD simulations of this thesis were done without indicating the solid phase as granular particles due to the unavailability of data. Therefore it is recommended to do these simulations while specifying the secondary phase as granular in order to enhance the accuracy of these simulations.

Six sedimentation tanks are operated in the VEAS and one was selected by the VEAS to do CFD simulations. The length between the inlet zone and the plate locate below the inlet zone is different for each and every tank. It is suggested to do simulations for these cases and relocate the plates of tanks, if possible, in order to gain the maximum sedimentation efficiency.

References

[1] (20/05/2013). *Water*. Available: http://www.nrdc.org/water/

[2] N. R. M. a. E. Department. (1992, 03/05/2013). *Wastewater treatment and use in agriculture*. Available: http://www.fao.org/docrep/T0551E/T0551E00.htm

[3] (20/05/2013). *Effects of Dumping Sewage Water Directly Into the Sea*. Available: http://gobiidae.com/PN/dumpingsewage.html

[4] (10/05/2013). *VEAS*. Available: http://www.veas.nu/

[5] (2010, 20/05/2013). *Literature Review*. Available: http://library.uws.edu.au/infoGathering.php?case=litReview&s=litImportance

[6] (05/05/2013). *Sedimentation tank*. Available: http://www.britannica.com/EBchecked/topic/532321/sedimentation-tank

[7] B. Carlsson. (1998). *An introduction to sedimentation theory in wastewater treatment*. Available: http://www.it.uu.se/edu/course/homepage/h2orentek/WWT98/sett98.pdf

[8] J. B. Christian, "Improve clarifier and thickener design and operation," *Chemical Engineering Progress;(United States)*, vol. 90, 1994.

[9] G. J. Schroepfer, "Factors Affecting the Efficiency of Sewage Sedimentation," *Sewage Works Journal*, vol. 5, 1933.

[10] 05/05/2013). Sedimentation. Available: http://www.mrwa.com/OP-Sedimentation.pdf

[11] M. Dufresne, J. Vazquez, A. Terfous, A. Ghenaim, and J.-B. Poulet, "Experimental investigation and CFD modelling of flow, sedimentation, and solids separation in a combined sewer detention tank," *Computers & Fluids*, vol. 38, pp. 1042-1049, 2009.

[12] L. Fan, N. Xu, X. Ke, and H. Shi, "Numerical simulation of secondary sedimentation tank for urban wastewater," *Journal of the Chinese Institute of Chemical Engineers*, vol. 38, pp. 425-433, 2007.

[13] (10-05-2013). *Water/Wastewater Distance Learning Website*. Available: http://water.me.vccs.edu/courses/ENV110/lesson5_2.htm

[14] (20/05/2013). *Lamella Plate Clarifier*. Available: http://www.hydro-int.com/uk/products/lamella-plate-clarifier

[15] E. Loth. (10/05/2013). *Dispersed Multiphase Flow Book*. Available: http://www.ae.illinois.edu/~loth/CUP/Text.pdf

[16] H. K. Versteeg and W. Malalasekera, *An introduction to computational fluid dynamics: the finite volume method*. Harlow: Pearson/Prentice Hall, 1995.

[17] (2012, 20/05/2013). *Fluid Dynamics Solutions*. Available: http://www.mallett.com/ansys-cfd-solutions.php

[18] (2009, 05/05/2013). ANSYS FLUENT 12.0 User's Guide Available: http://www.sharcnet.ca/Software/Fluent12/html/ug/node1484.htm

[19] M. D. Mattson. (2011, Euler-Lagrangian Simulations of Turbulent Bubbly Flow. Available: http://www.aem.umn.edu/~mahesh/publpdf/thesis/mattson_thesis.pdf

[20] R. Groll, S. Jakirlić, and C. Tropea, "Comparative study of Euler/Euler and Euler/Lagrange approaches simulating evaporation in a turbulent gas–liquid flow," *International journal for numerical methods in fluids*, vol. 59, pp. 873-906, 2009.

Appendix A: Thesis Task Description

Telemark University College
Faculty of Technology

FMH606 Master's Thesis

Title: Simulation of flow in sedimentation tank using Fluent

TUC supervisor: Knut Vågsæther

External partner: VEAS

Task description:

- Make a literature review on sedimentation tanks in sewage treatment plants and solid-liquid flow in tanks.
- Make computational mesh of one of the sedimentation tanks at VEAS.
- Simulate the flow in the sedimentation tank with Fluent.
- Investigate how the boundary conditions influence the flow field.
- Analyse data and discuss the behaviour of the flow field
- If possible: recommend changes in operation and justify these recommendations with simulations.
- Write report

Task background:

VEAS (veas.nu) is a sewage treatment plant located in Røyken at the Oslo-fjord. It serves over 500 000 people in Oslo and Akershus.

The flow field in a sedimentation tank is crucial for good sedimentation so that the particles don't follow the produced water but falls to the bottom of the pool. The flow field in these tanks can be very complicated and it is very difficult to measure velocities in such a large tank. CFD simulations with software like Fluent can be used to understand the flow-field in the sedimentation chamber.

Address: Kjølnes ring 56, NO-3918 Porsgrunn, Norway. **Phone:** 35 57 50 00. **Fax:** 35 55 75 47

Student category:

PT and EET (CFD course)

Practical arrangements:

The student will work at TUC but a few visits to the VEAS plant are needed.

Signatures:

Student: Achini Weerasooriya 2013-02-04

Supervisor: Knut Vågsæther 2013-02-04

Appendix B: Volume Fraction Profiles of Solid Phase

Flow pattern of 250 µm diameter solid particles with 0.5 m3/h flow rate

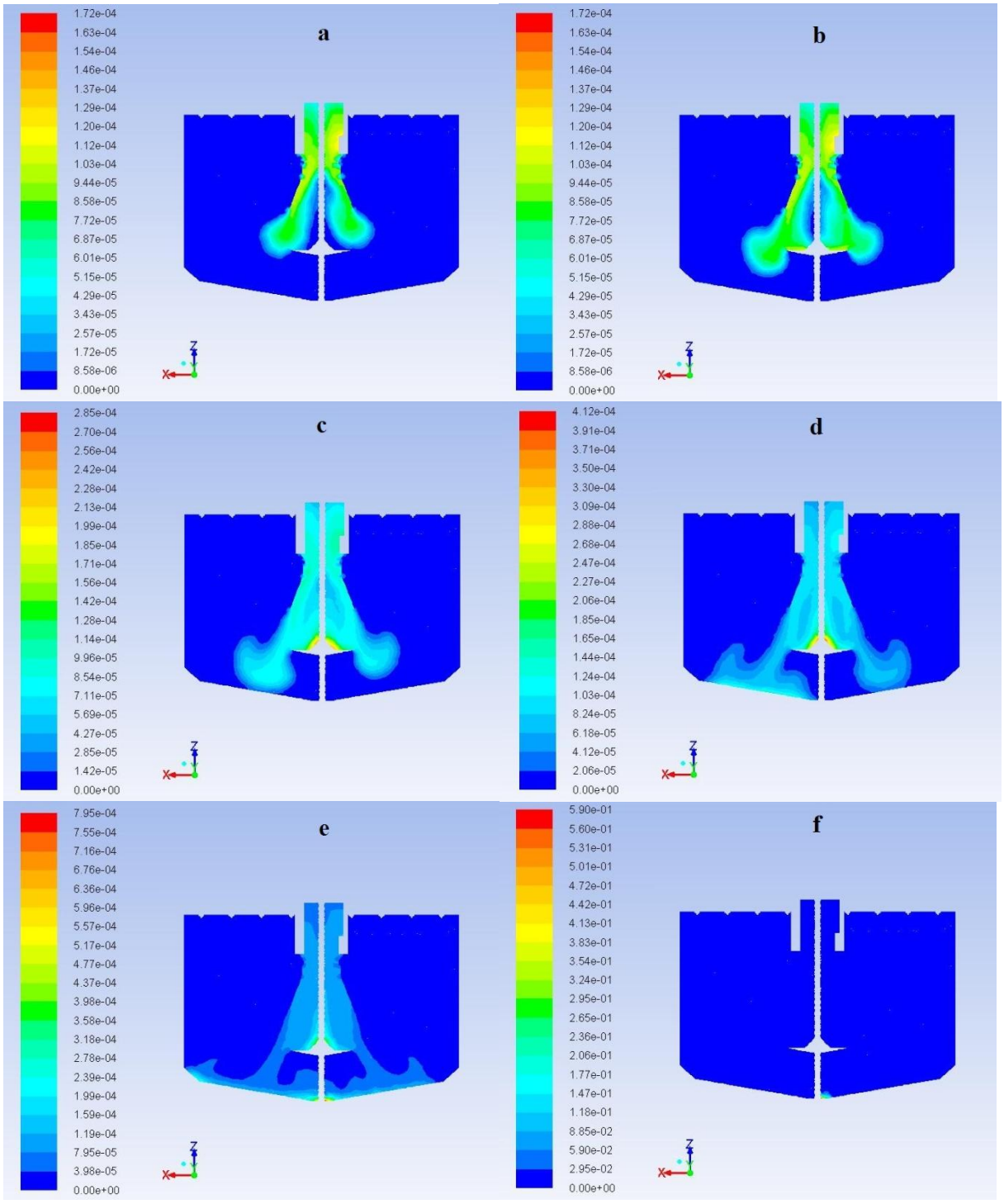

Figure B- 1: Flow pattern of 250 µm diameter solid particles with 0.5 m3/h flow rate at flow time a) 230 s; b) 350 s; c) 500 s; d) 660 s; e) 820; f) 7400s.

Flow pattern of 100 µm diameter solid particles with 0.5 m3/h flow rate

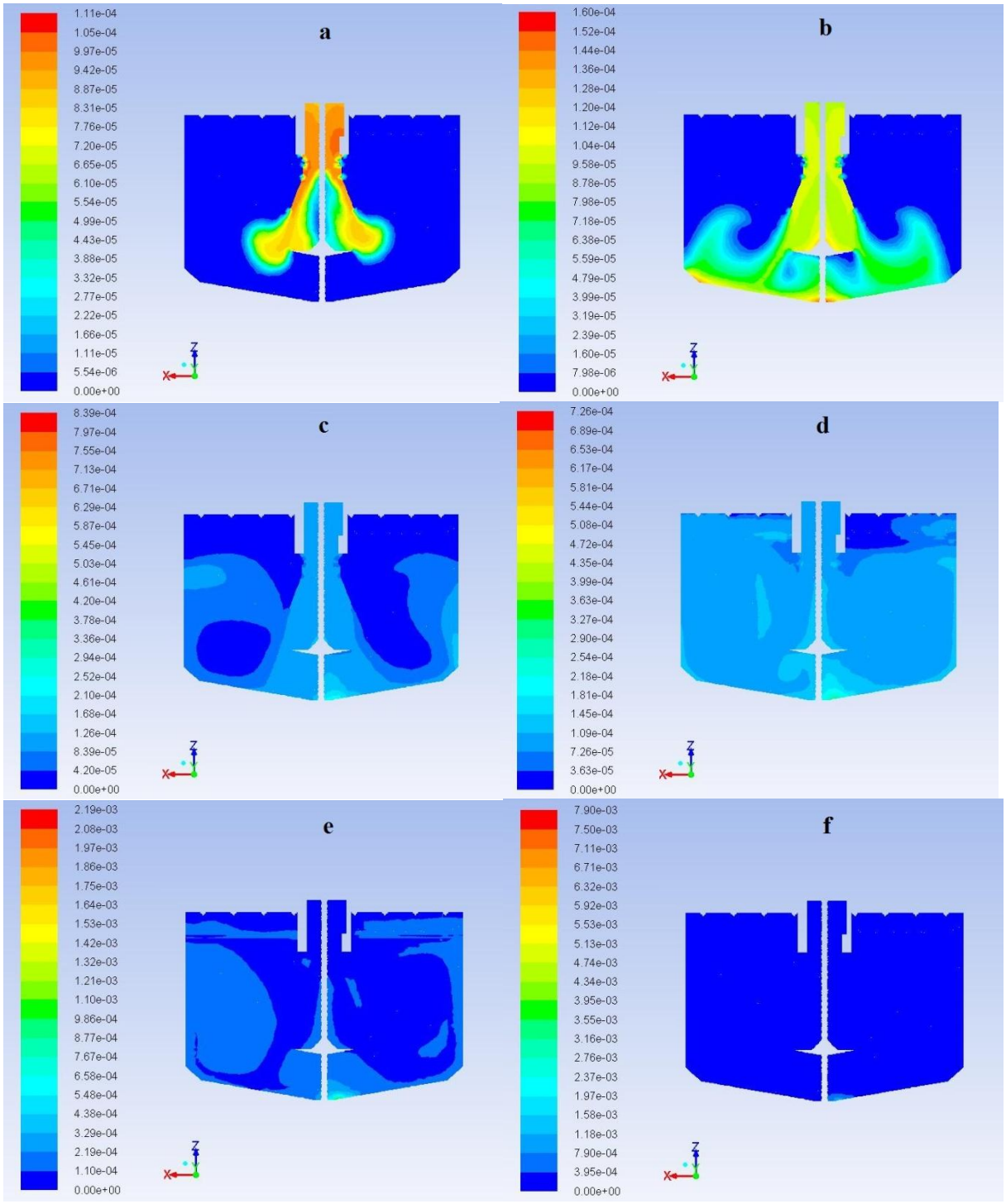

Figure B- 2: Flow pattern of 100 µm diameter solid particles with 0.5 m3/h flow rate at flow time a) 360 s; b) 1370 s; c) 4270 s; d) 9070 s; e) 20770 s; f) 44670 s.

Flow pattern of 50 µm diameter solid particles with 0.5 m3/h flow rate

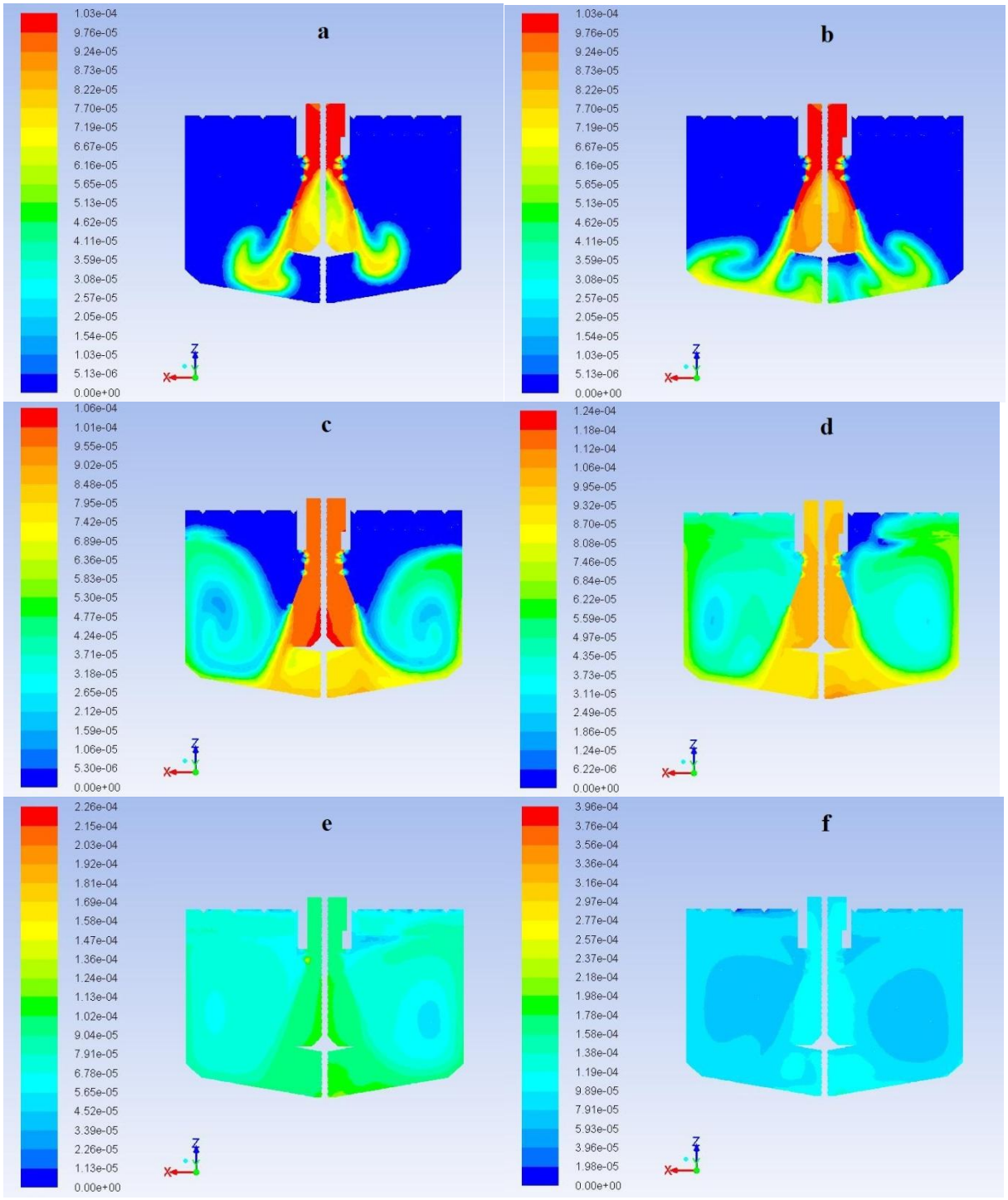

Figure B- 3: Flow pattern of 50 µm diameter solid particles with 0.5 m3/h flow rate at flow time a) 590 s; b) 886 s; c) 3403 s; d) 6463 s; e) 13723 s; f) 18328 s.

Flow pattern of 340 µm diameter solid particles with 1 m3/h flow rate

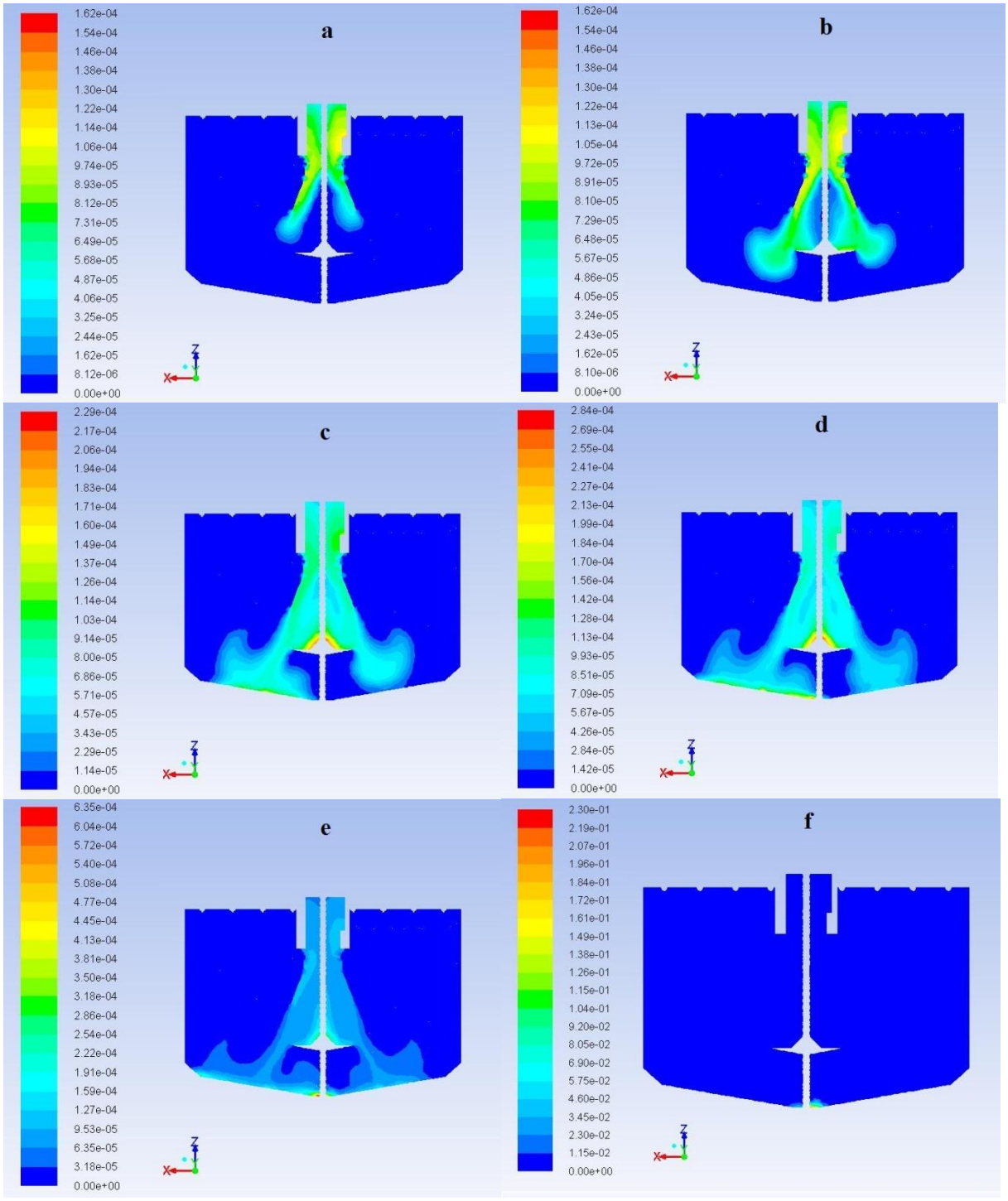

Figure B- 4: Flow pattern of 340 µm diameter solid particles with 1 m3/h flow rate at flow time a) 70 s; b) 160 s; c) 310 s; d) 360 s; e) 410 s; f) 4295 s.

Flow pattern of 250 µm diameter solid particles with 1 m3/h flow rate

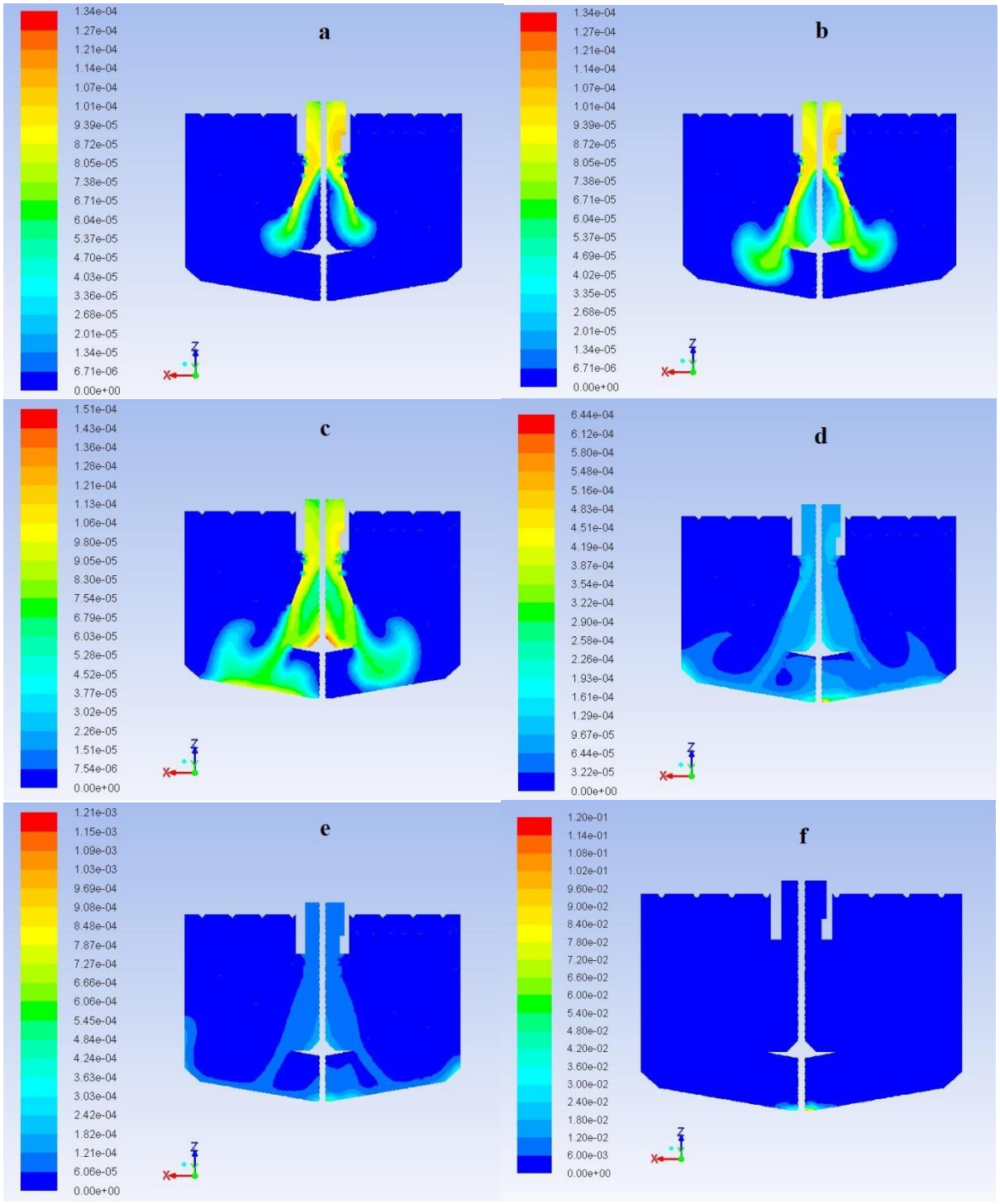

Figure B- 5: Flow pattern of 250 µm diameter solid particles with 1 m3/h flow rate at flow time a) 102 s; b) 202 s; c) 352 s; d) 552 s; e) 752 s; f) 44294 s.

Appendix C: Velocity Profiles of Solid Phase

Velocity Profile of 250 µm diameter solid particles with 0.5 m3/h flow rate

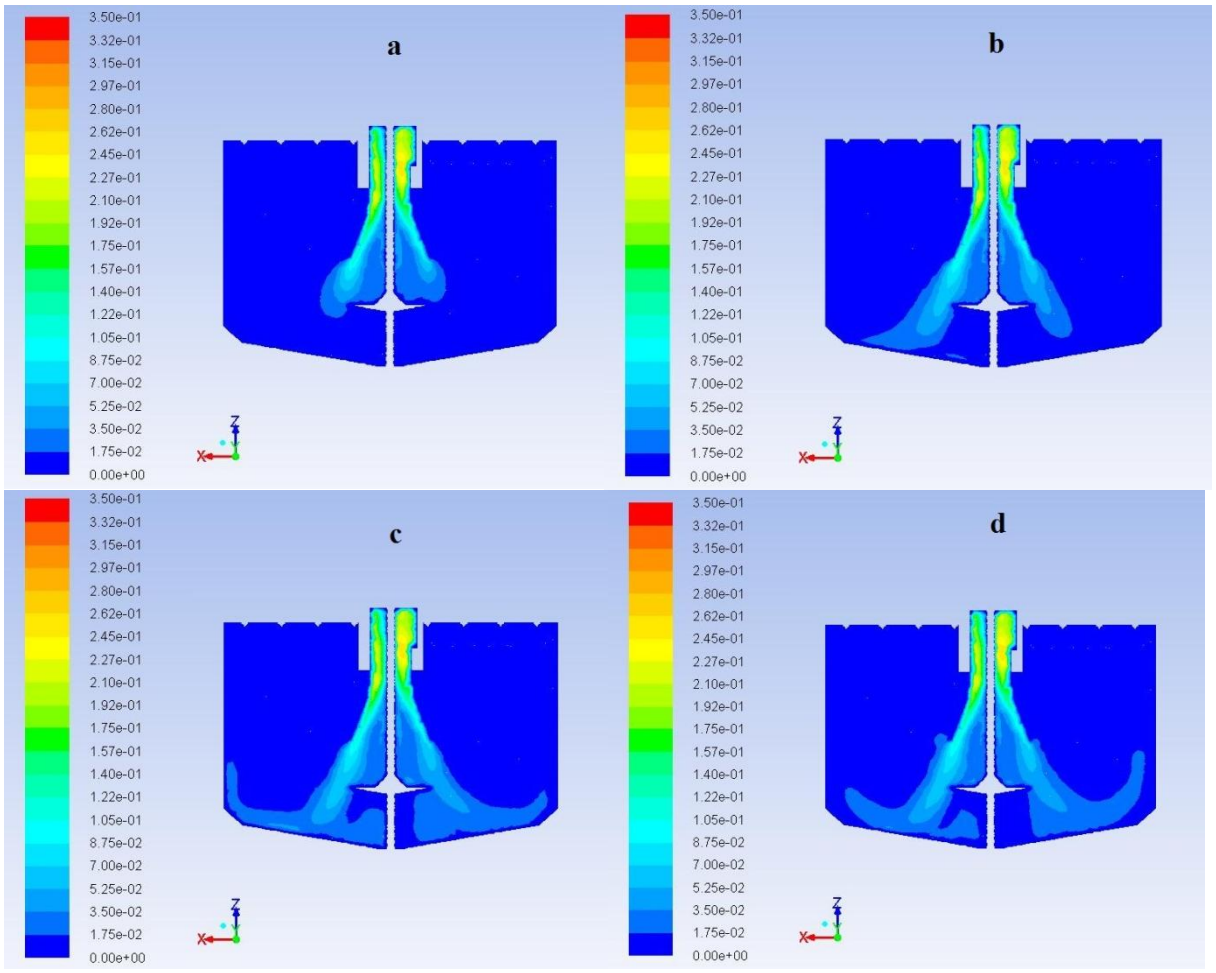

Figure C- 1: Velocity Profile of 250 µm diameter solid particles with 0.5 m3/h flow rate at flow time a) 300 s; b) 660 s; c) 2190 s; d) 7510.

Velocity Profile of 100 µm diameter solid particles with 0.5 m3/h flow rate

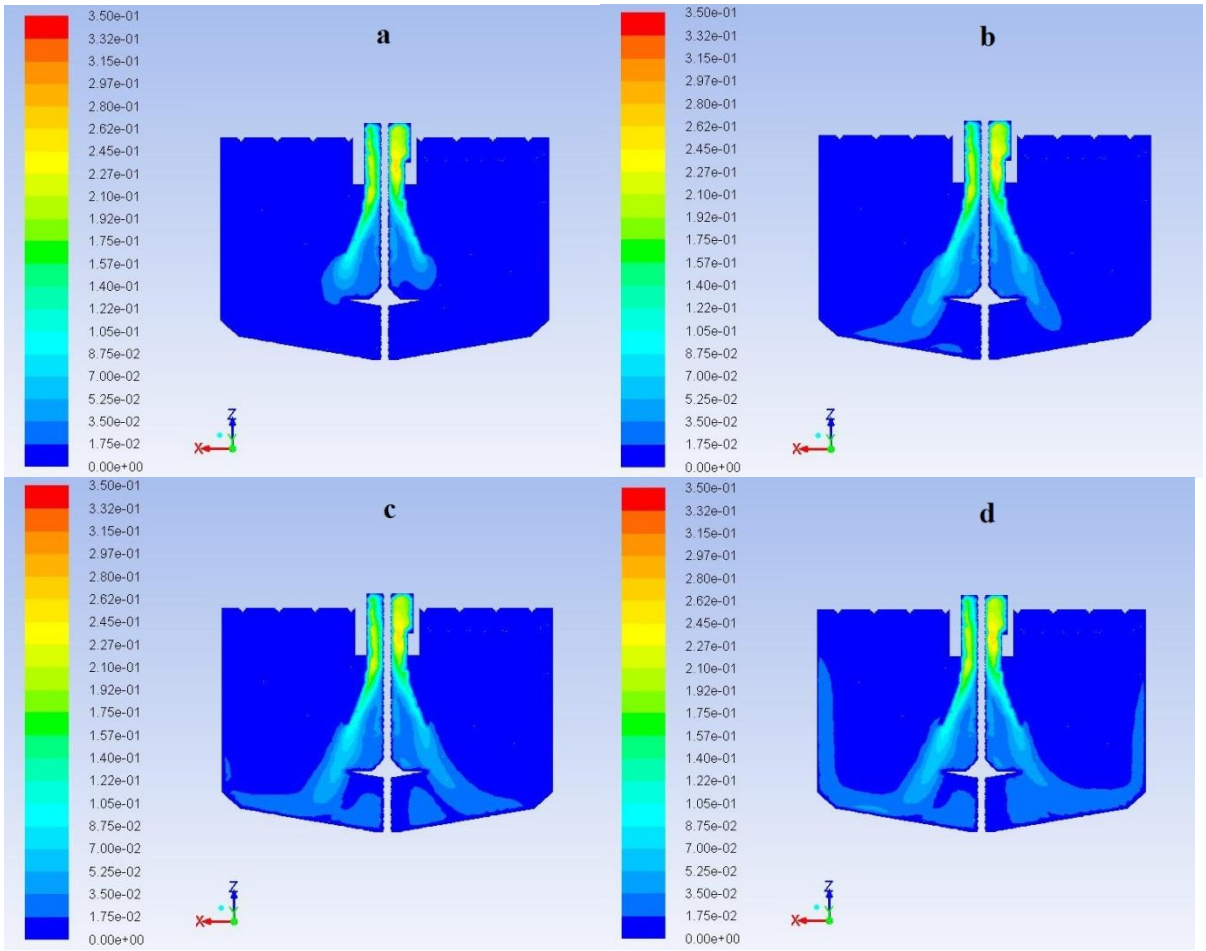

Figure C- 2: Velocity Profile of 100 µm diameter solid particles with 0.5 m3/h flow rate at flow time a) 310 s; b) 1870 s; c) 3870 s; d) 46070 s.

Velocity Profile of 50 µm diameter solid particles with 0.5 m3/h flow rate

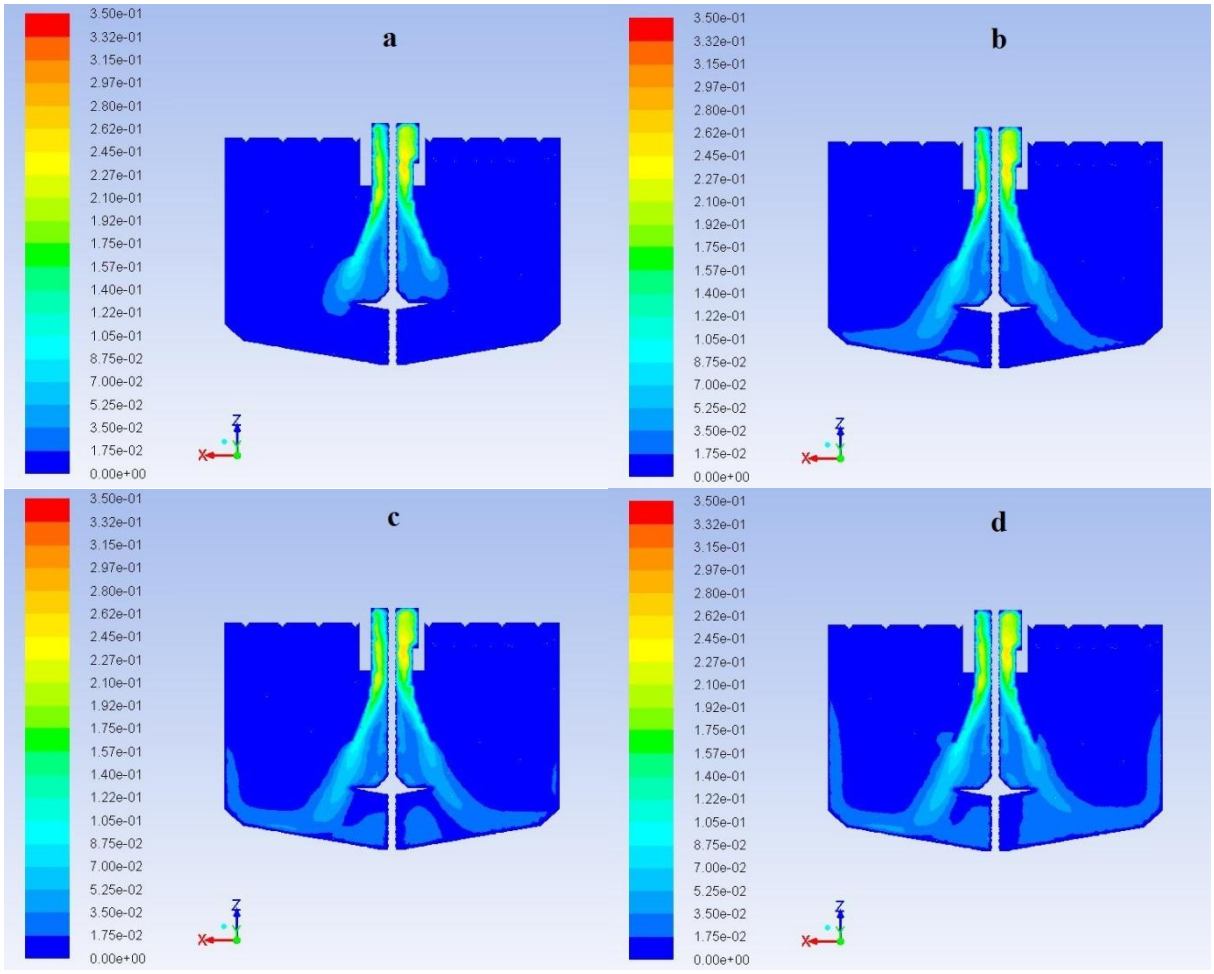

Figure C- 3: Velocity Profile of 50 µm diameter solid particles with 0.5 m3/h flow rate at flow time a) 329 s; b) 819 s; c) 1349 s; d) 12288 s.

Velocity Profile of 340 µm diameter solid particles with 1 m3/h flow rate

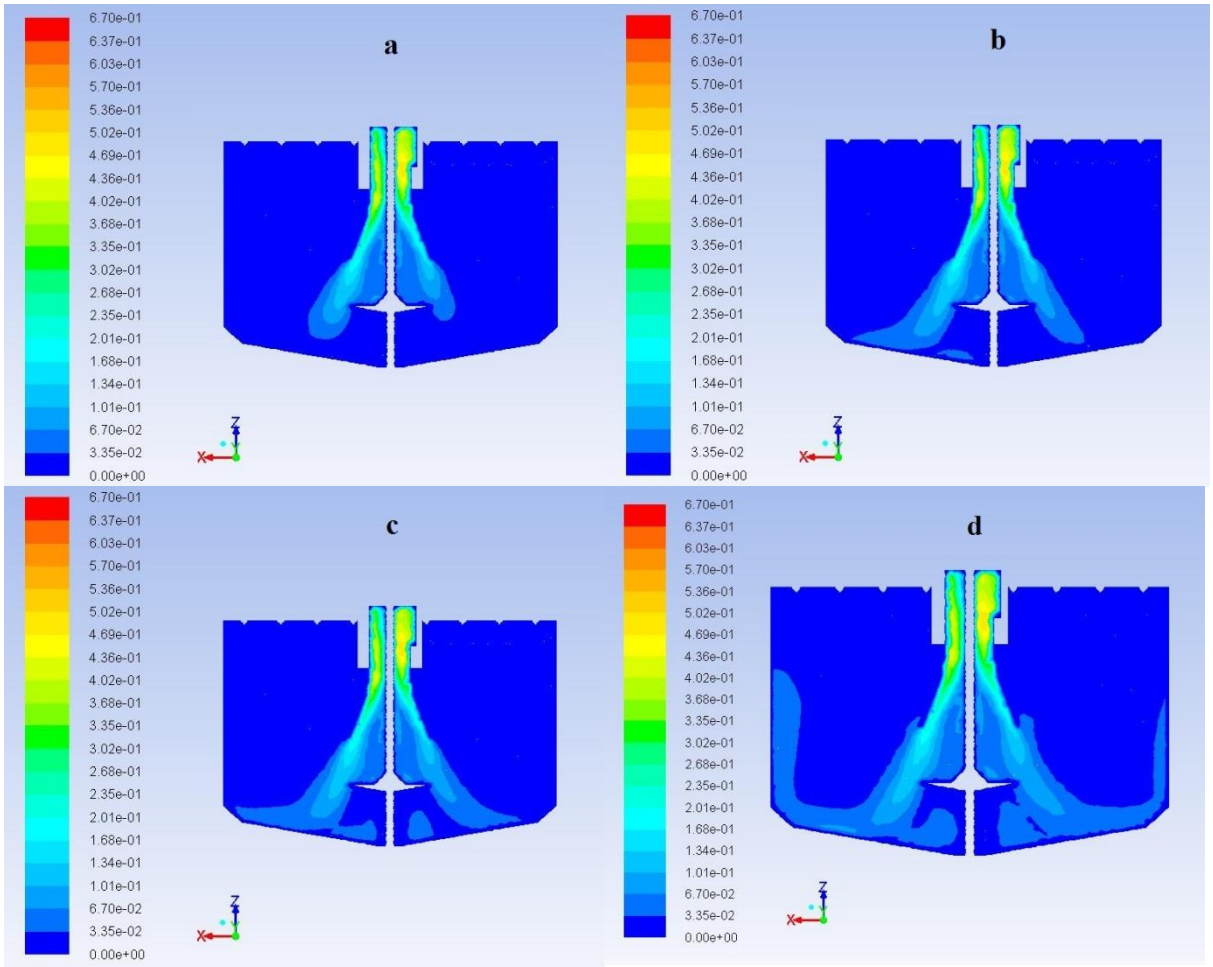

Figure C- 4: Velocity Profile of 340 µm diameter solid particles with 1 m3/h flow rate at flow time a) 260 s; b) 575 s; c) 875 s; d) 3575 s.

Velocity Profile of 250 µm diameter solid particles with 1 m3/h flow rate

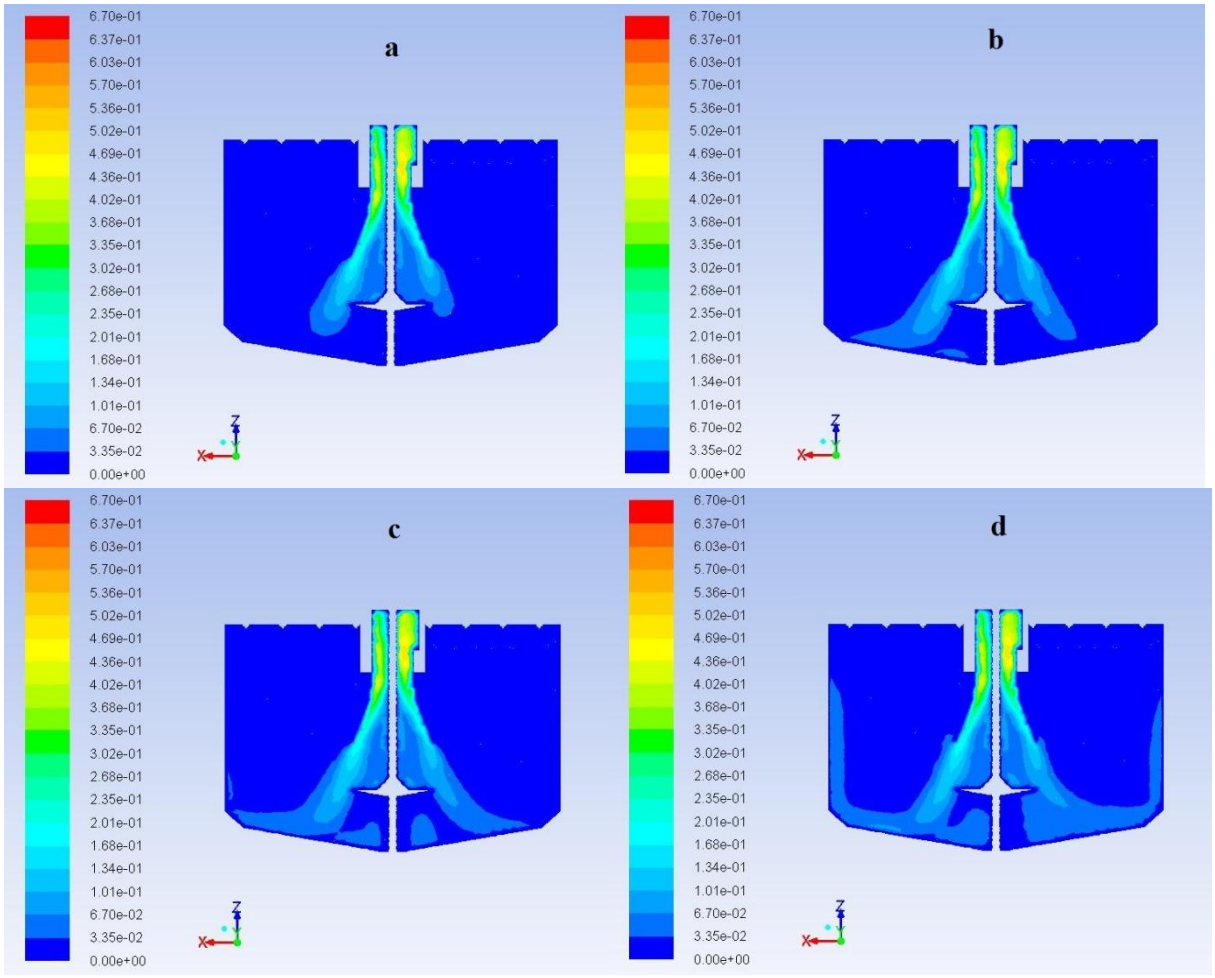

Figure C- 5: Velocity Profile of 250 µm diameter solid particles with 1 m3/h flow rate at flow time a) 252 s; b) 552 s; c) 952 s; d) 22952 s.

Appendix D: Detailed Lamella Description

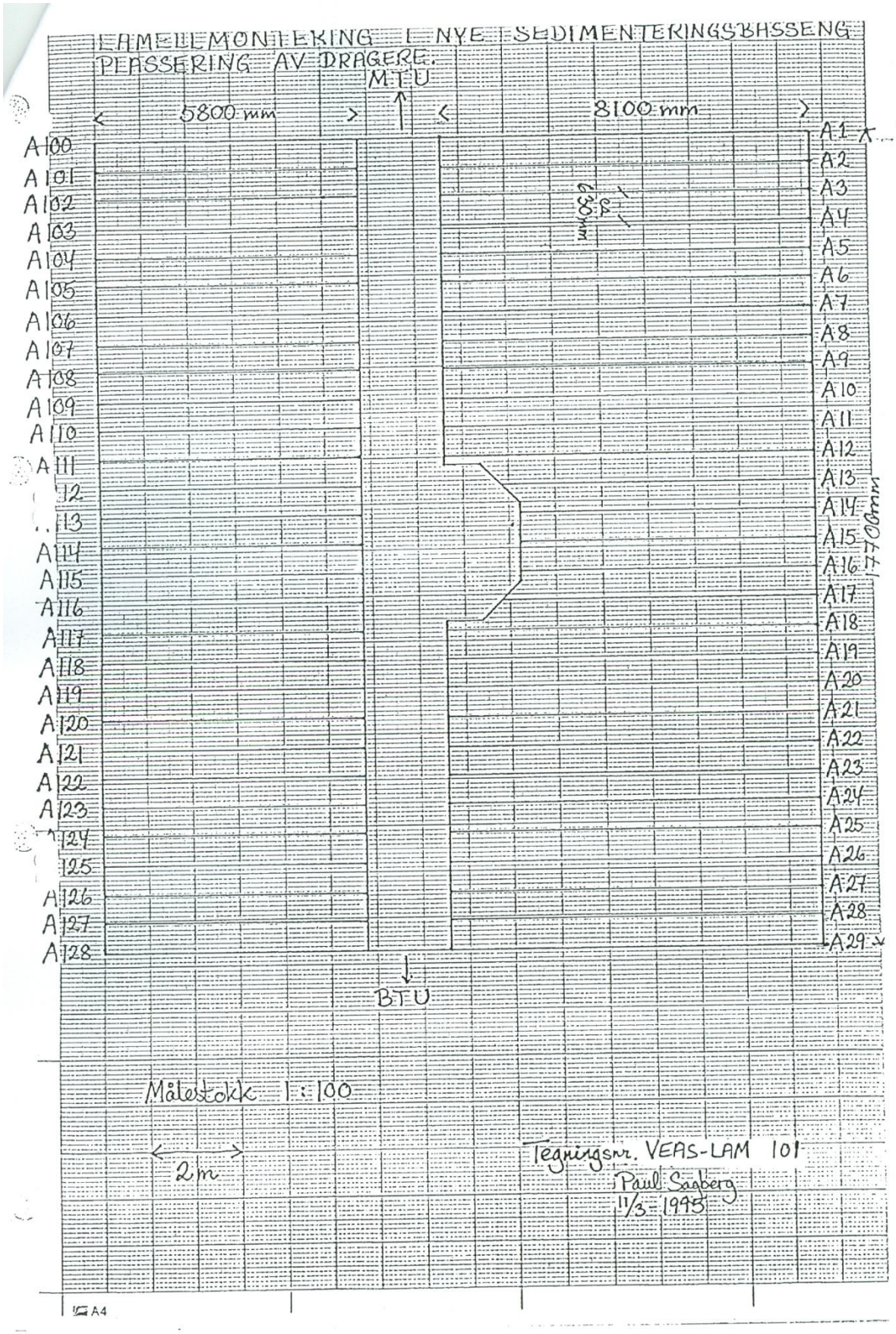

MONTERING AV VINKLER OG AVSTIVERLAMELLER PÅ DRAGERE
EKSEMPEL FRA DRAGER A-2
ca. 8100 mm
Ø12 mm
625 mm
889 mm
1m
2m
6m
7m
8m
1:10
1:2
Ø 12 mm
50 mm
Punktsveis
Ø 6 mm
Målestokk 1:20
400 mm
Tegn. nr. VEAS-LAM 106
Paul Saxberg
27/3 - 1995